Appendix A.13:

Bower Ave – CPT 3937

Table 1: Site Description for Bower Ave (CPT 3937 – CC LIQ 4).

Attribute	Yes/No			Description/Date	Symbol in Figure 1
	10-m Buffer	20-m Buffer	50-m Buffer		
Near a body of surface water or other free face features?	No	No	No	The center of the site is 350 m away from a pond (~2.0 m high, N-S free face) and 1140 m away from the Avon River (~1.5 m high, NW-SE free face).	NA
Lateral spreading observed during the CES?	No	No	No	Absence of ground cracks indicates no lateral spreading, as observed by the mapping team.[1]	NA
Nearby buildings or structures?	Yes	Yes	Yes	Building coverage of the 10-m, 20-m, and 50-m buffers is 11%, 17%, and 15%, respectively.	White Fill + Brown Outline
Sloping land?	No	No	No	Flat land, residential area.	NA
Step changes in the ground surface?	No	No	No	NA	NA
Retaining walls?	No	No	No	NA	NA
Vegetation?	Yes	Yes	Yes	Trees and bushes cover 27% of the 10-m buffer, 12% of the 20-m buffer and 16% of the 50-m buffer. They are spread throughout all quadrants of the three buffers.	White Fill + Green Outline
Anthropogenic changes to the site between the LiDAR surveys?	Yes	Yes	Yes	Minor earthwork was performed after Feb 2011 EQ in the NE quadrant of the 50-m buffer. Building complex was built in the E portion of the 50-m buffer in Mar 2011. The same complex was removed between Sep 2013 and Feb 2014. Road construction took place in the NW quadrant of the 50-m buffer between Aug 2013 and Aug 2014. Between Aug 2014 and Sep 2014, a building in the E portion of the 10-m, 20-m, and 50-m buffers was demolished. Another dwelling was built at the same location by Jan 2015.	Building Construction and Earthwork: White Fill + Yellow Outline; Road Construction: Gray Fill + Yellow Outline; Dwelling Removal in 2014: Orange Crossline
Other important factors?	Yes	Yes	Yes	Moderate-motor-vehicle-volume, two-way roadways occupy 20% of the 50-m buffer, and are in its NE, NW, and SW quadrants. Only W portion of the 10-m and 20-m buffers is occupied by the roadway that covers 3% and 23% of their respective areas.	Road: Gray Fill + Red Outline

Note: Buffer is the area within a circle of a specified radius with CPT investigations done at its center (172.711488°, -43.492600°).

[1] Canterbury Geotechnical Database. (2012). "Observed Ground Crack Locations", Map Layer CGD0400 - 23 July 2012, retrieved July 09, 2018 from https://canterburygeotechnicaldatabase.projectorbit.com/

Figure 1: Site plan with areas where LiDAR survey data is considered.

Note 1: Eight patches (outlined in red) in free field were initially selected for settlement assessment as areas free of vegetation and structures. Further analyses such as proximity of a patch to a CPT, proximity of a patch to a property subjected to addition and/or demolition of a structure, front yard/backyard alterations (e.g., ploughing, rubble, scrap), aerial distribution of sediment ejecta, and density of LiDAR points for 2003 resulted in Patches A and B being selected for detailed settlement assessment and other patches being discarded in detailed settlement assessment. In addition, since significant amounts of ejecta were observed on roads in the CES, the entire portion of the road within the 50-m buffer was considered for settlement assessment. Roads as hard, relatively flat surfaces provide many ground-classified points.

Table 2: LiDAR flight error adjustments, global adjustments for the difference between average LiDAR point elevations and benchmark survey elevations, and vertical tectonic movement adjustments.

	Adjustments (mm)		
Earthquake Event(s)	LiDAR Flight Error	Global Offset[2]	Tectonic Vertical Movement
Sep-10	-100	-3	0
Feb-11	+50	16	-30
Jun-11	0	38	-40
Dec-11	0	-65	0
CES	-50	-14	-70
Post Sep 2010 LiDAR survey affected by ejecta?			No

Note: The negative sign indicates the subtraction from the ground surface subsidence, while the positive sign indicates the addition to the ground surface subsidence.

Table 3a: LiDAR Measurement Error for Patch A.

Surveys	Buffer	Area Averaged Difference Indicating Repeat Measurement Error (mm)	$\sigma^*_{\text{individual LiDAR points}}$ (mm)	%Reduction in σ due to Area Averaging of LiDAR Points
Post Feb 2011: Mar 2011 and May 2011	10-m	51	59	[86,86]
	20-m	51		
	50-m	51		
Post Dec 2011: Feb 2012 and Oct 2015	10-m	NA	70	[NA,NA]
	20-m	NA		
	50-m	NA		

*Standard deviation.

[2] Russell, J., & van Ballegooy, S. (2015). *Canterbury Earthquake Sequence: Increased liquefaction vulnerability assessment methodology*. New Zealand: Tonkin & Taylor Ltd.

Table 3b: LiDAR Measurement Error for Patch B.

Surveys	Buffer	Area Averaged Difference Indicating Repeat Measurement Error (mm)	$\sigma^*_{\text{individual LiDAR points}}$ (mm)	%Reduction in σ due to Area Averaging of LiDAR Points
Post Feb 2011: Mar 2011 and May 2011	10-m	NA	59	[127,127]
	20-m	NA		
	50-m	75		
Post Dec 2011: Feb 2012 and Oct 2015	10-m	NA	70	[33,33]
	20-m	NA		
	50-m	23		

*Standard deviation.

Table 3c: LiDAR Measurement Error for Road.

Surveys	Buffer	Area Averaged Difference Indicating Repeat Measurement Error (mm)	$\sigma^*_{\text{individual LiDAR points}}$ (mm)	%Reduction in σ due to Area Averaging of LiDAR Points
Post Feb 2011: Mar 2011 and May 2011	10-m	35	59	[59,88]
	20-m	52		
	50-m	59		
Post Dec 2011: Feb 2012 and Oct 2015	10-m	7	70	[10,59]
	20-m	41		
	50-m	64		

*Standard deviation.

Table 4a: Ground surface subsidence adjustments due to LiDAR measurement error for Patch A.

Earthquake Event(s)	$\sigma_{\text{pre-EQ LiDAR survey}}$ (mm)	$\sigma_{\text{post-EQ LiDAR survey}}$ (mm)	σ_{total} (mm)	Area Average Adjusted σ (mm) **
Sep-10	158	56	134	±116
Feb-11	56	59	59	±51
Jun-11	59	61	62	±54
Dec-11	61	70	87	±75
CES	158	70	124	±108

**Based on the highest %Reduction in Table 3a.

Table 4b: Ground surface subsidence adjustments due to LiDAR measurement error for Patch B.

Earthquake Event(s)	$\sigma_{\text{pre-EQ LiDAR survey}}$ (mm)	$\sigma_{\text{post-EQ LiDAR survey}}$ (mm)	σ_{total} (mm)	Area Average Adjusted σ (mm) **
Sep-10	158	56	134	±170
Feb-11	56	59	59	±75
Jun-11	59	61	62	±79
Dec-11	61	70	87	±110
CES	158	70	124	±158

**Based on the highest %Reduction in Table 3b.

Table 4c: Ground surface subsidence adjustments due to LiDAR measurement error for Road.

Earthquake Event(s)	$\sigma_{\text{pre-EQ LiDAR survey}}$ (mm)	$\sigma_{\text{post-EQ LiDAR survey}}$ (mm)	σ_{total} (mm)	Area Average Adjusted σ (mm) **
Sep-10	158	56	134	±118
Feb-11	56	59	59	±52
Jun-11	59	61	62	±55
Dec-11	61	70	87	±76
CES	158	70	124	±110

**Based on the highest %Reduction in Table 3c.

Table 5a: Raw liquefaction-related ground surface subsidence using original LiDAR points for Patch A.

	Average Ground Surface Subsidence (mm)		
Earthquake Event(s)	10-m Buffer	20-m Buffer	50-m Buffer
Sep-10	49	49	49
Feb-11	185	185	185
Jun-11	42	42	42
Dec-11	91	91	91
CES	367	367	367

Table 5b: Raw liquefaction-related ground surface subsidence using original LiDAR points for Patch B.

	Average Ground Surface Subsidence (mm)		
Earthquake Event(s)	10-m Buffer	20-m Buffer	50-m Buffer
Sep-10	NA	NA	62
Feb-11	NA	NA	102
Jun-11	NA	NA	91
Dec-11	NA	NA	24
CES	NA	NA	279

Table 5c: Raw liquefaction-related ground surface subsidence using original LiDAR points for Road.

	Average Ground Surface Subsidence (mm)		
Earthquake Event(s)	10-m Buffer	20-m Buffer	50-m Buffer
Sep-10	156	77	100
Feb-11	198	209	173
Jun-11	59	82	91
Dec-11	75	56	62
CES	488	424	426

Table 6a: Corrected liquefaction-related ground surface subsidence using original LiDAR points for Patch A with the calculated adjustments in Table 2.

	Average Calculated Ground Surface Subsidence (mm)		
Earthquake Event(s)	10-m Buffer	20-m Buffer	50-m Buffer
Sep-10	-54±125	-54±125	-54±125
Feb-11	221±50	221±50	221±50
Jun-11	40±50	40±50	40±50
Dec-11	26±75	26±75	26±75
CES	233±100	233±100	233±100

Notes: Plus/minus values are same as those in Table 4a, but rounded to the nearest 25; Positive overall values indicate ground surface subsidence, while negative overall values indicate ground surface uplift.

Table 6b: Corrected liquefaction-related ground surface subsidence using original LiDAR points for Patch B with the calculated adjustments in Table 2.

	Average Calculated Ground Surface Subsidence (mm)		
Earthquake Event(s)	10-m Buffer	20-m Buffer	50-m Buffer
Sep-10	NA	NA	-41±175
Feb-11	NA	NA	138±75
Jun-11	NA	NA	89±75
Dec-11	NA	NA	-41±100
CES	NA	NA	145±150

Notes: Plus/minus values are same as those in Table 4b, but rounded to the nearest 25; Positive overall values indicate ground surface subsidence, while negative overall values indicate ground surface uplift.

Table 6c: Corrected liquefaction-related ground surface subsidence using original LiDAR points for Road with the calculated adjustments in Table 2.

	Average Calculated Ground Surface Subsidence (mm)		
Earthquake Event(s)	10-m Buffer	20-m Buffer	50-m Buffer
Sep-10	53±125	-26±125	-3±125
Feb-11	234±50	245±50	209±50
Jun-11	57±50	80±50	89±50
Dec-11	10±75	-9±75	-3±75
CES	354±100	290±100	292±100

Notes: Plus/minus values are same as those in Table 4c, but rounded to the nearest 25; Positive overall values indicate ground surface subsidence, while negative overall values indicate ground surface uplift.

Table 7a: Corrected liquefaction-related ground surface subsidence for Patch A using LiDAR DEMs.

	Estimated Ground Surface Subsidence (mm)								
	10-m Buffer			20-m Buffer			50-m Buffer		
Earthquake Event(s)	16th %ile	50th %ile	84th %ile	16th %ile	50th %ile	84th %ile	16th %ile	50th %ile	84th %ile
Sep-10	50	50	50	50	50	50	50	50	50
Feb-11	200	200	200	200	200	200	200	200	200
Jun-11	50	50	50	50	50	50	50	50	50
Dec-11	50	50	50	50	50	50	50	50	50
CES	300	350	400	300	350	400	300	350	400

Note: These percentiles are not the exact statistical measures; they indicate the spatial variability of ground surface subsidence.

Table 7b: Corrected liquefaction-related ground surface subsidence for Patch B using LiDAR DEMs.

	Estimated Ground Surface Subsidence (mm)								
	10-m Buffer			20-m Buffer			50-m Buffer		
Earthquake Event(s)	16th %ile	50th %ile	84th %ile	16th %ile	50th %ile	84th %ile	16th %ile	50th %ile	84th %ile
Sep-10	NA	NA	NA	NA	NA	NA	50	50	50
Feb-11	NA	NA	NA	NA	NA	NA	100	100	150
Jun-11	NA	NA	NA	NA	NA	NA	50	50	50
Dec-11	NA	NA	NA	NA	NA	NA	50	50	50
CES	NA	NA	NA	NA	NA	NA	200	200	250

Note: These percentiles are not the exact statistical measures; they indicate the spatial variability of ground surface subsidence.

Table 7c: Corrected liquefaction-related ground surface subsidence for Road using LiDAR DEMs.

	Estimated Ground Surface Subsidence (mm)								
	10-m Buffer			20-m Buffer			50-m Buffer		
Earthquake Event(s)	16th %ile	50th %ile	84th %ile	16th %ile	50th %ile	84th %ile	16th %ile	50th %ile	84th %ile
Sep-10	<50	<50	<50	<50	<50	50	<50	<50	50
Feb-11	200	200	200	200	200	200	150	200	200
Jun-11	50	50	50	50	50	50	50	50	50
Dec-11	50	50	50	50	50	50	50	50	50
CES	300	300	300	300	300	300	250	300	350

Note: These percentiles are not the exact statistical measures; they indicate the spatial variability of ground surface subsidence.

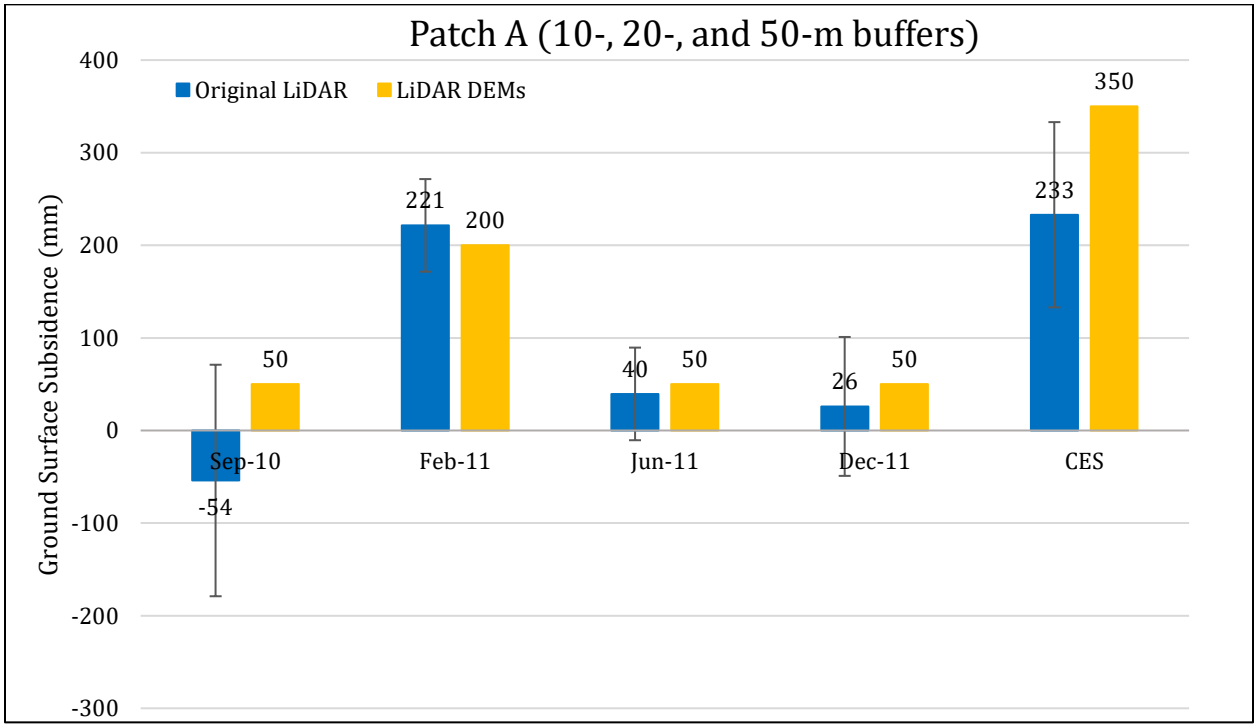

Figure 2: Comparison between ground surface subsidence determined from original LiDAR survey points and ground surface subsidence (50th %ile) estimated using LiDAR DEMs for Patch A.

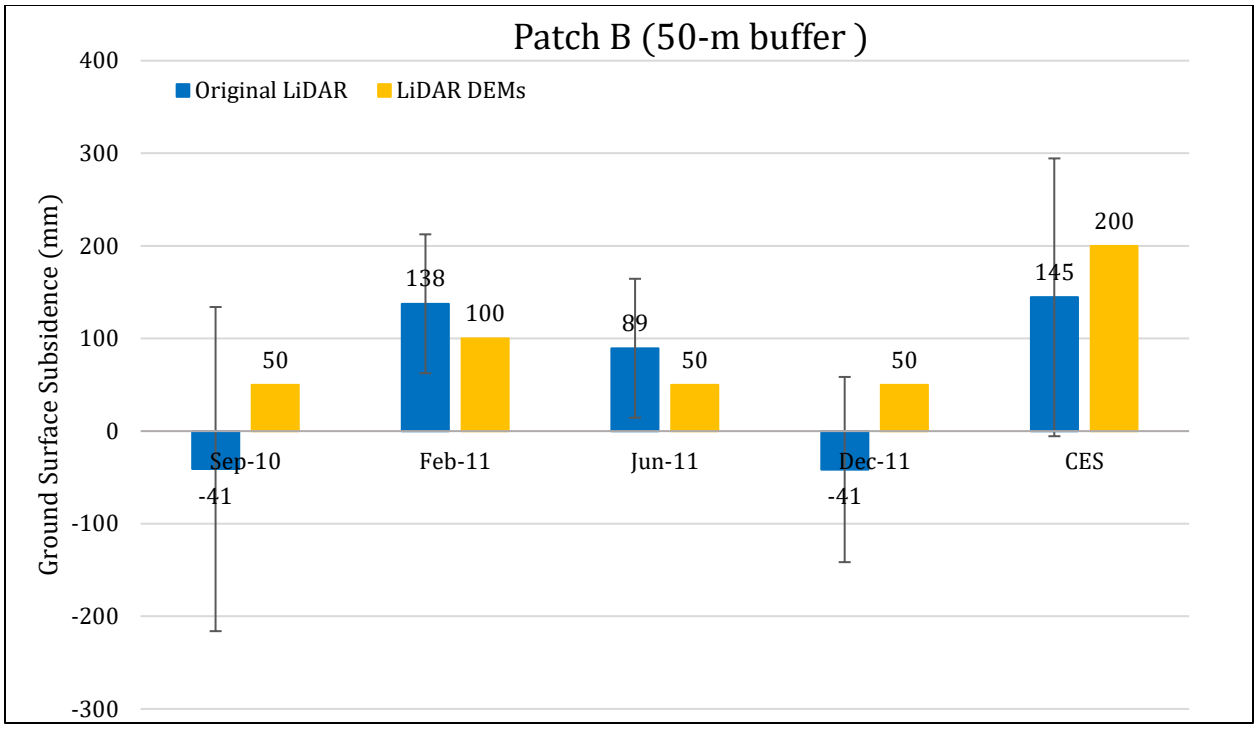

Figure 3: Comparison between ground surface subsidence determined from original LiDAR survey points and ground surface subsidence (50th %ile) estimated using LiDAR DEMs for Patch B for the 50-m buffer.

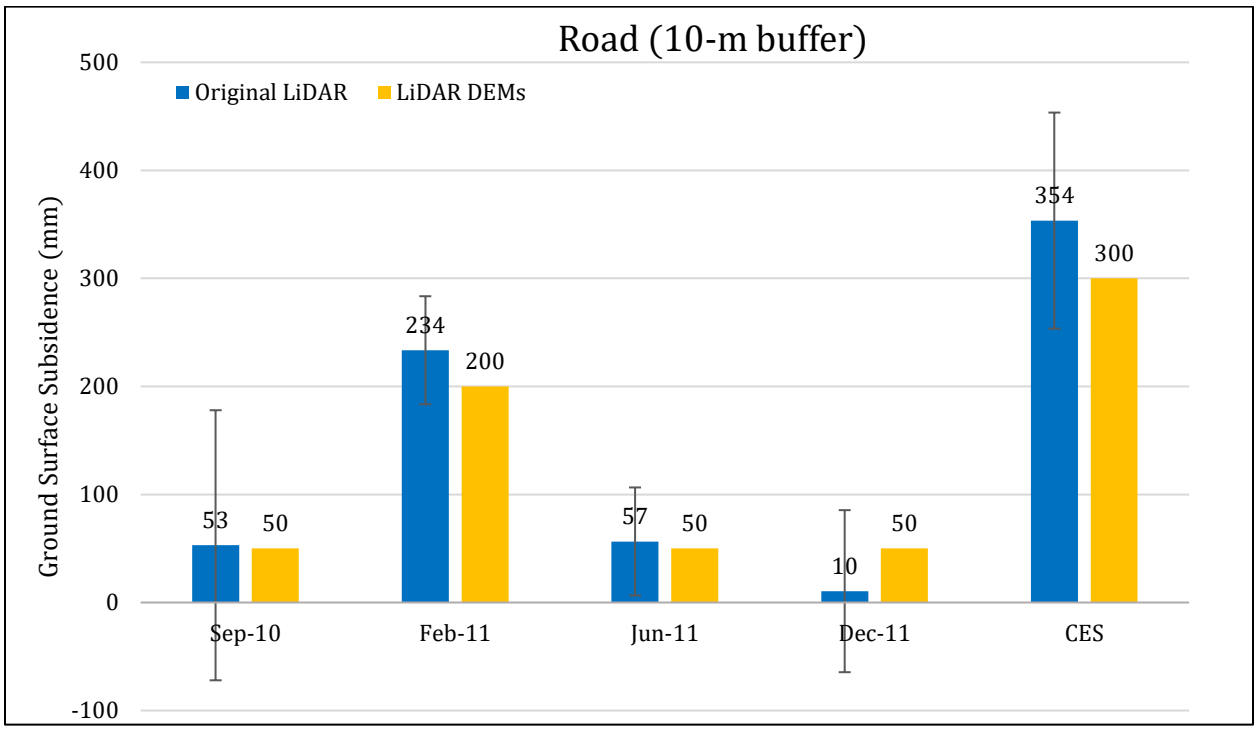

Figure 4: Comparison between ground surface subsidence determined from original LiDAR survey points and ground surface subsidence (50th %ile) estimated using LiDAR DEMs for Road for the 10-m buffer.

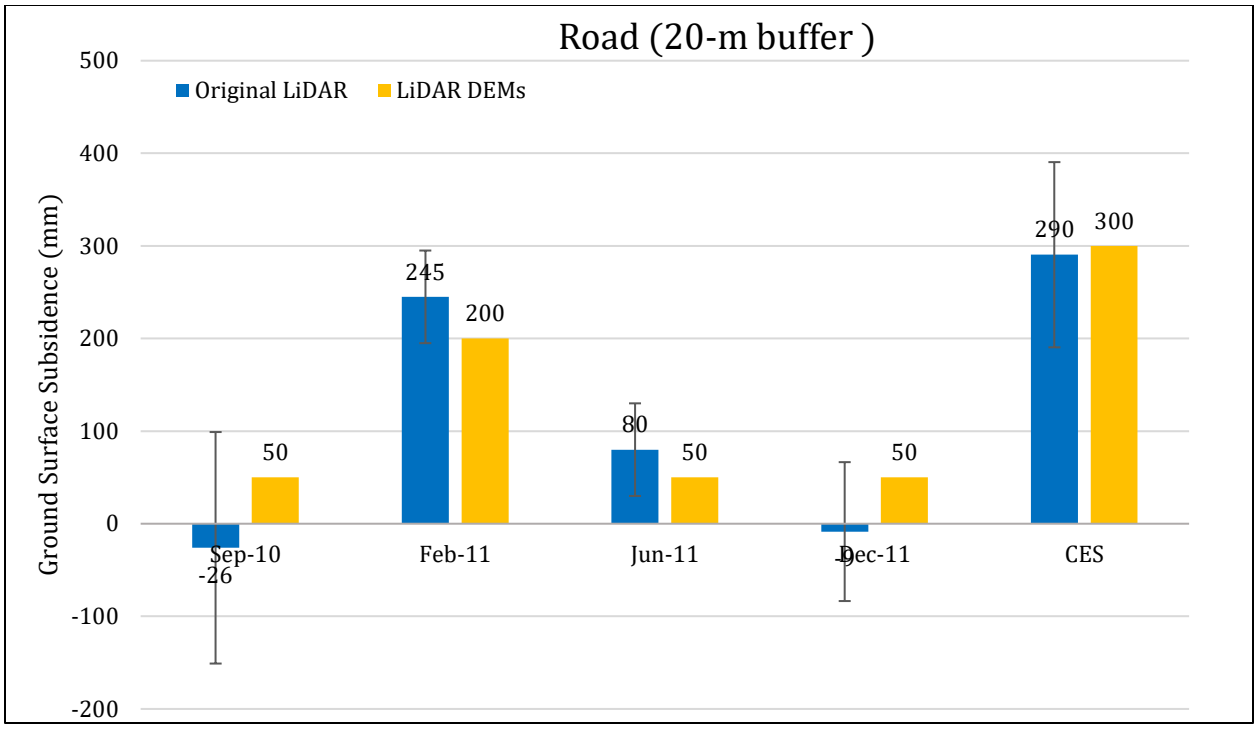

Figure 5: Comparison between ground surface subsidence determined from original LiDAR survey points and ground surface subsidence (50th %ile) estimated using LiDAR DEMs for Road for the 20-m buffer.

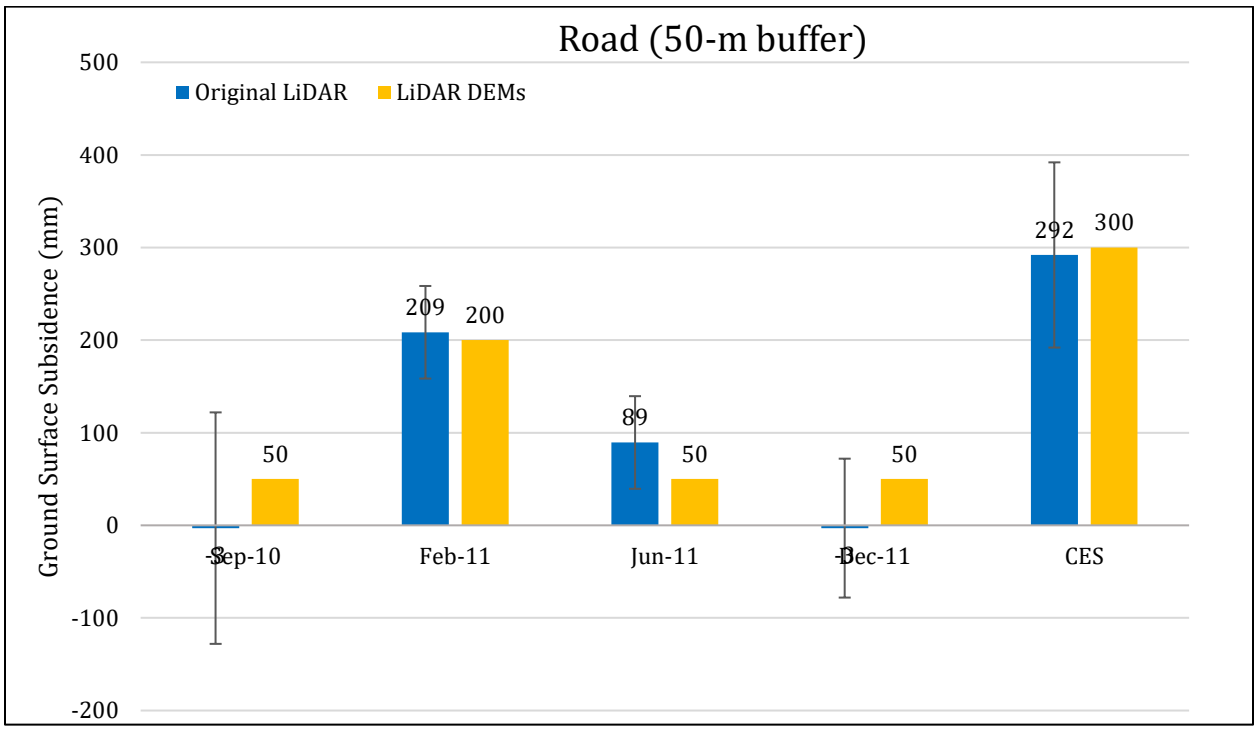

Figure 6: Comparison between ground surface subsidence determined from original LiDAR survey points and ground surface subsidence (50th %ile) estimated using LiDAR DEMs for Road for the 50-m buffer.

Note 2: The ground surface subsidence values determined from original LiDAR survey points are in agreement with the ground surface subsidence values estimated using LiDAR DEMs for all earthquake events.

Table 8a: Ejecta-Induced settlement for the top 20 m of the soil profile for Patch A for the 50th %ile PGA, P_L=50%, and C_{FC}=0.13 using BI-2014, ZRB-2002, and I_C cutoff of 2.6.

Earthquake Event(s)	M_W	PGA (g)	Depth to Groundwater (m)	S_T(mm)	S_{V1D} (mm)	$S_{E,L}$ (mm)
Sep-10	7.1	0.18	2.5	-54±125	16±20	-70±127
Feb-11	6.2	0.47	2.2	221±50	98±50	123±71
Jun-11	6.2	0.22	2.5	40±50	20±25	20±56
Dec-11	6.1	0.36	1.5	26±75	65±50	-39±90

Notes: S_T = Total settlement (Table 6); S_{V1D} = Average vertical settlement due to volumetric compression using Boulanger and Idriss (2014) (BI-2014), Zhang et al. (2002) (ZRB-2002) procedures and de Greef and Lengkeek (2018) thin-layer correction; $S_{E,L}$ = Ejecta-induced settlement as the difference between the LiDAR-based S_T and S_{V1D}.

Table 8b: Ejecta-Induced settlement for the top 20 m of the soil profile for Patch B for the 50th %ile PGA, P_L=50%, and C_{FC}=0.13 using BI-2014, ZRB-2002, and I_C cutoff of 2.6.

Earthquake Event(s)	M_W	PGA (g)	Depth to Groundwater (m)	S_T(mm)	S_{V1D} (mm)	$S_{E,L}$ (mm)
Sep-10	7.1	0.18	2.5	-41±175	8±20	-49±176
Feb-11	6.2	0.47	2.2	138±75	45±50	93±90
Jun-11	6.2	0.22	2.5	89±75	11±25	78±79
Dec-11	6.1	0.36	1.5	-41±100	36±50	-77±112

Notes: S_T = Total settlement (Table 6); S_{V1D} = Average vertical settlement due to volumetric compression using Boulanger and Idriss (2014) (BI-2014), Zhang et al. (2002) (ZRB-2002) procedures and de Greef and Lengkeek (2018) thin-layer correction; $S_{E,L}$ = Ejecta-induced settlement as the difference between the LiDAR-based S_T and S_{V1D}.

Table 8c: Ejecta-Induced settlement for the top 20 m of the soil profile for Road within the 50-m buffer for the 50th %ile PGA, P_L=50%, and C_{FC}=0.13 using BI-2014, ZRB-2002, and I_C cutoff of 2.6.

Earthquake Event(s)	M_W	PGA (g)	Depth to Groundwater (m)	S_T(mm)	S_{V1D} (mm)	$S_{E,L}$ (mm)
Sep-10	7.1	0.18	2.5	-3±125	10±20	-13±127
Feb-11	6.2	0.47	2.2	209±50	63±50	146±71
Jun-11	6.2	0.22	2.5	89±50	13±25	76±56
Dec-11	6.1	0.36	1.5	-3±75	44±50	-47±90

Notes: S_T = Total settlement (Table 6); S_{V1D} = Average vertical settlement due to volumetric compression using Boulanger and Idriss (2014) (BI-2014), Zhang et al. (2002) (ZRB-2002) procedures and de Greef and Lengkeek (2018) thin-layer correction; $S_{E,L}$ = Ejecta-induced settlement as the difference between the LiDAR-based S_T and S_{V1D}.

Note 3: The uncertainty for volumetric settlement was derived based on the sensitivity of volumetric settlement to PGA, C_{FC}, and P_L for each earthquake event for VsVp 57203 *Shirley Intermediate School* and CC LIQ 1 – CPT 5586 – *Vivian St* sites. Taking the 50th percentile as the baseline case, the minimum and maximum values corresponding to the difference between the 25th percentile and the 50th percentile and the 75th percentile and the 50th percentile were determined. The arithmetic mean of the range of the minimum and maximum difference was evaluated for each patch at the two sites. The maximum arithmetic mean for each earthquake event was rounded to the nearest five and used as the uncertainty value. Accordingly, the 1-D volumetric settlement uncertainties of ±20, ±50, ±25, and ±50 mm for the Sep-10, Feb-11, Jun-11, and Dec-11 earthquake events, respectively, were used for all sites in this study.

Table 9a: Coverage area and height of ejecta estimates for Patch A using photographs.

Earthquake Event	$A_{E,thick}$ (m^2)	$H_{E,thick}$ (mm)	$A_{E,thin}$ (m^2)	$H_{E,thin}$ (mm)	A_T (m^2)
Sep-10	0	0	0	0	29.3
Feb-11	0	0	0	0	29.3
Jun-11	0	0	0	0	29.3
Dec-11	0	0	0	0	29.3

Notes: $A_{E,thick/thin}$ = Coverage area of thick/thin ejecta layers; $H_{E,thick/thin}$ = Lower-upper estimate of height of thick/thin ejecta layers; A_T = Total assessment area of a buffer being considered; Thin and thick layers correspond to light gray and dark gray colors of ejecta observed in aerial photographs.

Table 9b: Coverage area and height of ejecta estimates for Patch B using photographs.

Earthquake Event	$H_{E,thin}$ (mm)	$A_{E,thin}$ (m^2)	$H_{E,thick}$ (mm)	$A_{E,thick}$ (m^2)	A_T (m^2)
Sep-10	0	0	0	0	28.0
Feb-11	20-40	8.9	100-160	19.1	28.0
Jun-11	0	0	0	0	28.0
Dec-11	0	0	0	0	28.0

Notes: $A_{E,thick/thin}$ = Coverage area of thick/thin ejecta layers; $H_{E,thick/thin}$ = Lower-upper estimate of height of thick/thin ejecta layers; A_T = Total assessment area of a buffer being considered; Thin and thick layers correspond to light gray and dark gray colors of ejecta observed in aerial photographs.

Table 9c: Coverage area and height of ejecta estimates for Road within the 50-m buffer using photographs.

Earthquake Event	Sep-10	Feb-11	Jun-11	Dec-11
$H_{E,thin1}$ (mm)	0	3-6	3-6	0
$A_{E,thin1}$ (m^2)	0	60.7	1083	0
$H_{E,thin2}$ (mm)	0	5-10	0	5-10
$A_{E,thin2}$ (m^2)	0	66.9	0	45.3
$H_{E,thick1}$ (mm)	0	8-16	0	0
$A_{E,thick1}$ (m^2)	0	33.9	0	0
$H_{E,thick2}$ (mm)	0	15-25	15-25	15-25
$A_{E,thick2}$ (m^2)	0	32.5	38.5	21.3
$H_{E,prism}$ (mm)	0	10-270	14-259	12-260
$V_{E,prism}$ (m^3)	0	5.69-11.1	8.32-15.3	6.44-11.6
$H_{E,t.prism1}$ (mm)	0	134-269	0	0
$H_{E,t.prism2}$ (mm)	0	15-25	0	0
$V_{E,t.prism}$ (m^3)	0	2.49-4.39	0	0
$H_{E,cone}$ (mm)	0	0	150-200	0
$A_{E,half\text{-}cone}$ (m^2)	0	0	10	0
$H_{E,cc}$ (mm)	0	0	421-566	0
$V_{E,cc}$ (m^3)	0	0	1.72	0
A_T (m^2)	1491	1438*	1377*	1491

Notes: $A_{E,thin/thick}$ = Coverage area of thin/thick ejecta layers; $H_{E,\ thin/thick}$ = Lower-upper estimate of height of thin/thick ejecta layers; $H_{E,prism}$ = Lower-upper estimate of ejecta height near the curb based on 2-4% cross slope of normal crown; $V_{E,prism}$ = Lower-upper estimate of total volume of prismatic-shape ejecta; $A_{E,cone}$ = Coverage area of conically shaped ejecta layers; $H_{E,t.prism1/2}$ = Lower-upper estimate of height of sides of ejecta layers shaped as a trapezoidal prism; $V_{E,t.prism}$ = Volume of ejecta layers shaped as a trapezoidal prism; ; $H_{E,cone}$ = Lower-upper estimate of height of conically shaped ejecta layers; $V_{E,cc}$ = Volume of conically shaped ejecta pile components; $H_{E,cc}$= Lower-upper estimate of height of conically shaped ejecta pile components (based on the repose angle of 30°); A_T= Total assessment area of a buffer being considered; * indicates the reduction in A_T due to the presence of objects within the assessment area.

Note 4: The values in Table 9 correspond to the coverage area of ejecta outlined in aerial photographs (Figures 85 through 89) and the lower and upper estimates of ejecta height based on geometry, ground photographs (Figure 90), and EQC LDAT property inspection notes (Figures 91 and 92) and reports from Aug 2011 (100-200 mm in height of ejected material near Patch B). The ejecta-induced settlement using photographs and engineering judgment, $S_{E,P}$, is estimated as

$$S_{E,P} = \frac{\sum_{i=1}^{a} A_{E,thick,i} * H_{E,thick,i} + \sum_{j=1}^{b} A_{E,thin,j} * H_{E,thin,j} + \frac{1}{3}\sum_{l=1}^{d} A_{E,cc,l} * R_{E,cc,l} * tan30°}{A_T}$$
$$+ \frac{\frac{1}{3}\sum_{m=1}^{e} A_{E,cone,m} * H_{E,cone,m} + \frac{1}{2}\sum_{n=1}^{f} W_{E,prism,n} * H_{E,prism,n} * L_{E,prism,n}}{A_T}$$
$$+ \frac{\frac{1}{2}\sum_{p=1}^{g} W_{E,t.prism,p} * L_{E,t.prism,p} * \left(H_{E,t.prism1,p} + H_{E,t.prism2,p}\right)}{A_T}$$
$$= \frac{\sum_{i=1}^{a} V_{E,thick,i} + \sum_{j=1}^{b} V_{E,thin,j} + \sum_{l=1}^{d} V_{E,conical\ component,l}}{A_T}$$
$$+ \frac{\sum_{m=1}^{e} V_{E,cone,m} + \sum_{n=1}^{f} V_{E,prism,n} + \sum_{p=1}^{g} V_{E,t.prism,p}}{A_T}$$

where

- $A_{E,thick,i}$ and $H_{E,thick,i}$ are the area and the height of a thick ejecta layer, respectively;
- $A_{E,thin,j}$ and $H_{E,thin,j}$ are the area and the height of a thin ejecta layer, respectively;
- $A_{E,cc,l}$ and $R_{E,cc,l}$ are the area and the radius of an ejecta pile component, respectively, shaped as a cone with the repose angle of 30°;
- $A_{E,cone,m}$ and $H_{E,cone,m}$ are the area and the height of a conically shaped ejecta, respectively;
- $W_{E,prism,n}$ and $L_{E,prism,n}$ are the width and the length of the coverage area of a prismatically shaped ejecta layer, respectively, and $H_{E,prism,n}$ is the height of a prism-like ejecta layer;
- $W_{E,t.prism,p}$ and $L_{E,t.prism,p}$ are the width and the length, respectively, of the coverage area of an ejecta layer shaped as a trapezoidal prism, and $H_{E,t.prism,p}$ is the height of a trapezoidal prism ejecta layer;
- A_T is the total assessment area for a buffer being considered (Figure 1).

Table 10: Ejecta-induced settlement estimates for Patches A and B and Road based on photographs.

EQ Event	Patch A (10-, 20-, and 50-m buffers)		Patch B (50-m buffer)		Road (50-m buffer)	
	$S_{E,P,lower}$ (mm)	$S_{E,P,upper}$ (mm)	$S_{E,P,lower}$ (mm)	$S_{E,P,upper}$ (mm)	$S_{E,P,lower}$ (mm)	$S_{E,P,upper}$ (mm)
Sep-10	0	0	0	0	0	0
Feb-11	0	0	75	122	7	12
Jun-11	0	0	0	0	10	18
Dec-11	0	0	0	0	5	9

Note: $S_{E,P,lower}$ and $S_{E,P,upper}$ correspond to lower and upper estimates of $S_{E,P}$, respectively.

Table 11: Best final estimates of ejecta-induced settlement for Patches A and B and Road.

EQ Event	Patch A (10-, 20-, and 50-m buffers)			Patch B (50-m buffer)			Road (50-m buffer)		
	$S_{E,L}$ (mm)	$S_{E,P}$ (mm)	$S_{E,final}$ (mm)	$S_{E,L}$ (mm)	$S_{E,P}$ (mm)	$S_{E,final}$ (mm)	$S_{E,L}$ (mm)	$S_{E,P}$ (mm)	$S_{E,final}$ (mm)
Sep-10	-70±127	0	0	-49±176	0	0	-13±127	0	0
Feb-11	123±71	0	0	93±90	99±23	95±35	146±71	9.5±2.5	25±10
Jun-11	20±56	0	0	78±79	0	0	76±56	14±4	20±5
Dec-11	-39±90	0	0	-77±112	0	0	-47±90	7±2	10±5

Notes: $S_{E,L}$ = Ejecta-induced settlement based on LiDAR data reported in Table 8; $S_{E,P}$ = Median ejecta-induced settlement for the range of values reported in Table 10; $S_{E,final}$ = Best final estimate of ejecta-induced settlement rounded to the nearest 5; Final plus/minus values are also rounded to the nearest 5.

Note 5:

- $S_{E,final}$ for Patch A is based solely on $S_{E,P}$ for all earthquake events. For Patch B, $S_{E,final}$ is equal to $S_{E,P}$ for the Sep-10, Jun-11, and Dec-11 EQs, while $S_{E,final}$ for the Feb-11 EQ is the weighted average of $S_{E,L}$ and $S_{E,P}$ with weights of 1/3 and 2/3, respectively.
- $S_{E,final}$ for Road is the weighted average of $S_{E,L}$ and $S_{E,P}$ with weights of 0.1 and 0.9, respectively, for the Feb-11 and Jun-11 EQs. For the Sep-10 and Dec-11 EQs, $S_{E,final}$ is based on $S_{E,P}$ only.
- The uncertainty associated with $S_{E,final}$ is also the weighted average of uncertainties associated with $S_{E,L}$ and $S_{E,P}$ with the same corresponding weights.
- The weights are based on the LiDAR error bands, LPI prediction error (Maurer et al. 2014[3]), presence of ejecta at the time of LiDAR surveys, and completeness of visual evidence (i.e., ground and aerial photographs and EQC LDAT property inspection reports for the site). The Bower Ave site is in the apparent zone of higher ground surface subsidence for the Sep-10 EQ and the apparent zone of lower ground surface subsidence for the Feb-11 EQ (i.e., the Jul-03 and Sep-10 LiDAR flight errors). The site is also in the zone of slight to moderate LPI overprediction of liquefaction severity for the Sep-10 and Feb-11 EQs. The LDAT property inspection report is available for Patches A and B. The height of ejecta at the property with Patch B was measured as 100-200 mm in Oct 2011. There are no ground photographs of the road.
- Ejecta did not occur within either Patch A or Patch B as a result of the Jun-11 EQ; however, it occurred at several properties (the N portion of the 20-m and 50-m buffers and the SW quadrant of the 50-m buffer).

Summary:

- **The best estimate of the ejecta-induced free-field ground settlement at the Bower Ave site for the SEP 2010, FEB 2011, JUN 2011, and DEC 2011 earthquake is 0 mm, 95±35 mm, 0 mm, and 0 mm, respectively.**

[3] Maurer, B. W., Green, R. A., Cubrinovski, M., & Bradley, B. A. (2014). Evaluation of the Liquefaction Potential Index for Assessing Liquefaction Hazard in Christchurch, New Zealand. *Journal of Geotechnical and Geoenvironmental Engineering*, 140(7), 04014032-1-11. doi:10.1061/(asce)gt.1943-5606.0001117

- **The best estimate of the ejecta-induced settlement of the road at the Bower Ave site for the SEP 2010, FEB 2011, JUN 2011, and DEC 2011 earthquake is 0 mm, 25±10 mm, 20±5 mm, and 10±5 mm, respectively.**

Note 6: CPT 3937 was initially named as CC LIQ 4.

Figure 7: Location of the site.

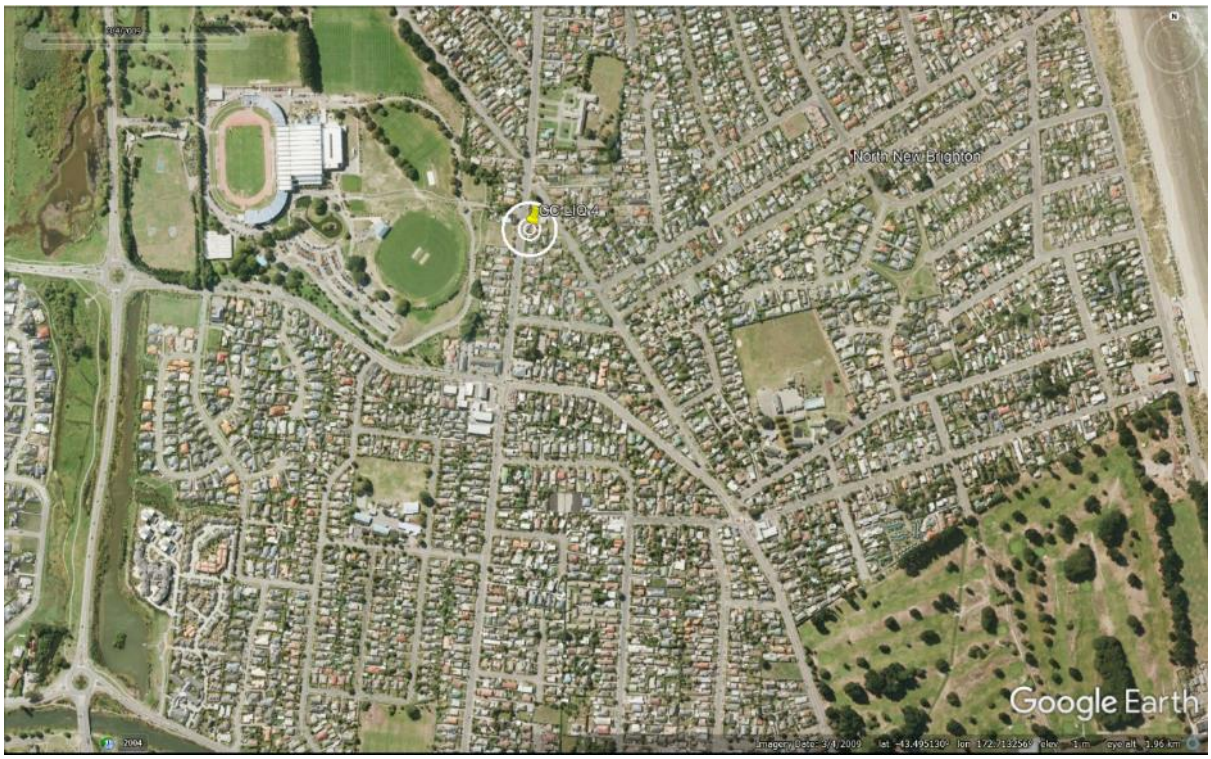

Figure 8: Position of the site relative to nearby buildings, vegetation, and free-face features.

Figure 9: Street view of the site showing flat land.

Figure 10: Satellite image of the site taken in Dec 2004.

Figure 11: Satellite image of the site taken in Mar 2009.

Figure 12: Satellite image of the site taken in Feb 2011.

Figure 13: Satellite image of the site taken in Mar 2011.

Figure 14: Satellite image of the site taken in Apr 2012.

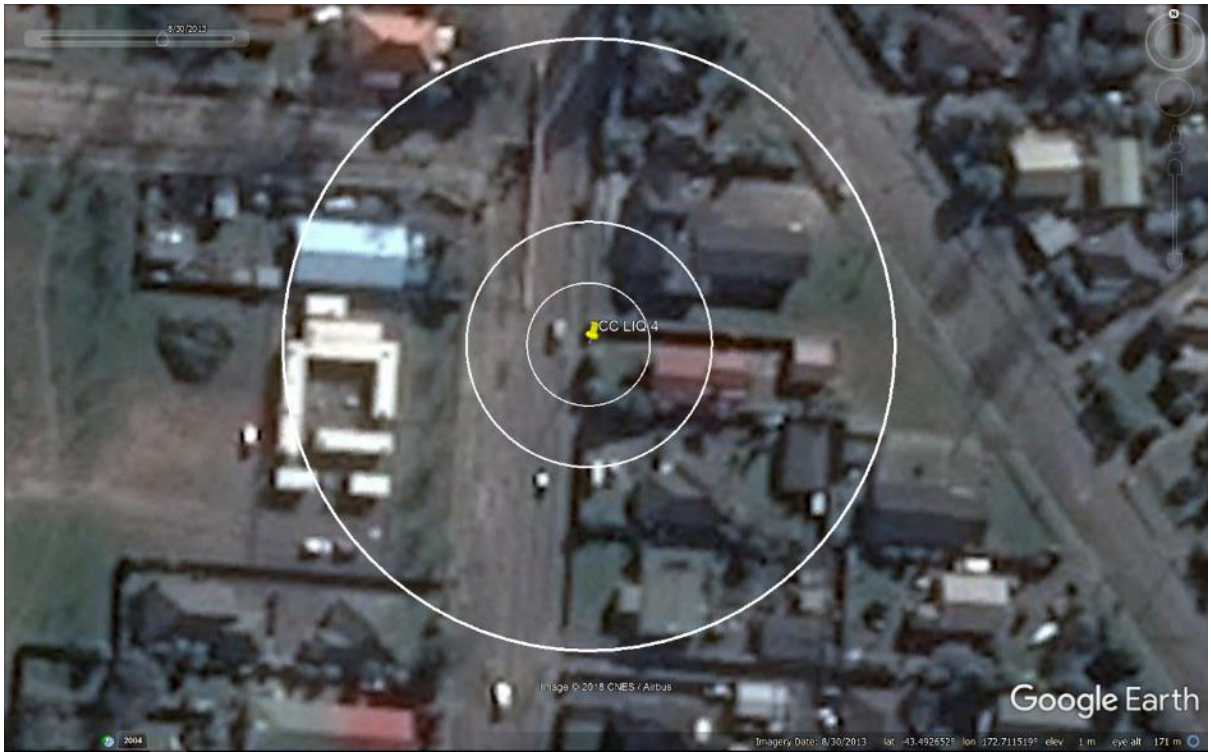

Figure 15: Satellite image of the site taken in Aug 2013.

Figure 16: Satellite image of the site taken in Sep 2013.

Figure 17: Satellite image of the site taken in Feb 2014.

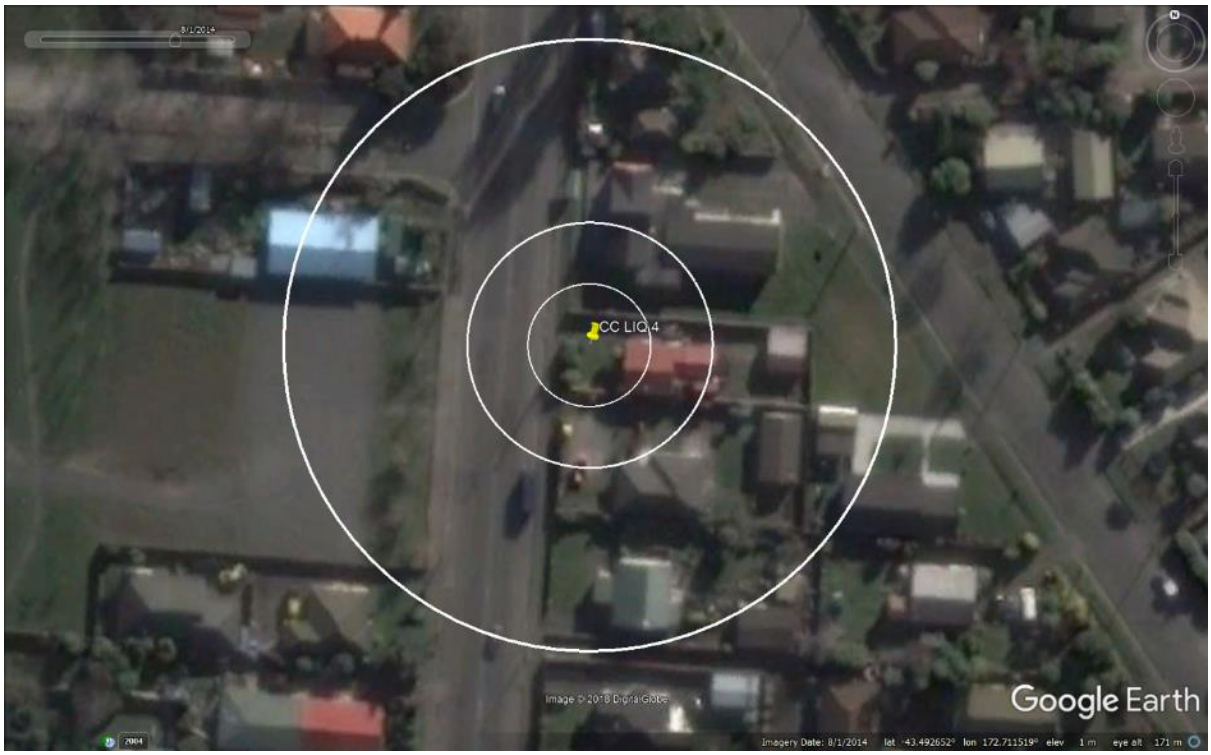

Figure 18: Satellite image of the site taken in Aug 2014.

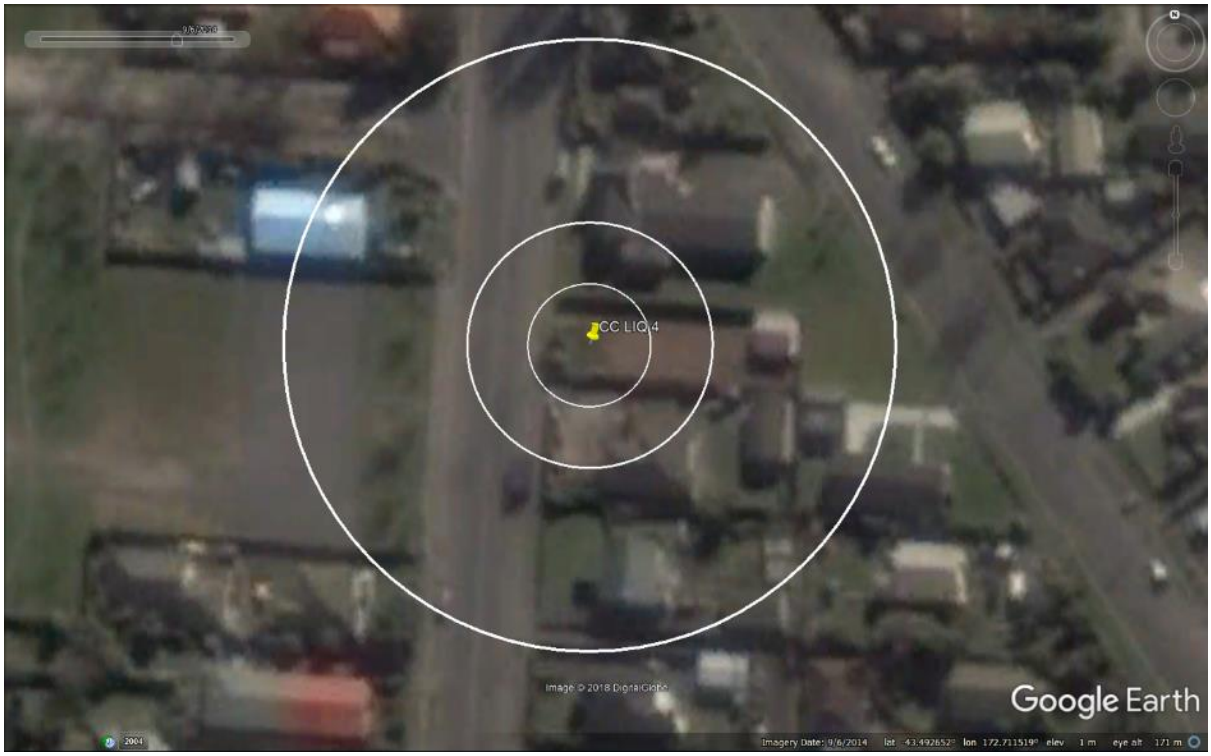

Figure 19: Satellite image of the site taken in Sep 2014.

Figure 20: Satellite image of the site taken in Jan 2015.

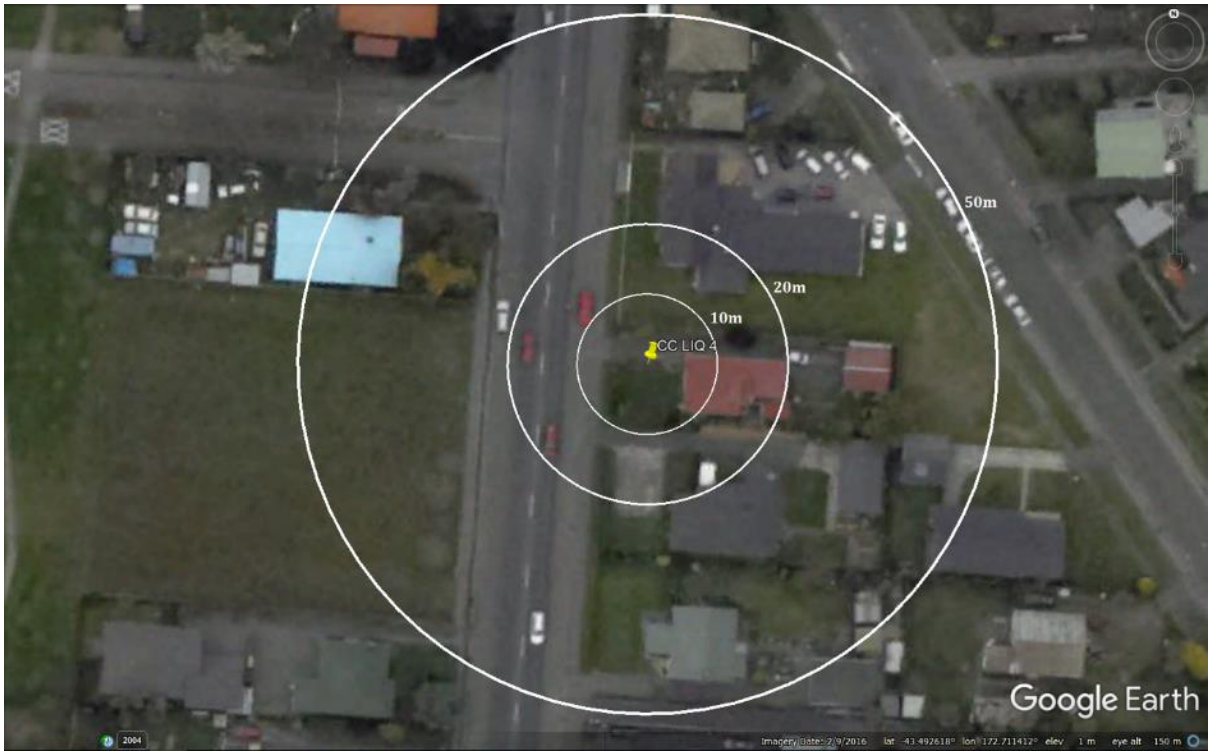

Figure 21: Aerial photograph of the site taken on Sep 4, 2010.

Figure 22: Aerial photograph of the site taken on Feb 24, 2011.

Figure 23: Aerial photograph of the site taken on June 14-15, 2011.

Figure 24: Aerial photograph of the site taken on Dec 24, 2012.

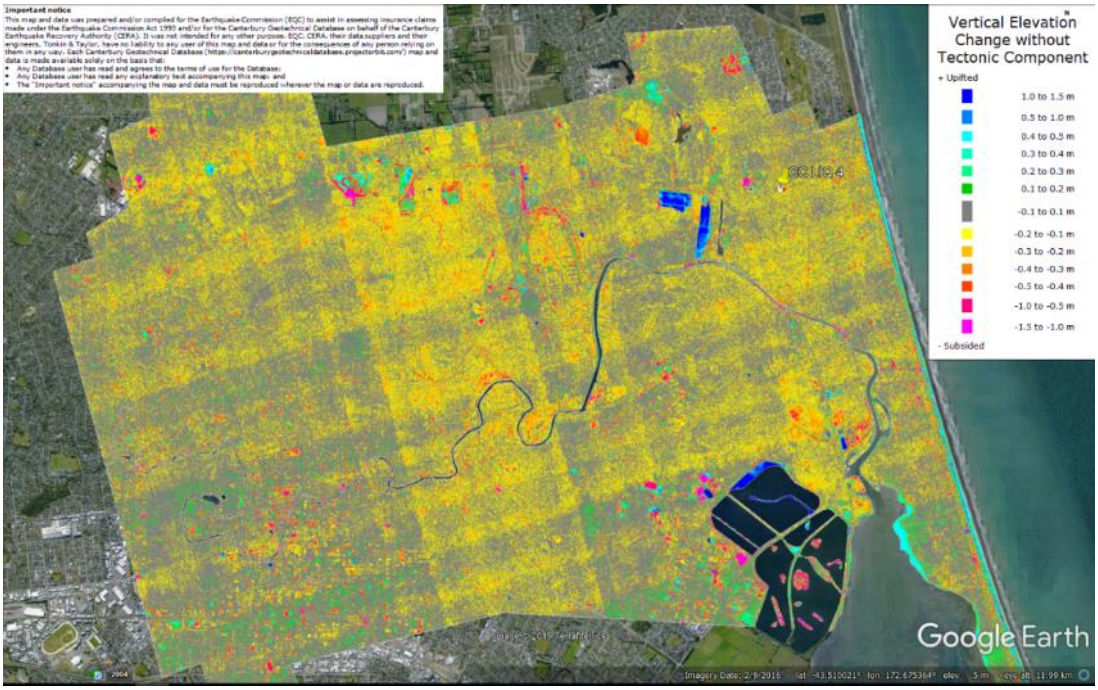

Figure 25: Vertical Ground Movements (Surface – Tectonic) for Sep 2010 Earthquake – the site is in the apparent zone of overestimated ground surface subsidence (i.e., Sep 2010 flight band error).

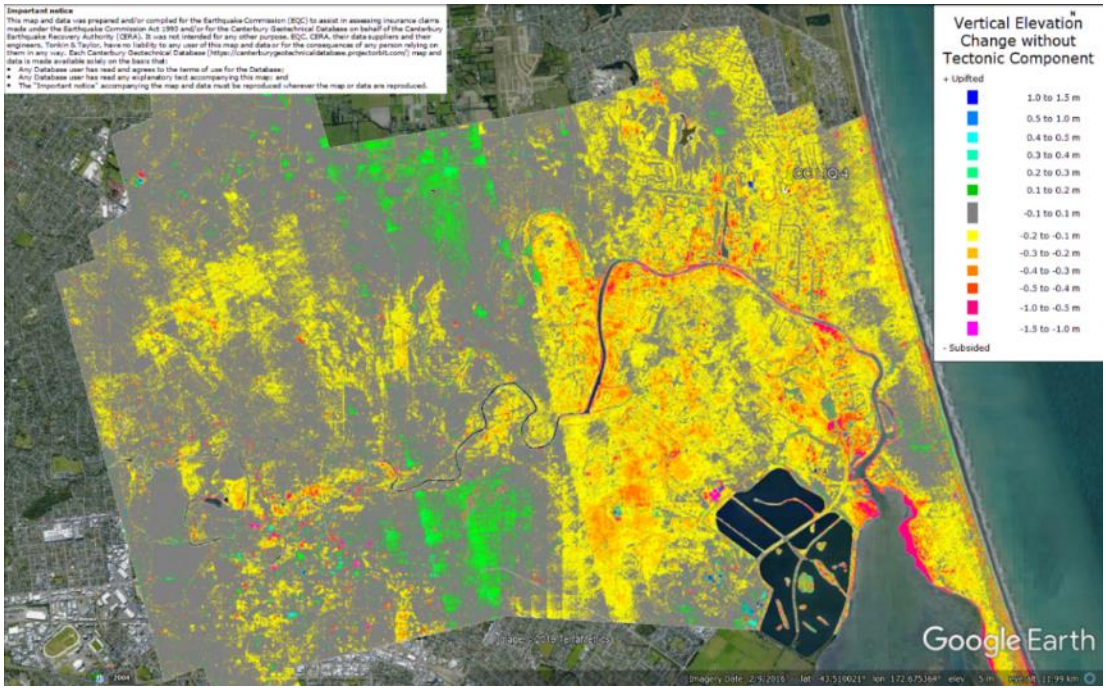

Figure 26: Vertical Ground Movements (Surface – Tectonic) for Feb 2011 Earthquake – the site is in the apparent zone of underestimated ground surface subsidence (i.e., Sep 2010 flight band error).

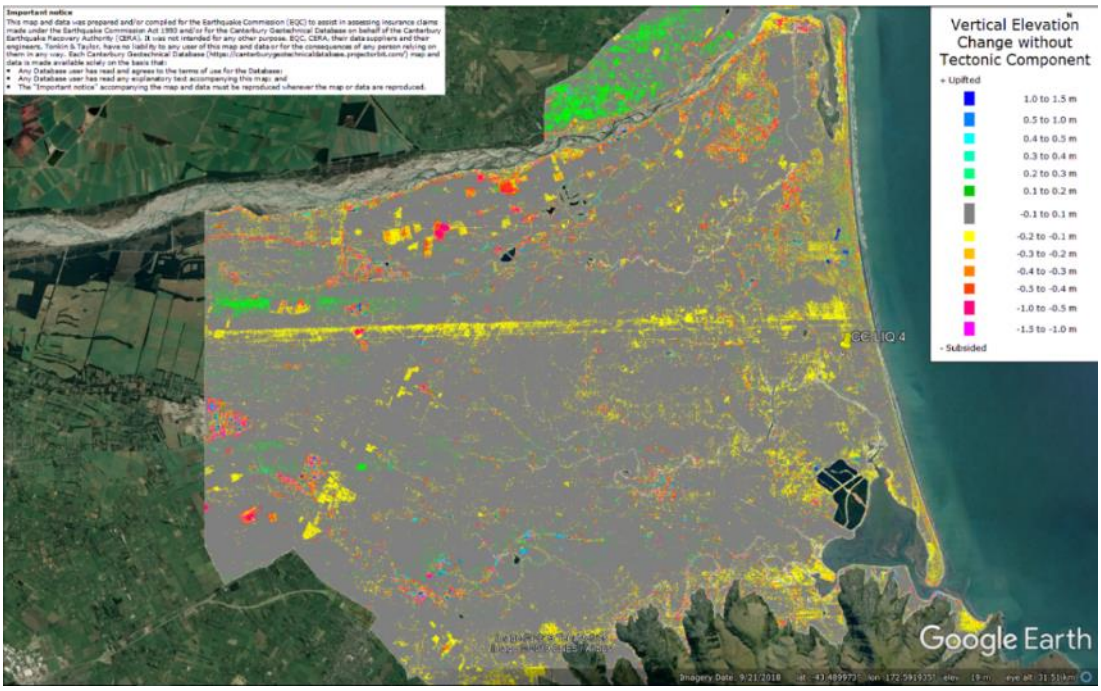

Figure 27: Vertical Ground Movements (Surface – Tectonic) for June 2011 Earthquake – the site is not in the apparent zone of overestimated or underestimated ground surface subsidence.

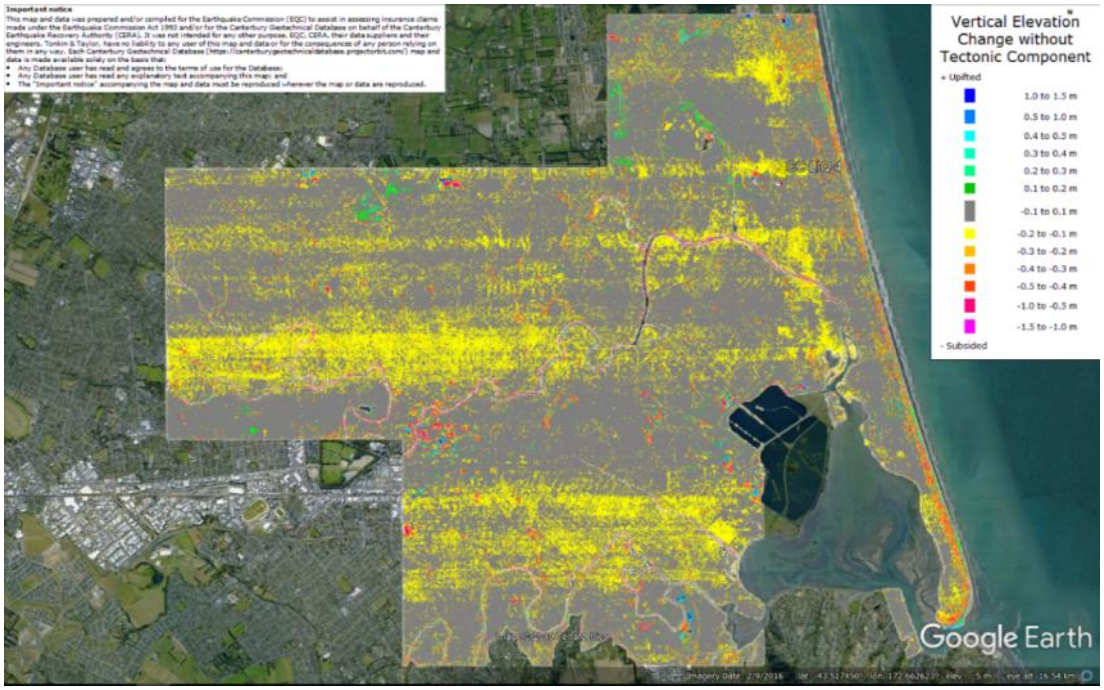

Figure 28: Vertical Ground Movements (Surface – Tectonic) for Dec 2011 Earthquake – the site is not in the apparent zone of overestimated or underestimated ground surface subsidence.

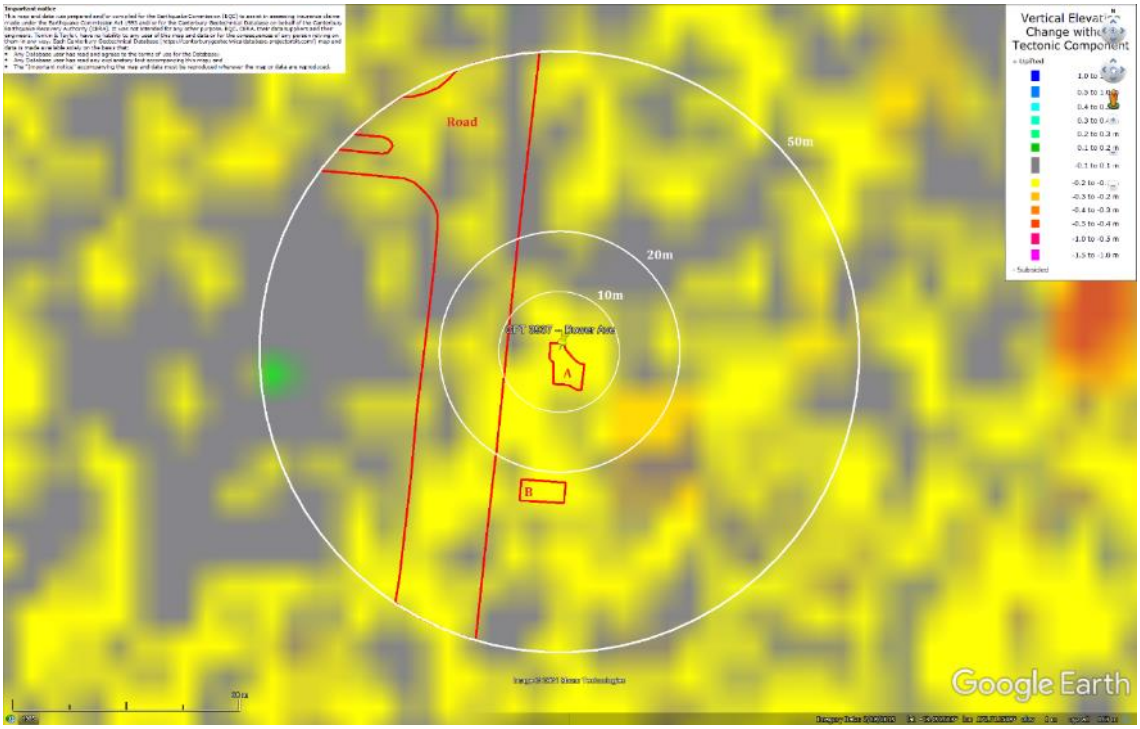

Figure 29: Ground surface subsidence without tectonic component for Sep 2010 Earthquake according to the LiDAR DEM.

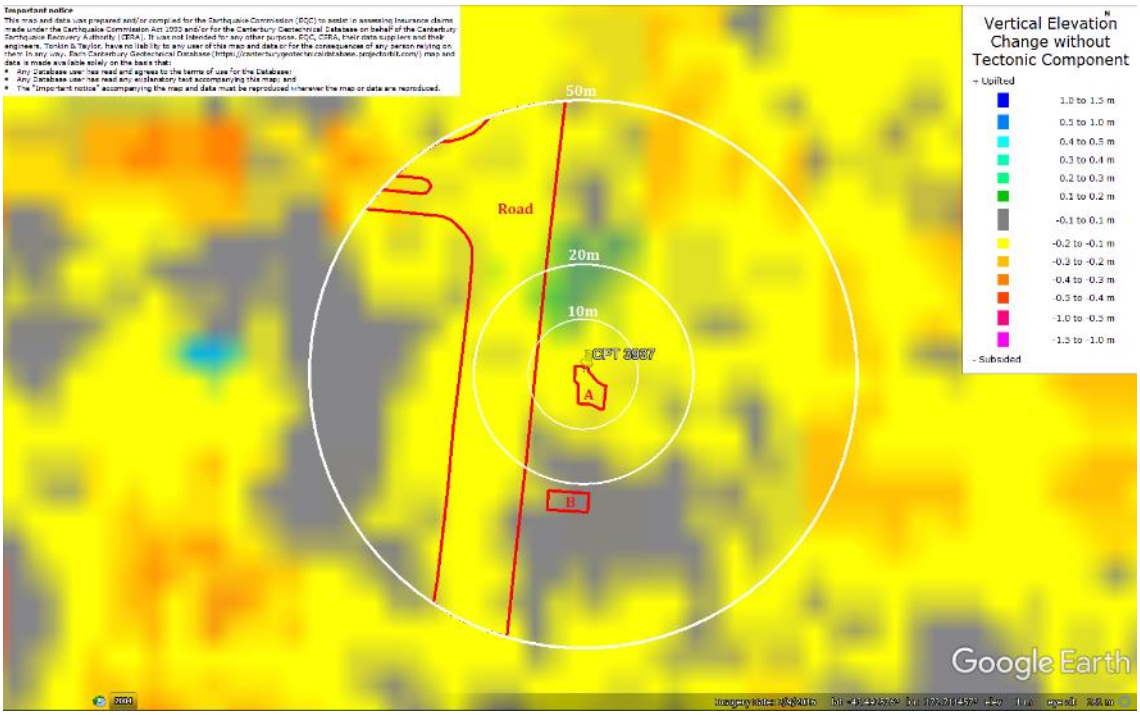

Figure 30: Ground surface subsidence without tectonic component for Feb 2011 Earthquake according to the LiDAR DEM.

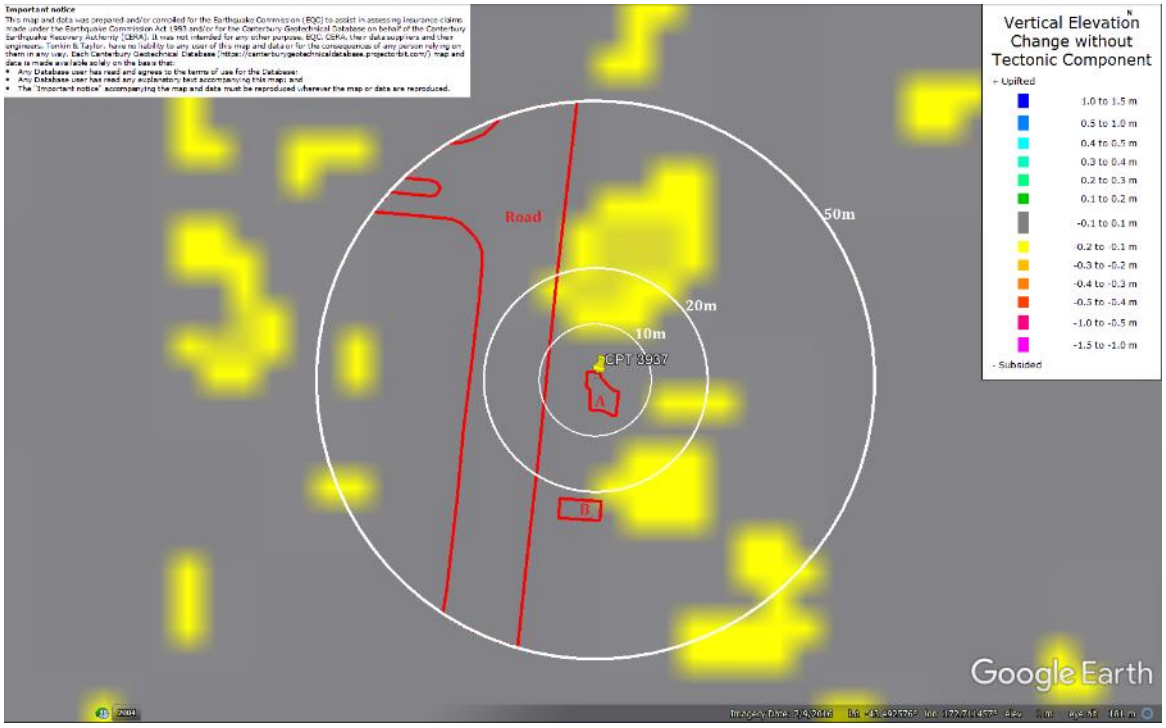

Figure 31: Ground surface subsidence without tectonic component for June 2011 Earthquake according to the LiDAR DEM.

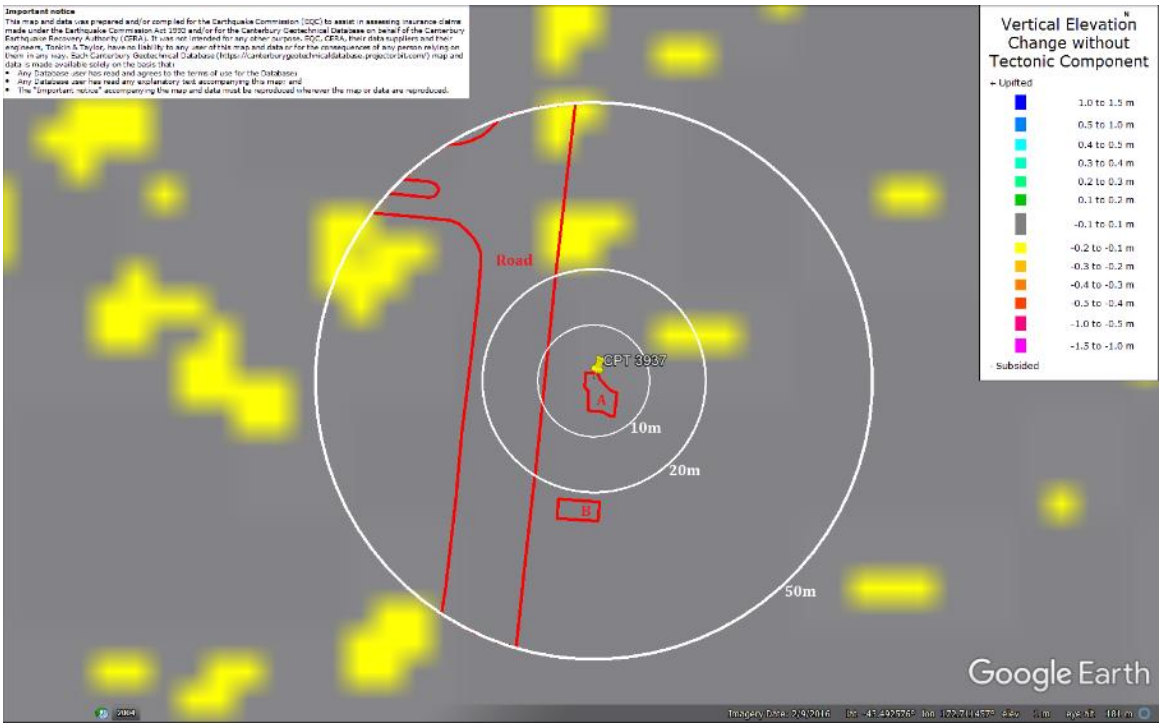

Figure 32: Ground surface subsidence without tectonic component for Dec 2011 Earthquake according to the LiDAR DEM.

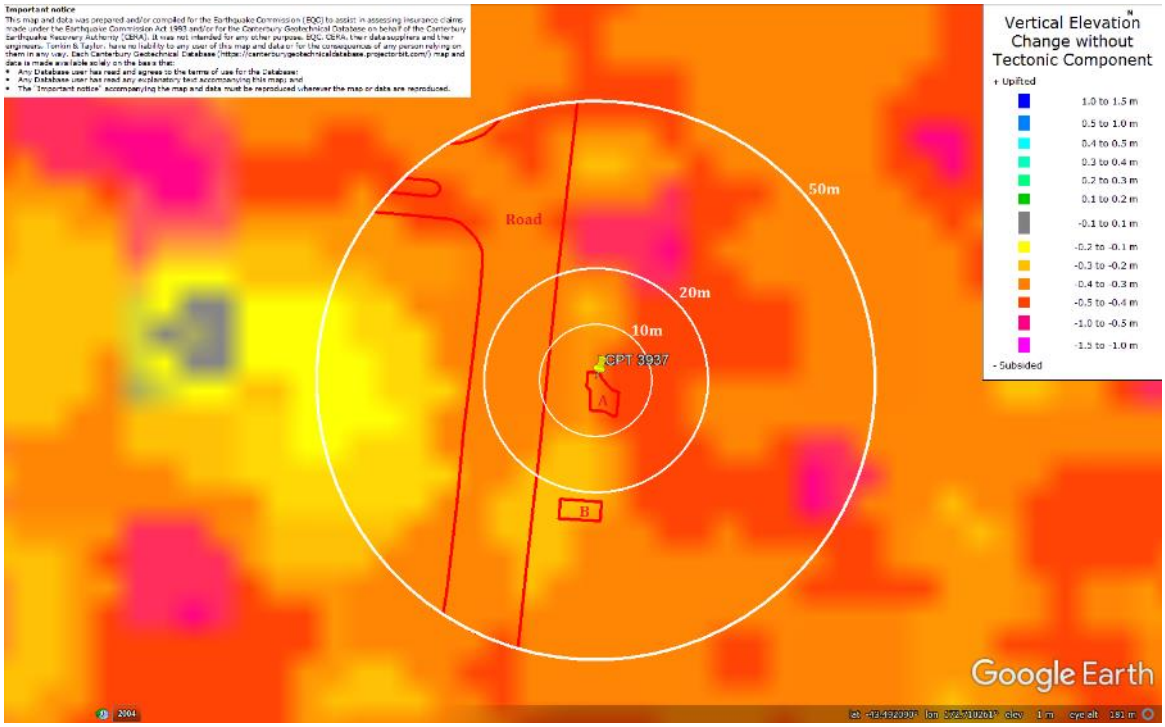

Figure 33: Ground surface subsidence without tectonic component for Canterbury Earthquake Sequence according to the LiDAR DEM.

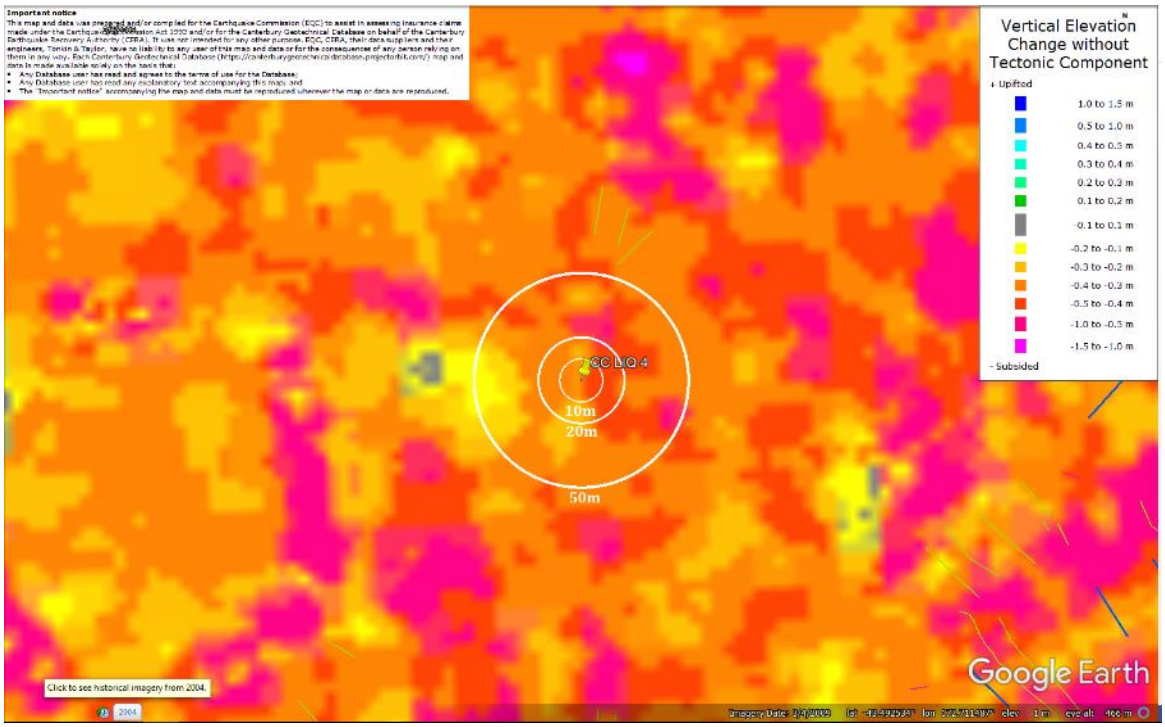

Figure 34: Absence of ground cracks indicating no lateral spreading for Canterbury Earthquake Sequence.

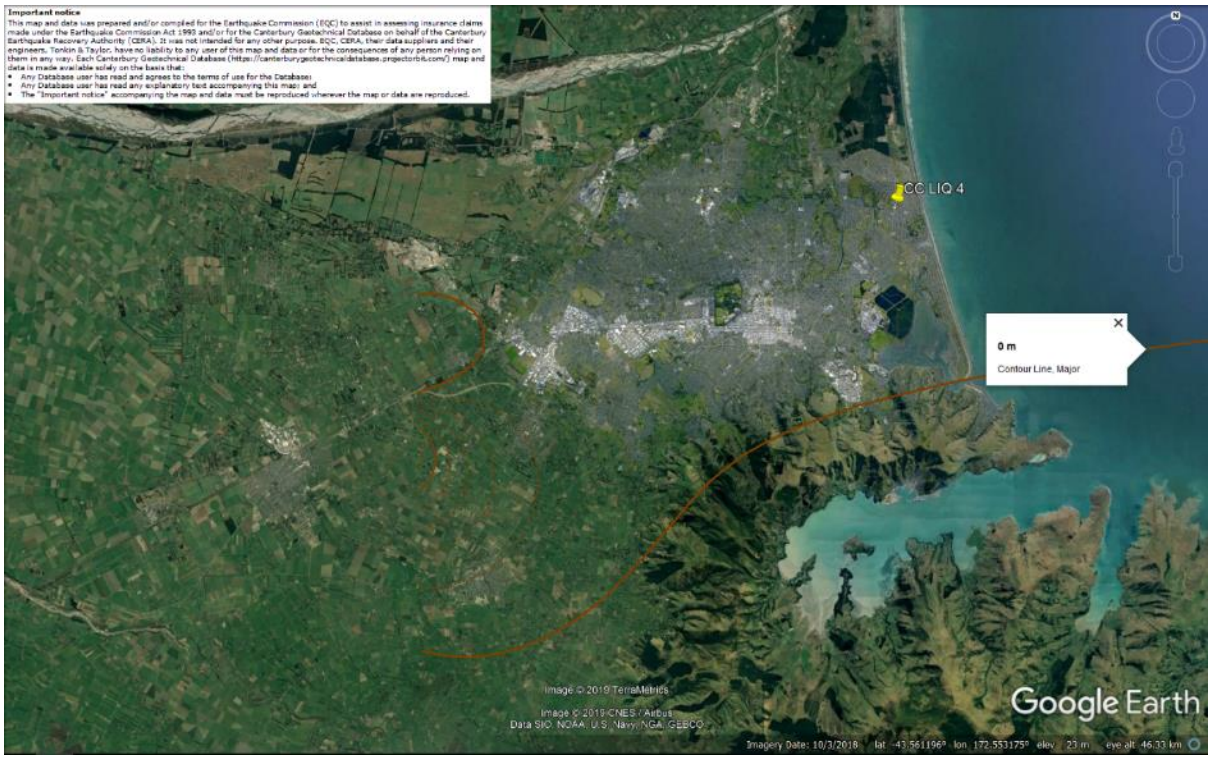

Figure 35: Vertical tectonic movements for Sep 2010 Earthquake.

Figure 36: Vertical tectonic movements for Feb 2011 Earthquake.

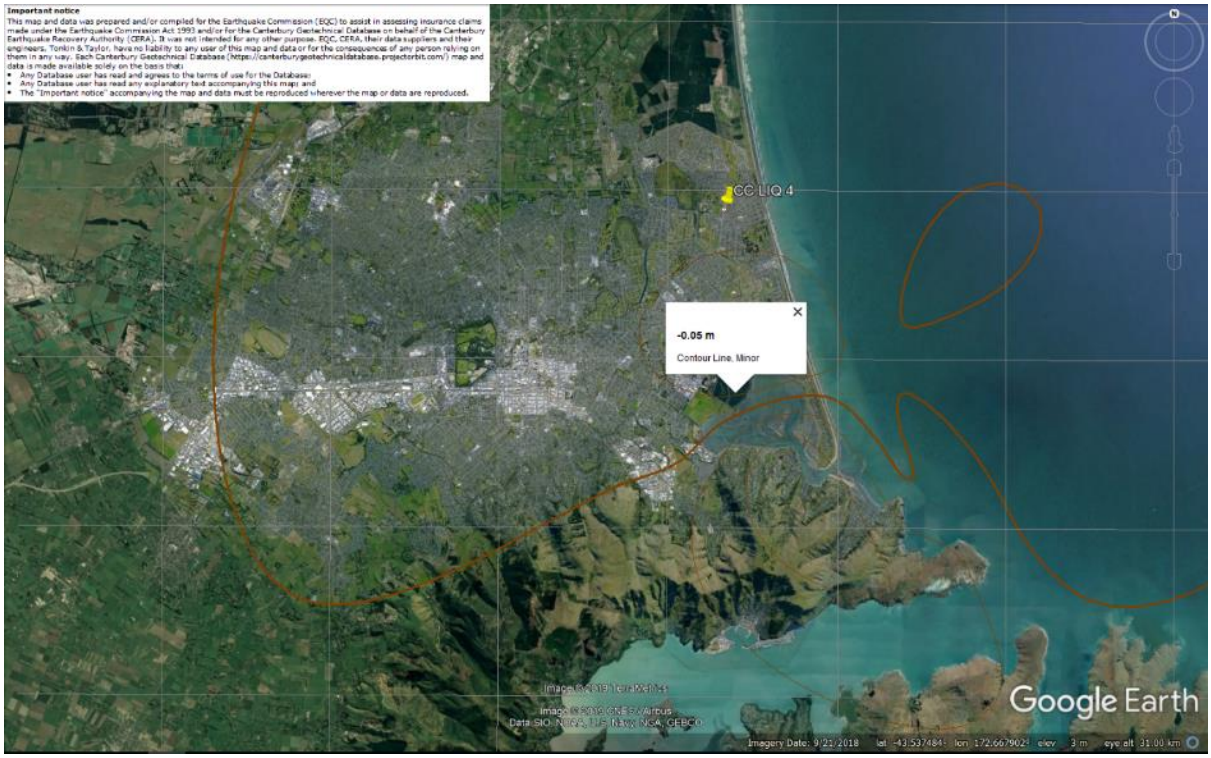

Figure 37: Vertical tectonic movements for June 2011 Earthquake.

Figure 38: Vertical tectonic movements for Dec 2011 Earthquake.

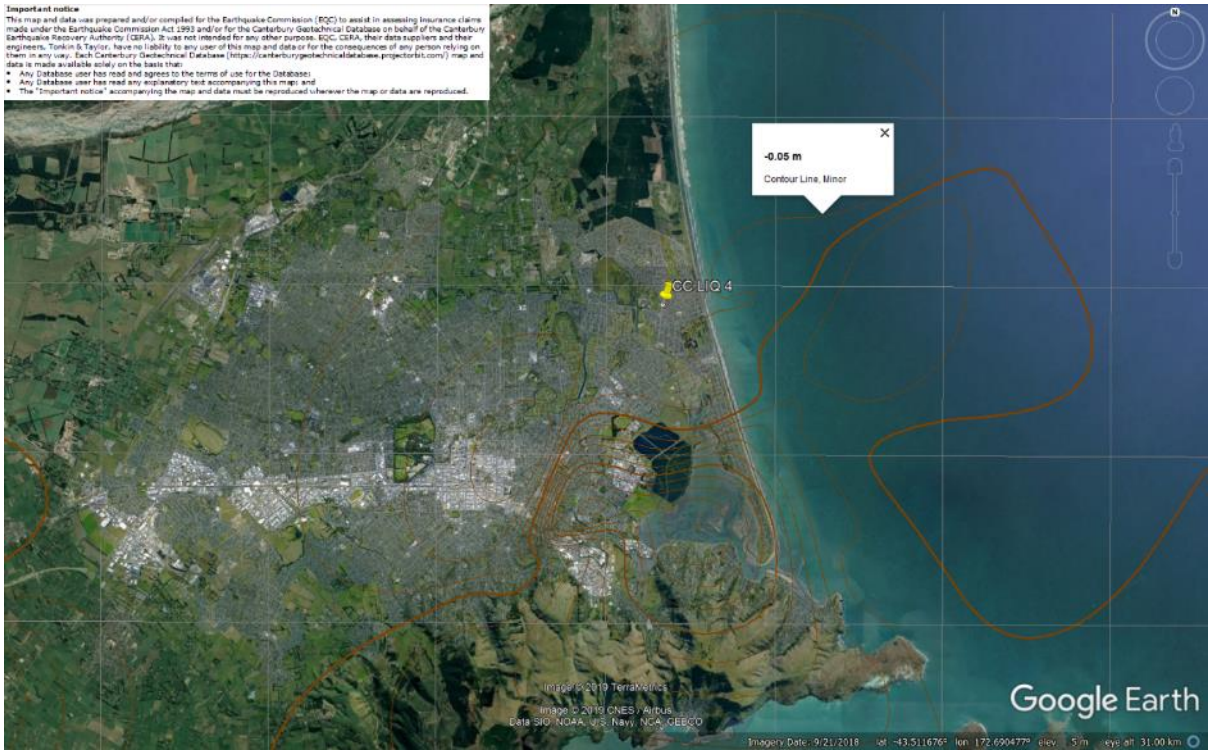

Figure 39: Vertical tectonic movements for Canterbury Earthquake Sequence.

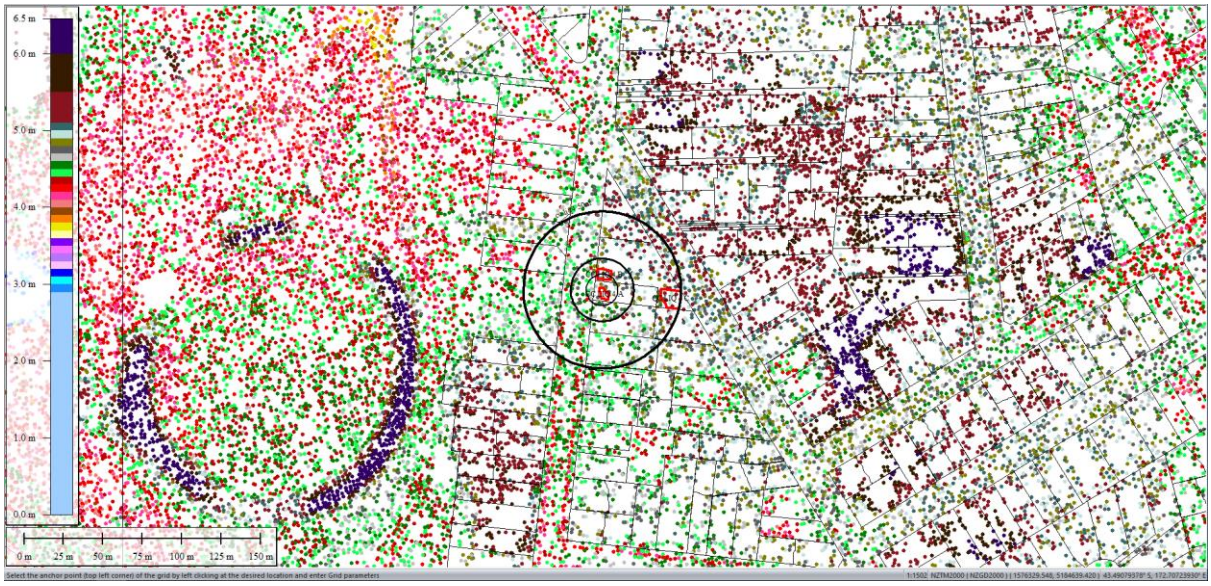

Figure 40: Jul 2003 LiDAR survey.

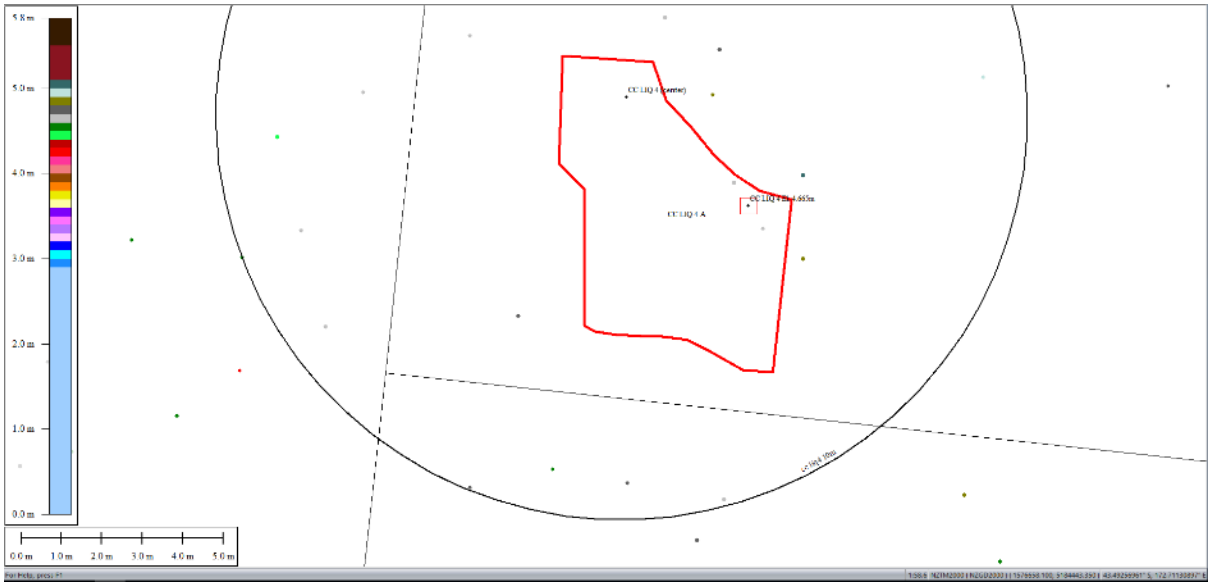

Figure 41: Ground surface elevation averaged over 10-m, 20-m, and 50-m buffers for Patch A for Jul 2003 LiDAR survey.

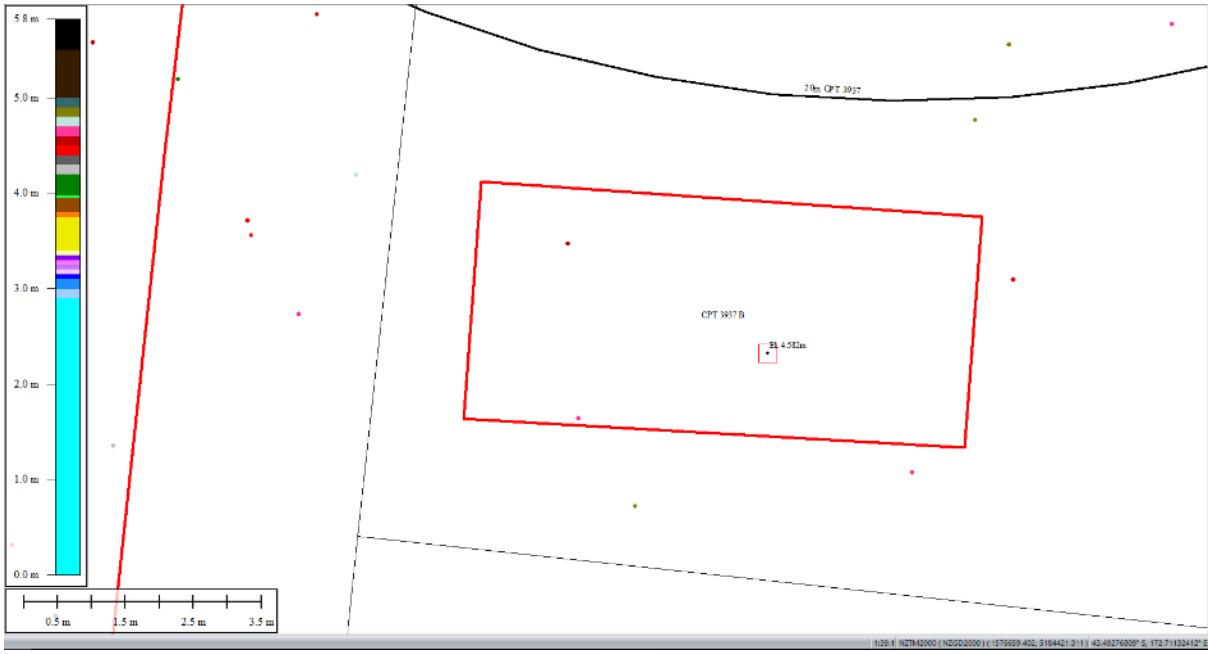

Figure 42: Ground surface elevation averaged over 50-m buffer for Patch B for July 2003 LiDAR survey.

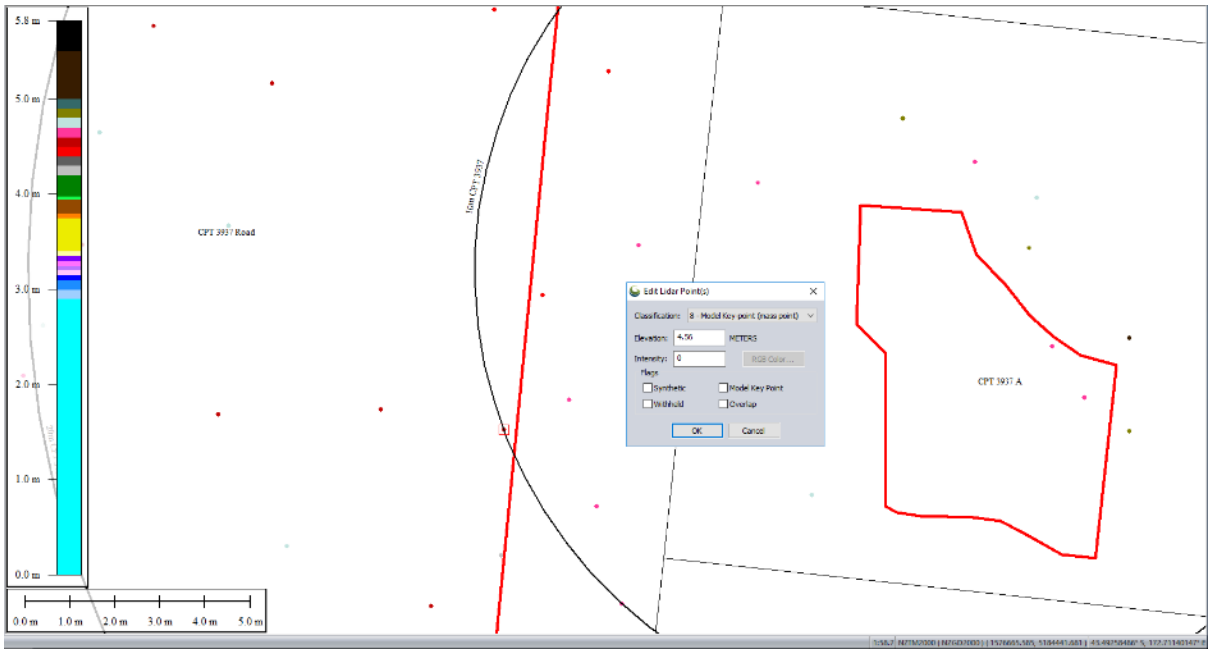

Figure 43: Ground surface elevation "averaged" over 10-m buffer for Road for July 2003 LiDAR survey.

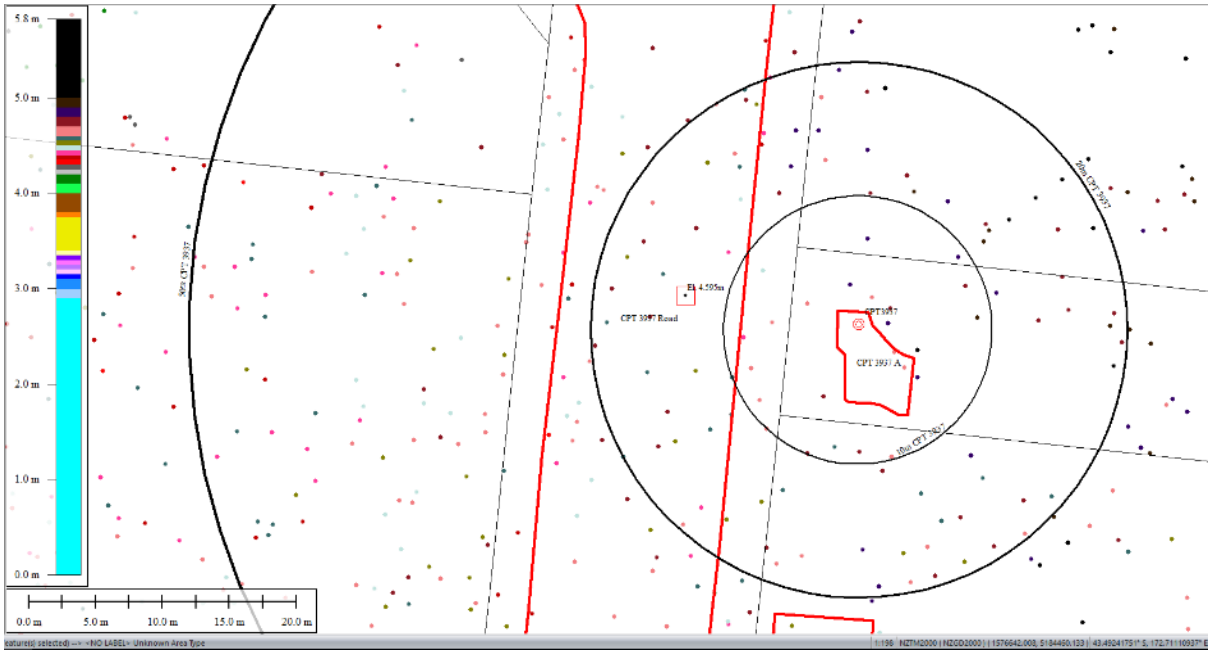

Figure 44: Ground surface elevation averaged over 20-m buffer for Road for July 2003 LiDAR survey.

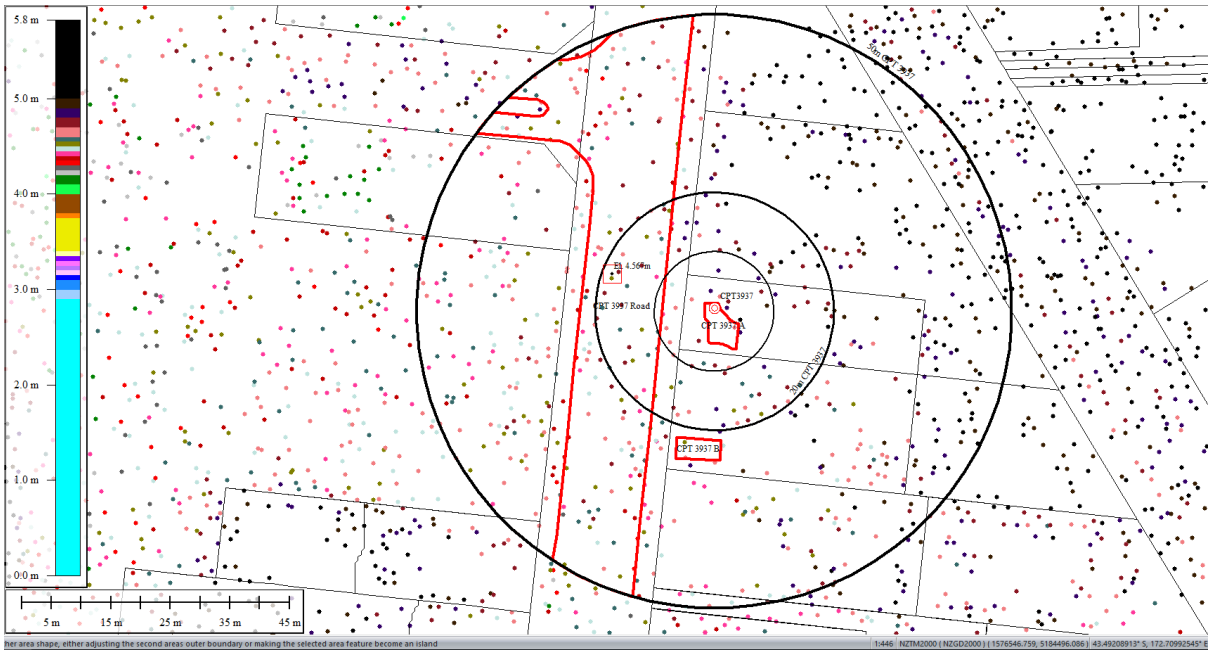

Figure 45: Ground surface elevation averaged over 50-m buffer for Road for July 2003 LiDAR survey.

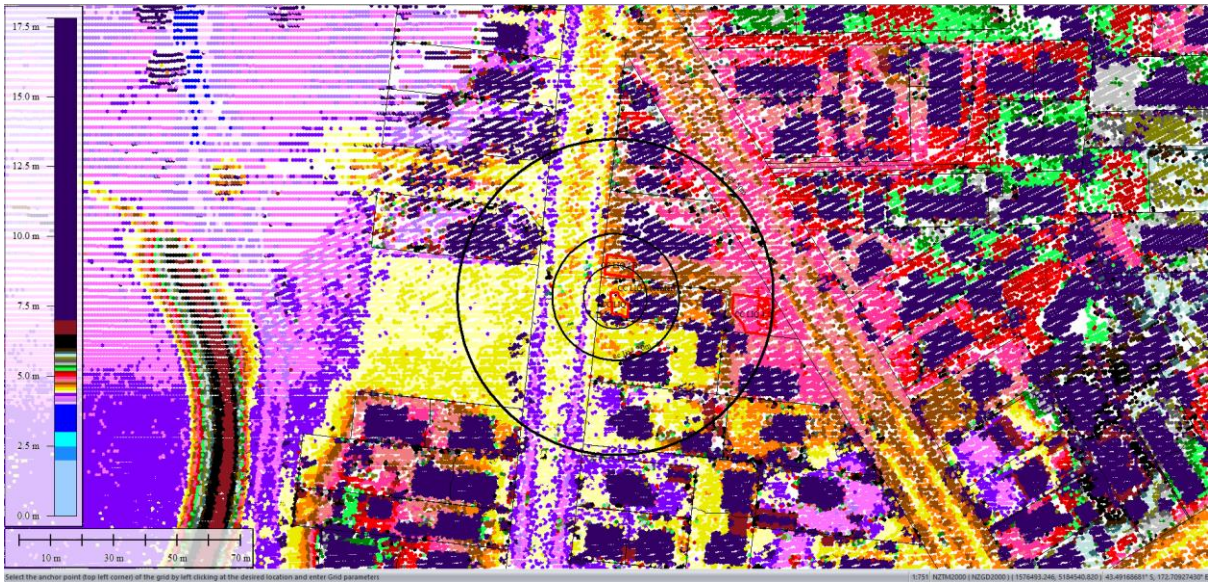

Figure 46: Sep 5, 2010 LiDAR survey.

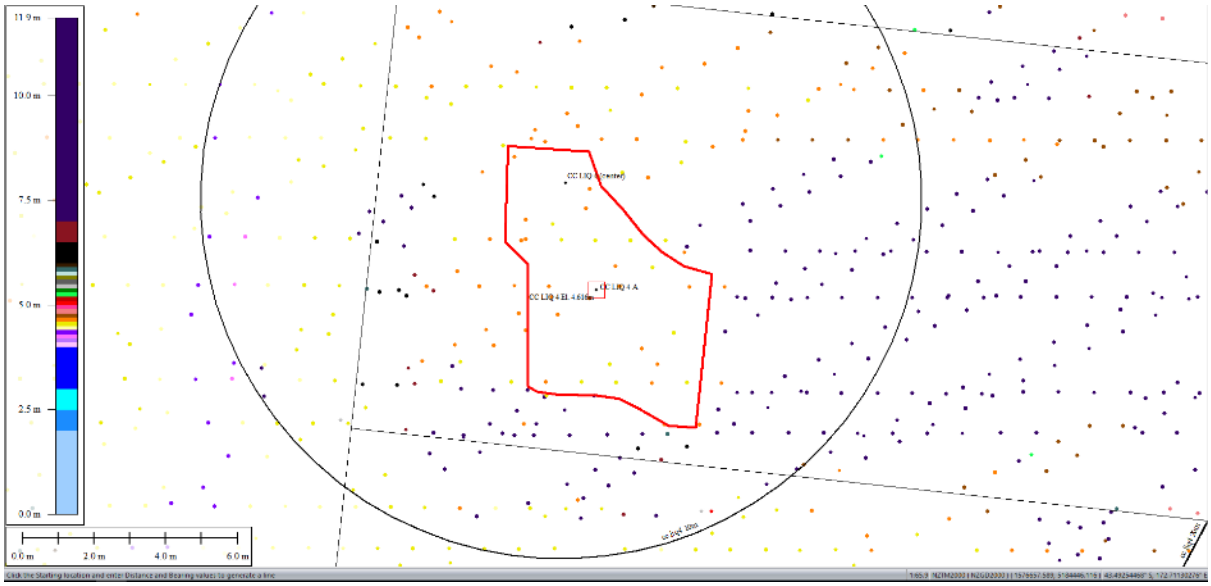

Figure 47: Ground surface elevation averaged over 10-m, 20-m, and 50-m buffers for Patch A for Sep 5, 2010 LiDAR survey.

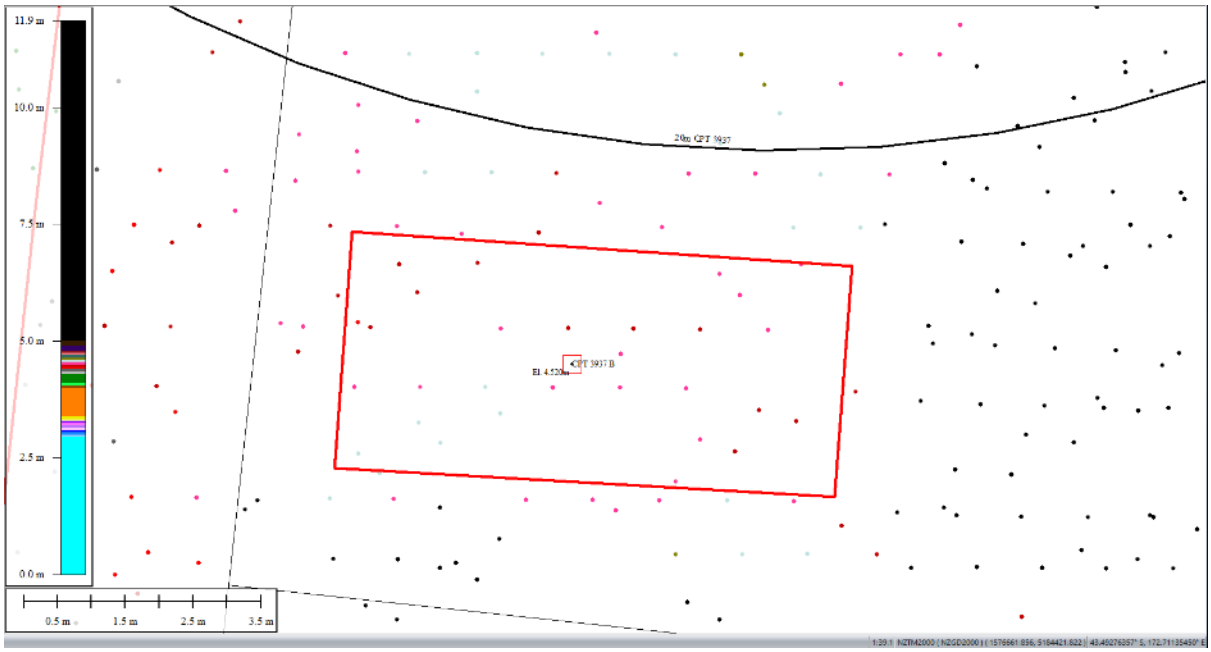

Figure 48: Ground surface elevation averaged over 50-m buffer for Patch B for Sep 5, 2010 LiDAR survey.

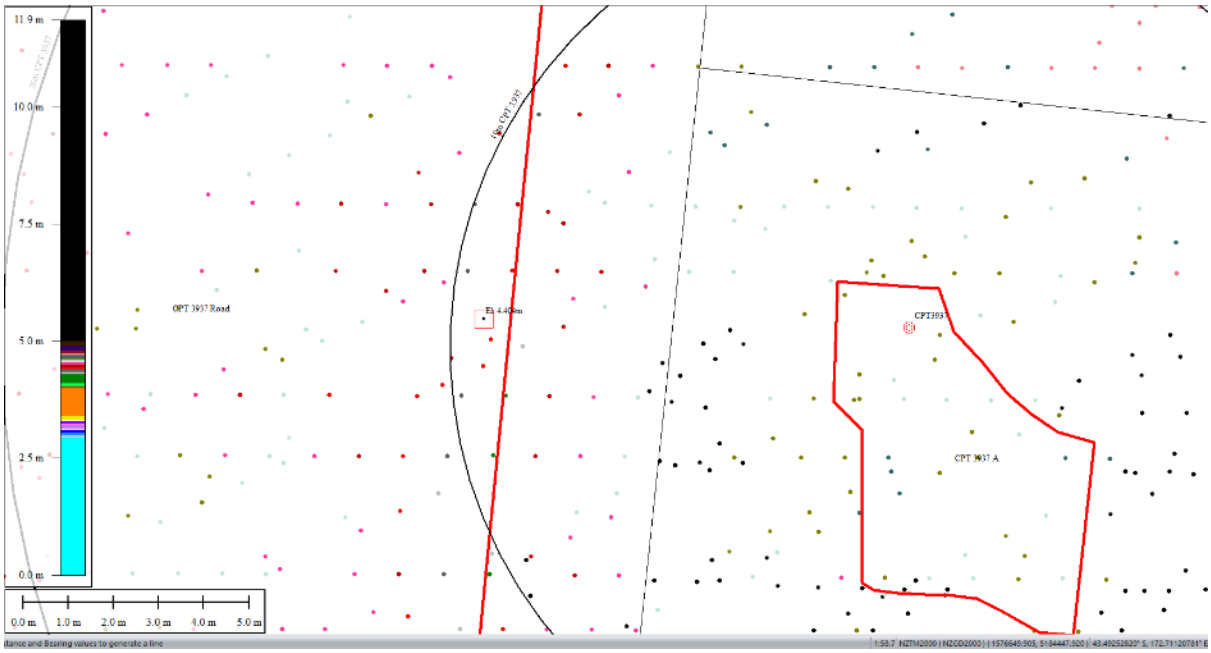

Figure 49: Ground surface elevation averaged over 10-m buffer for Road for Sep 5, 2010 LiDAR survey.

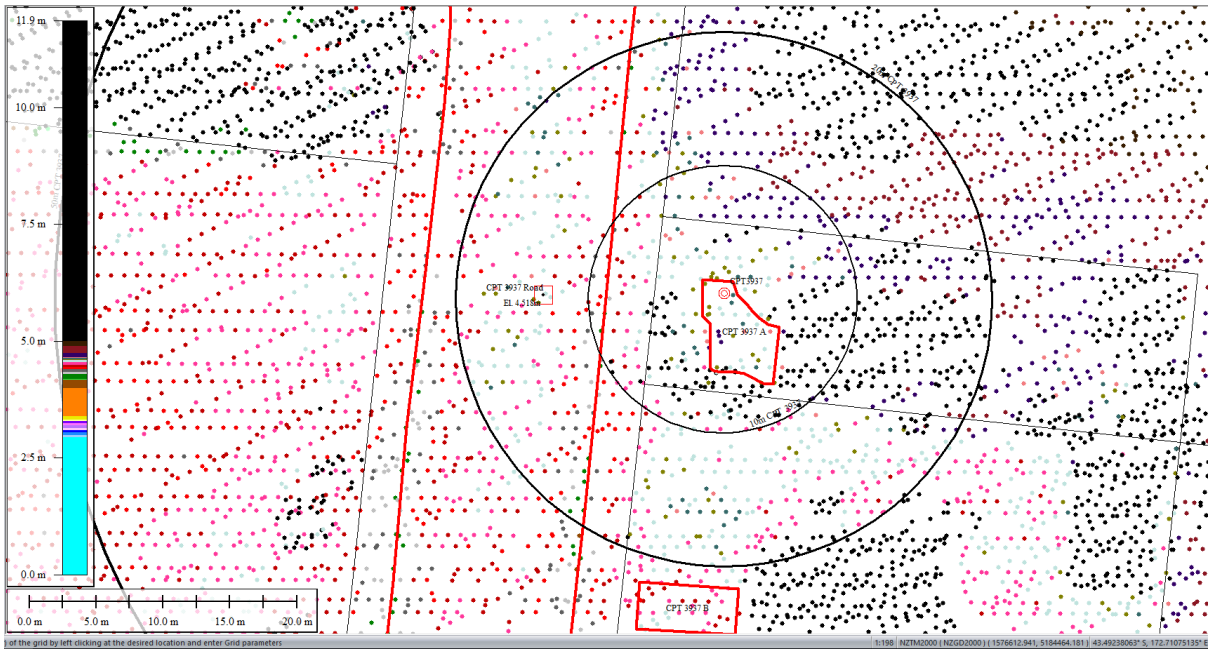

Figure 50: Ground surface elevation averaged over 20-m buffer for Road for Sep 5, 2010 LiDAR survey.

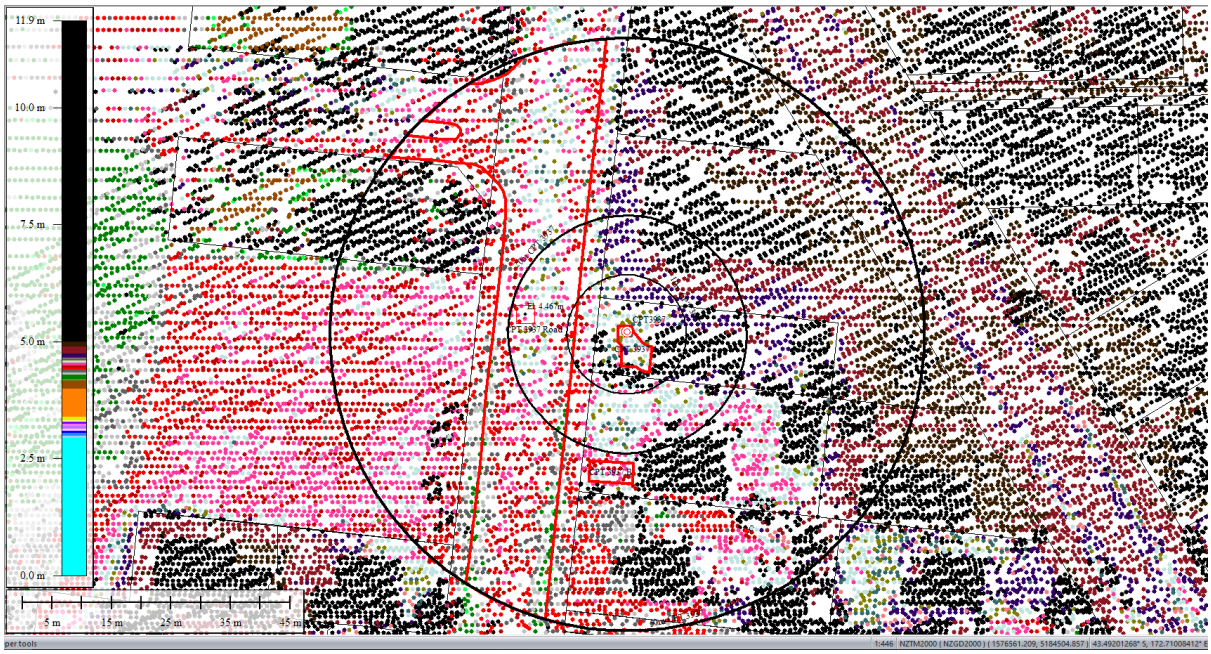

Figure 51: Ground surface elevation averaged over 50-m buffer for Road for Sep 5, 2010 LiDAR survey.

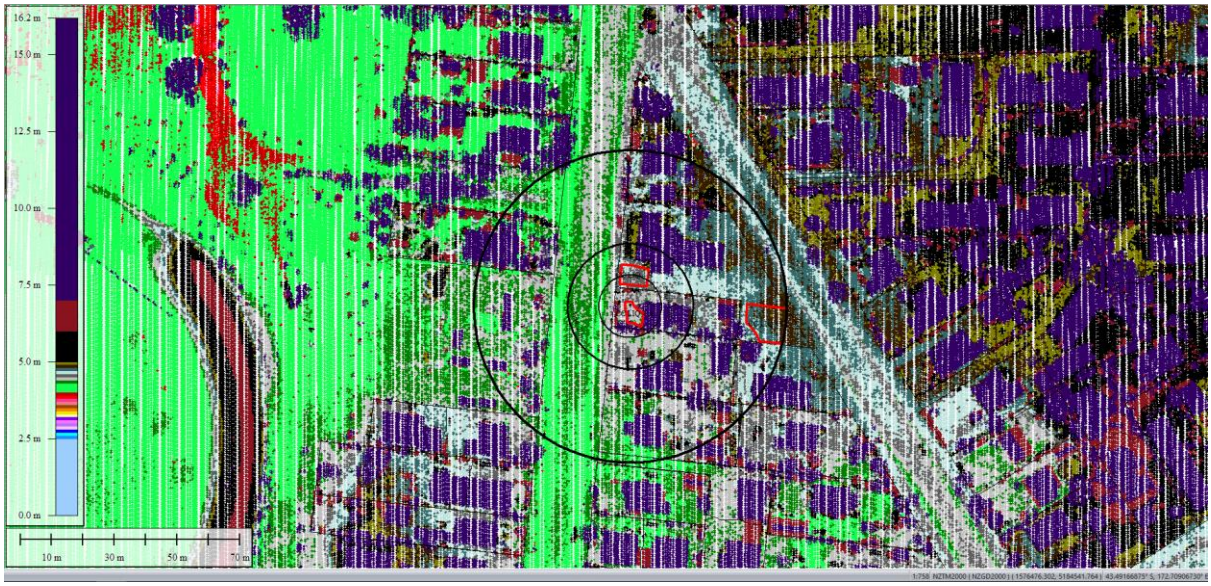

Figure 52: Mar 2011 LiDAR survey.

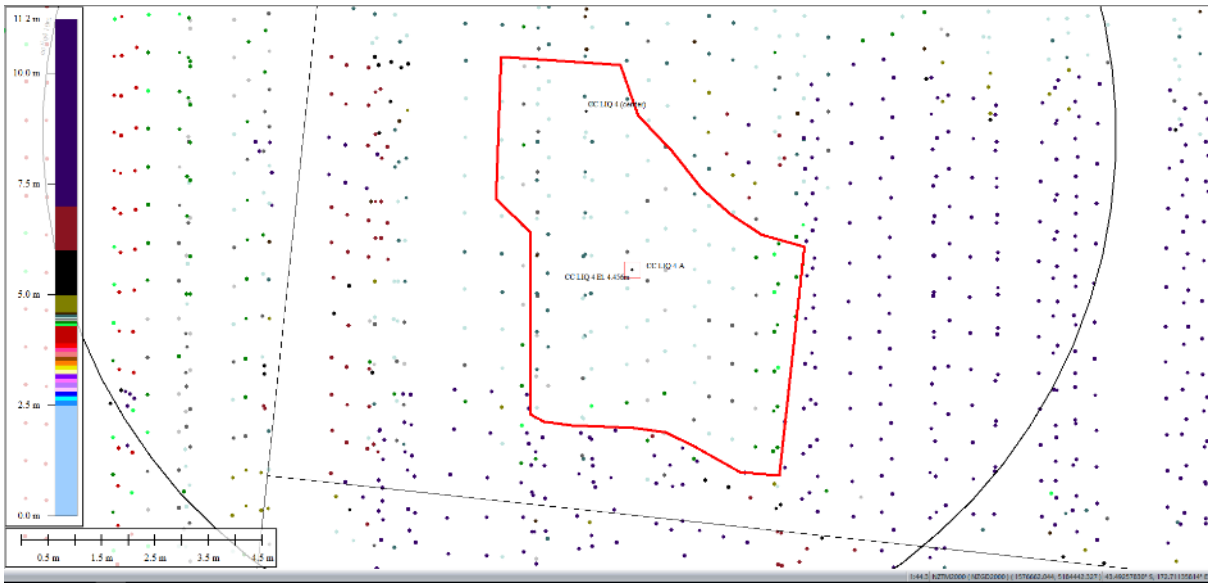

Figure 53: Ground surface elevation averaged over 10-m, 20-m, and 50-m buffers for Patch A for Mar 2011 LiDAR survey.

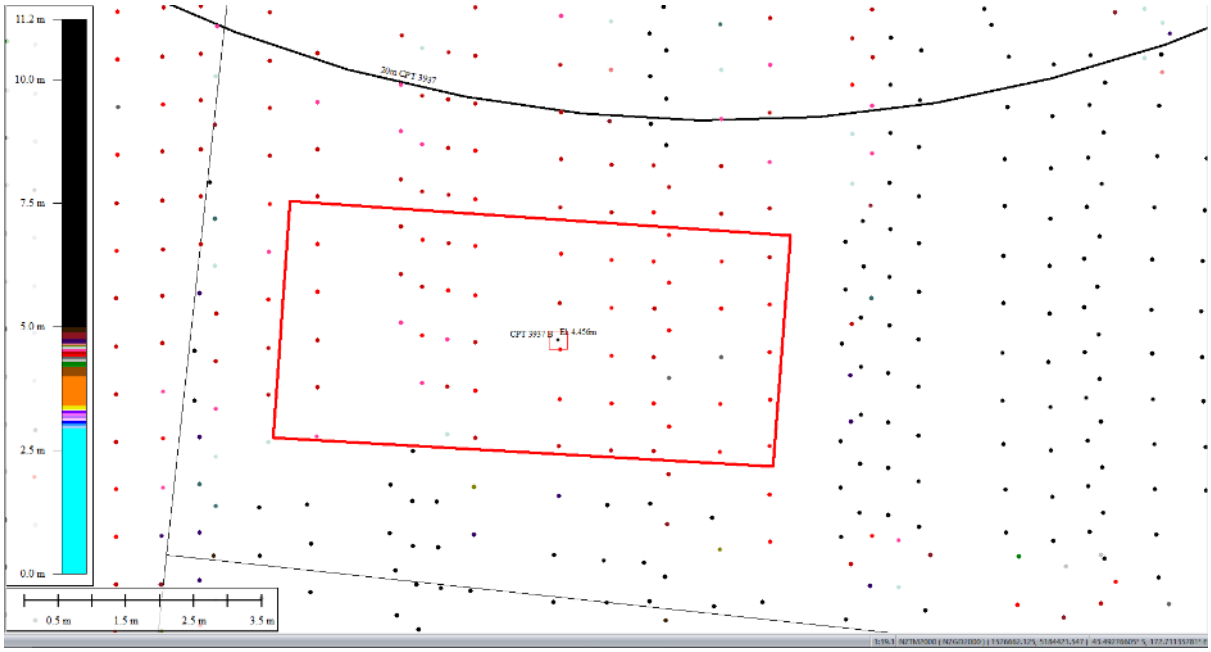

Figure 54: Ground surface elevation averaged over 50-m buffer for Patch B for Mar 2011 LiDAR survey.

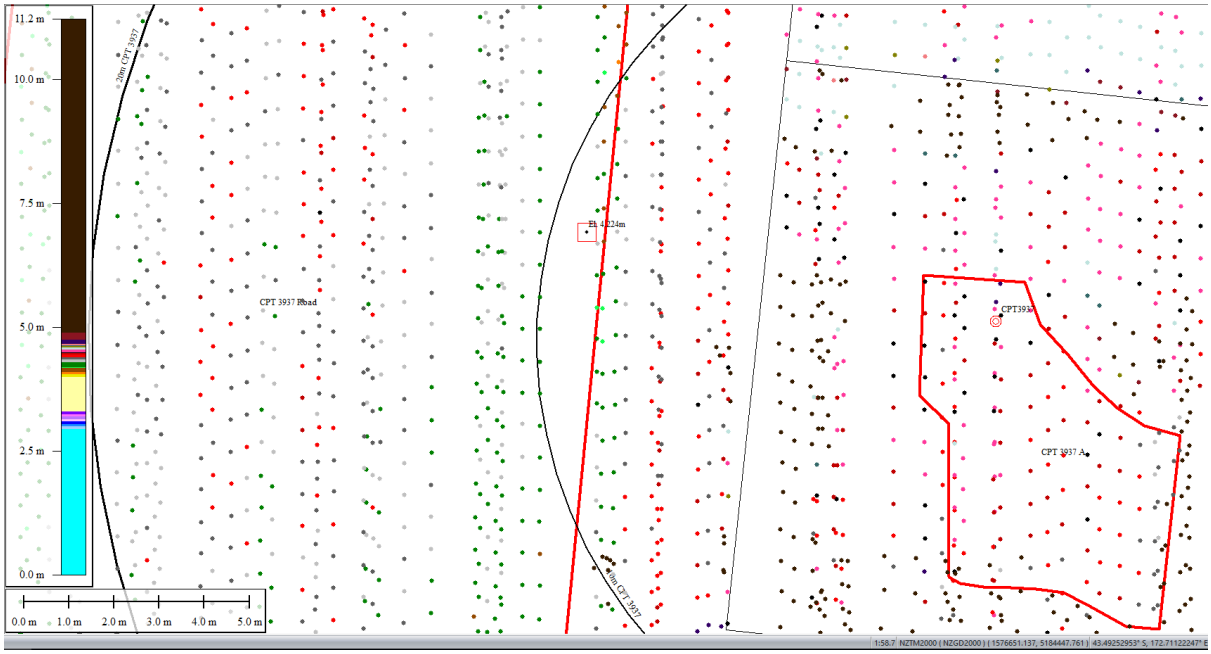

Figure 55: Ground surface elevation averaged over 10-m buffer for Road for Mar 2011 LiDAR survey.

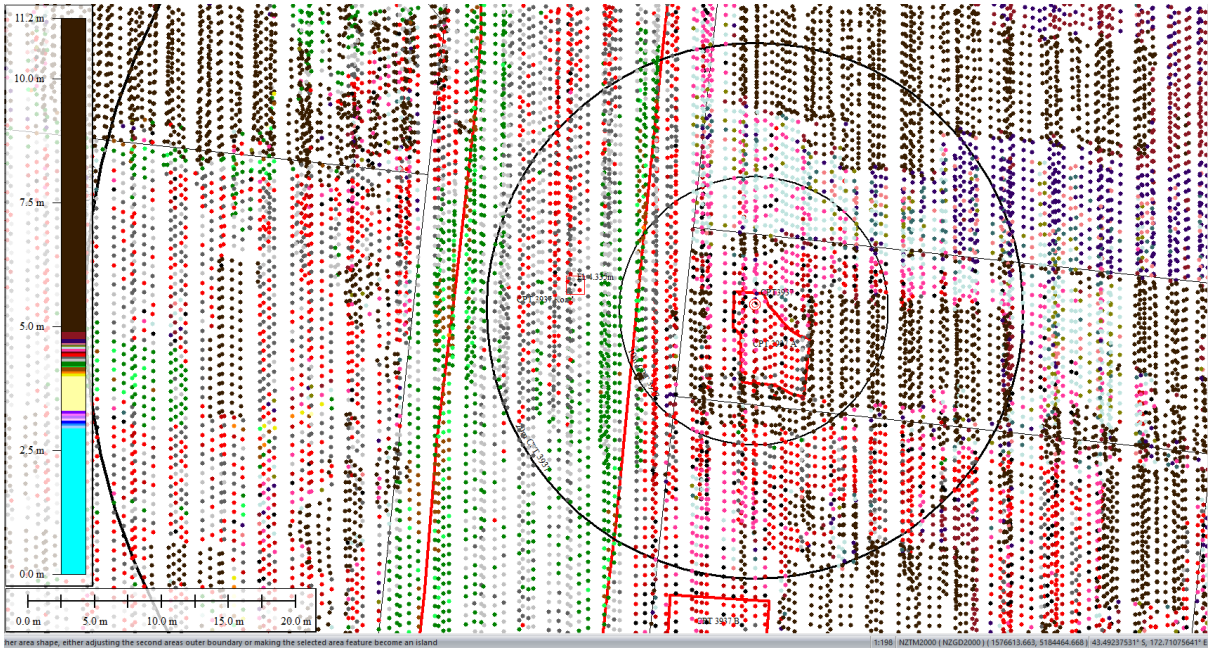

Figure 56: Ground surface elevation averaged over 20-m buffer for Road for Mar 2011 LiDAR survey.

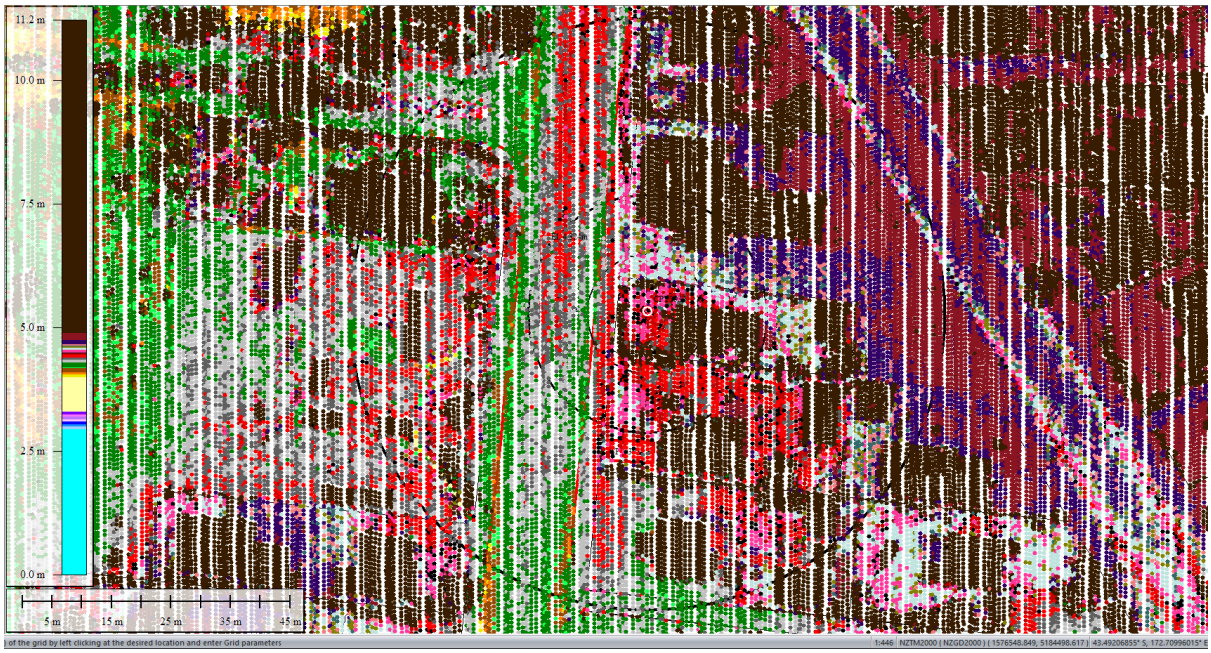

Figure 57: Ground surface elevation averaged over 50-m buffer for Road for Mar 2011 LiDAR survey.

Figure 58: May 2011 LiDAR survey.

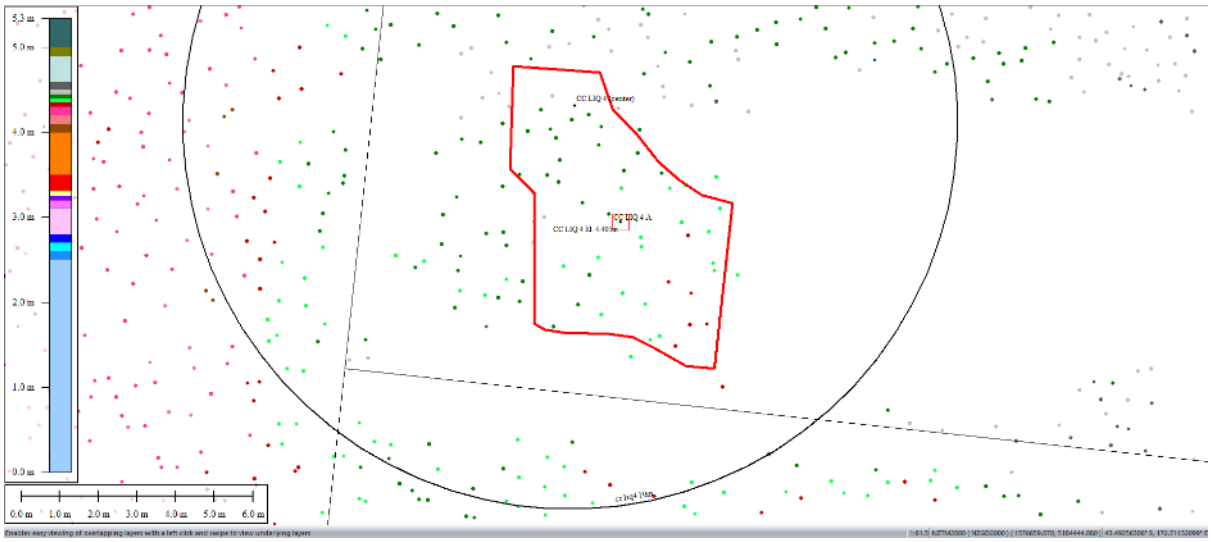

Figure 59: Ground surface elevation averaged over 10-m, 20-m, and 50-m buffers for Patch A for May 2011 LiDAR survey.

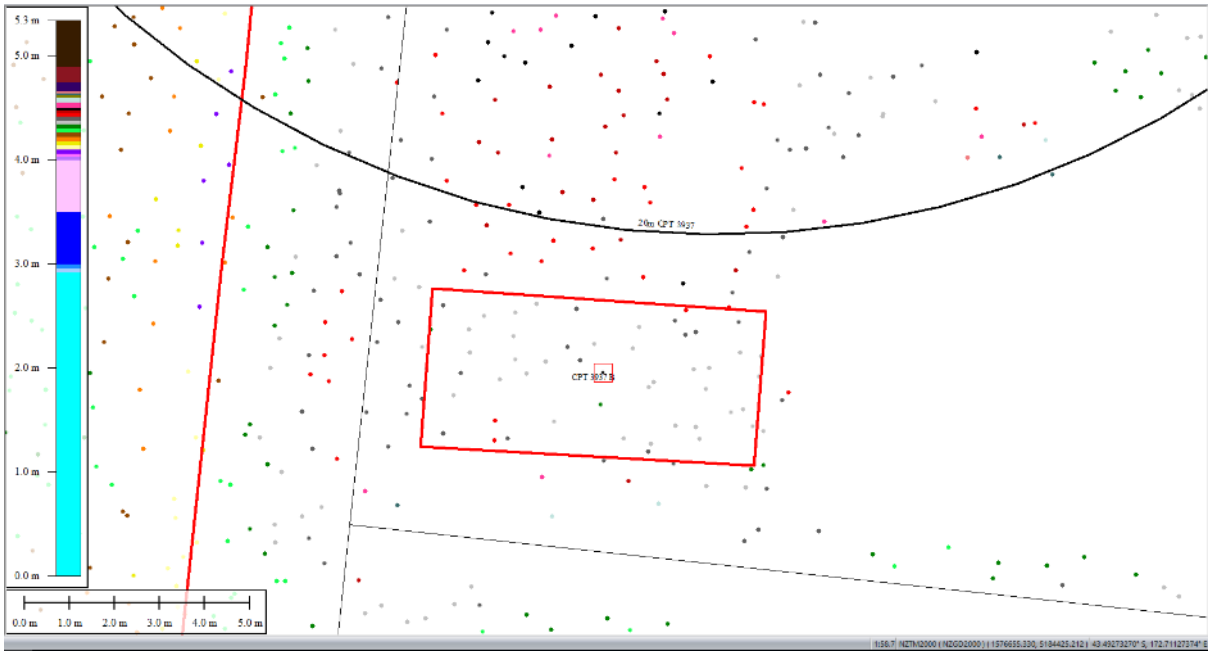

Figure 60: Ground surface elevation averaged over 50-m buffer for Patch B for May 2011 LiDAR survey.

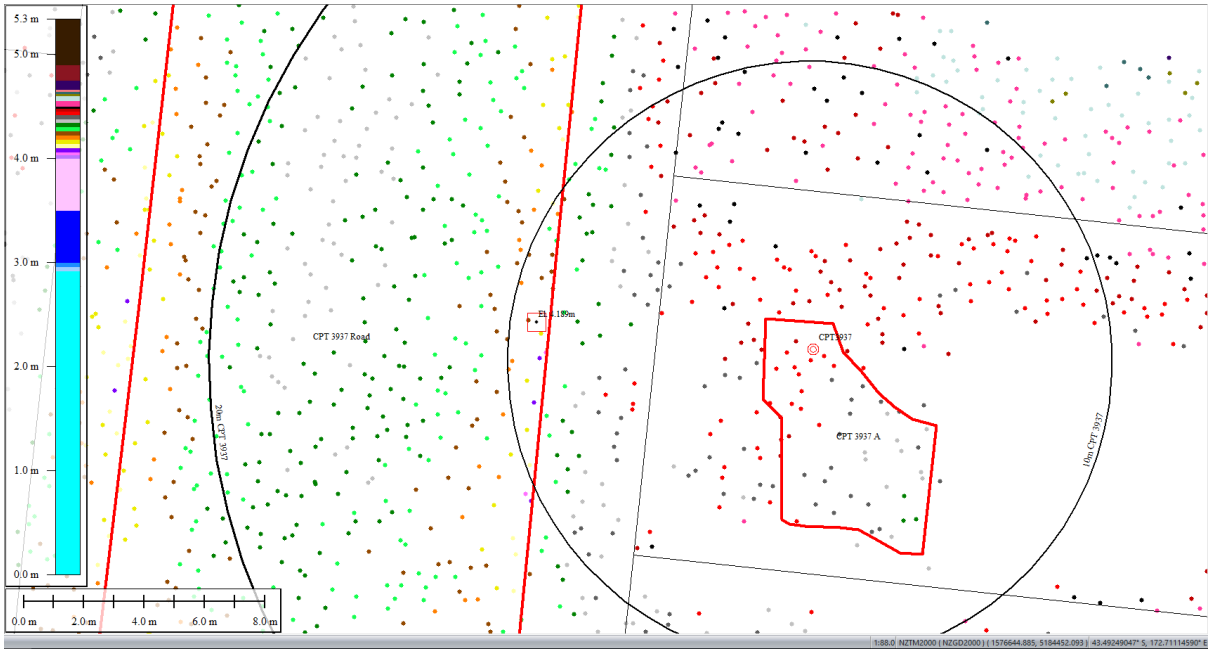

Figure 61: Ground surface elevation averaged over 10-m buffer for Road for May 2011 LiDAR survey.

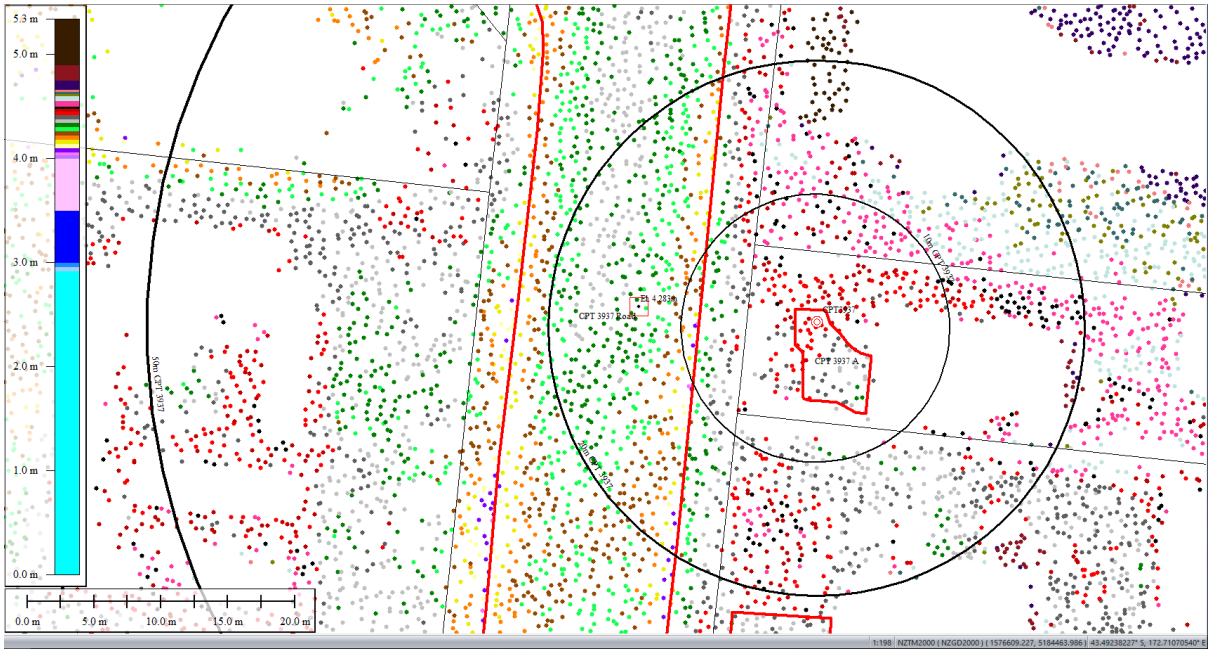

Figure 62: Ground surface elevation averaged over 20-m buffer for Road for May 2011 LiDAR survey.

Figure 63: Ground surface elevation averaged over 50-m buffer for Road for May 2011 LiDAR survey.

Figure 64: Sep 2011 LiDAR survey.

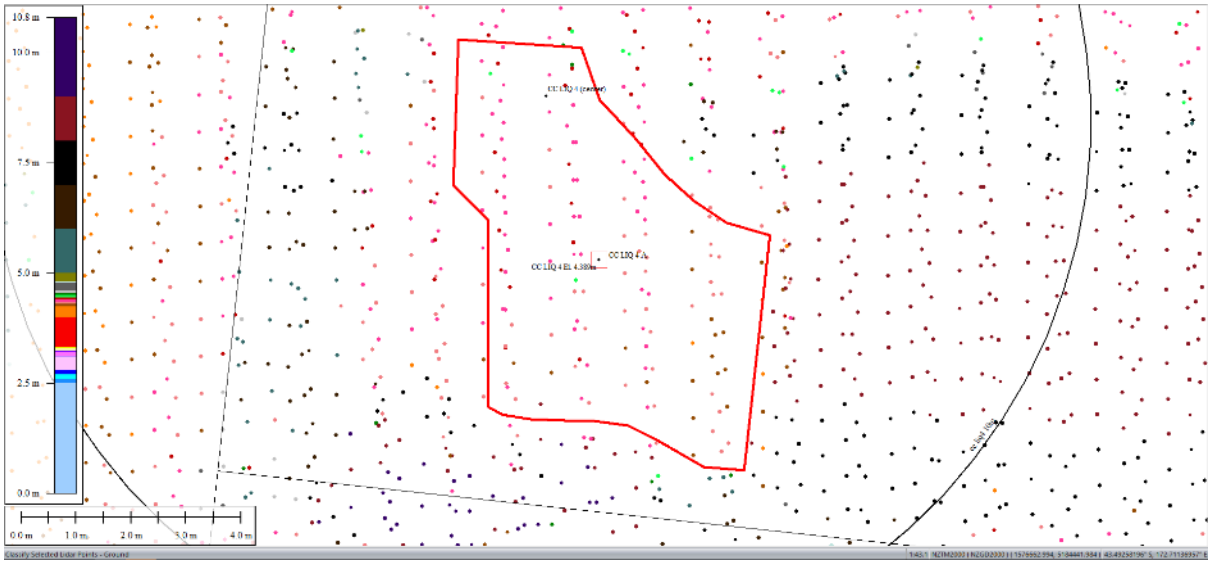

Figure 65: Ground surface elevation averaged over 10-m, 20-m, and 50-m buffers for Patch A for Sep 2011 LiDAR survey.

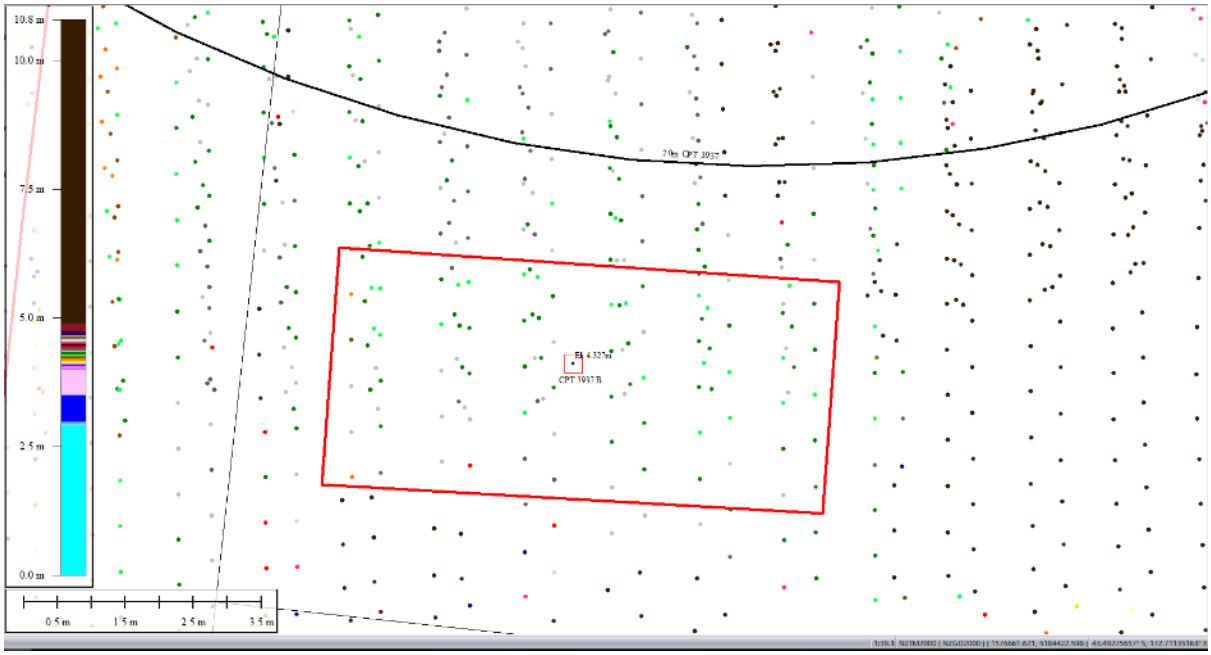

Figure 66: Ground surface elevation averaged over 50-m buffer for Patch B for Sep 2011 LiDAR survey.

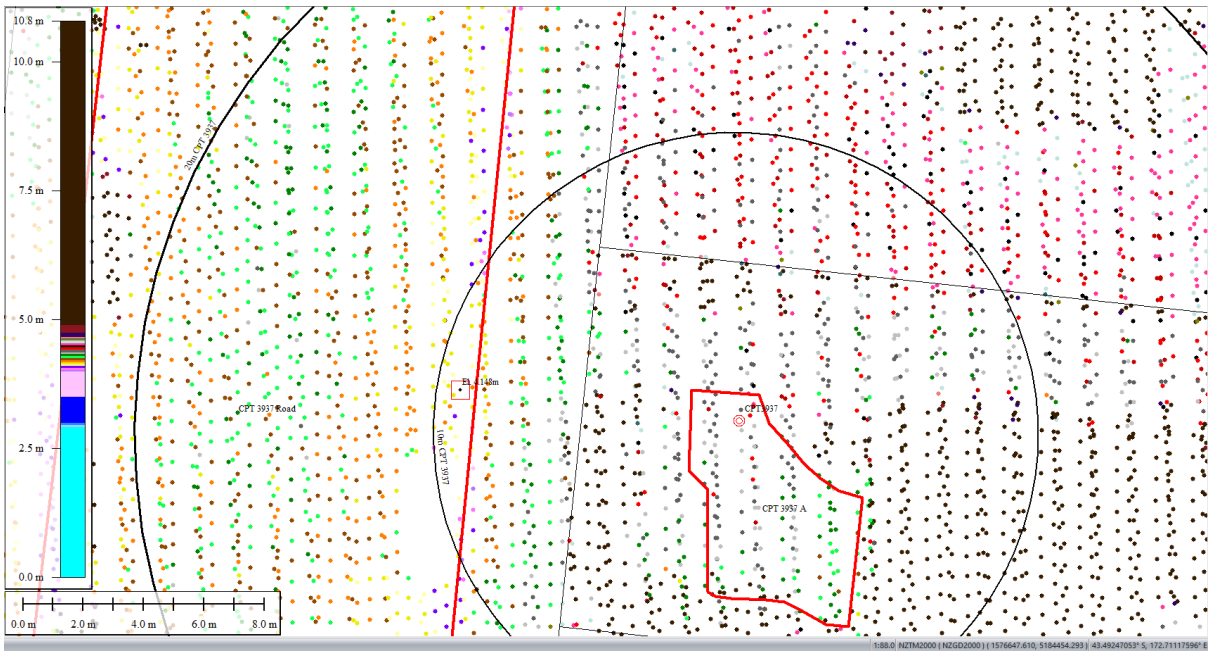

Figure 67: Ground surface elevation averaged over 10-m buffer for Road for Sep 2011 LiDAR survey.

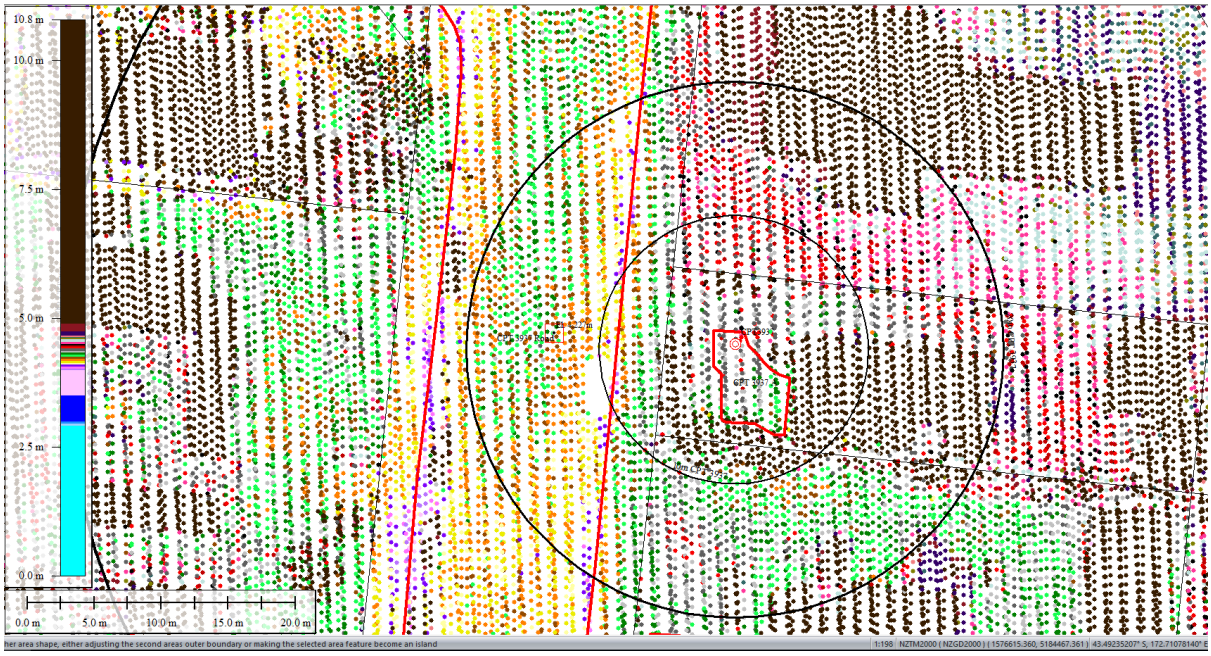

Figure 68: Ground surface elevation averaged over 20-m buffer for Road for Sep 2011 LiDAR survey.

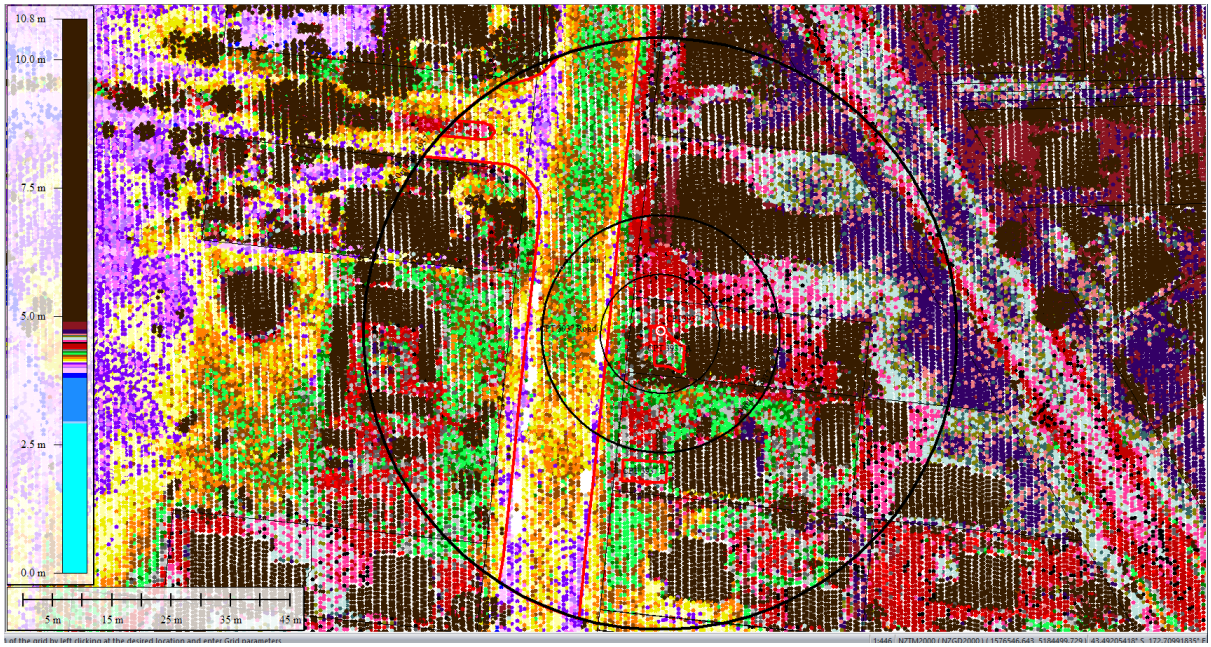

Figure 69: Ground surface elevation averaged over 50-m buffer for Road for Sep 2011 LiDAR survey.

Figure 70: Feb 2012 LiDAR survey.

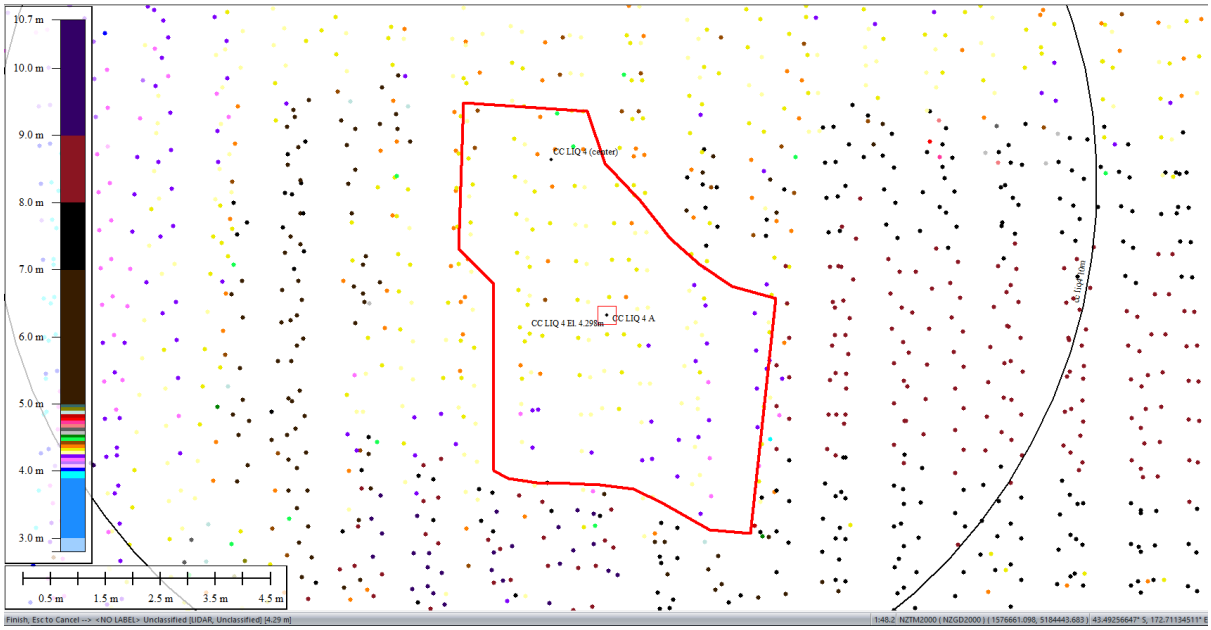

Figure 71: Ground surface elevation averaged over 10-m, 20-m, and 50-m buffers for Patch A for Feb 2012 LiDAR survey.

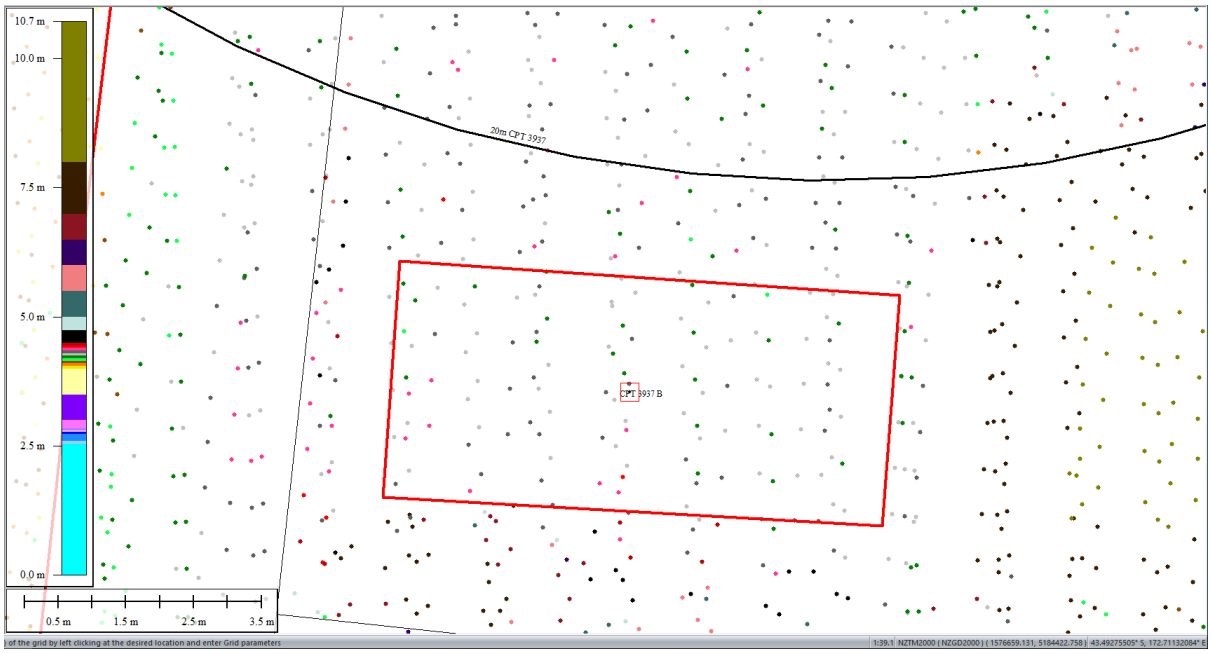

Figure 72: Ground surface elevation averaged over 50-m buffer for Patch B for Feb 2012 LiDAR survey.

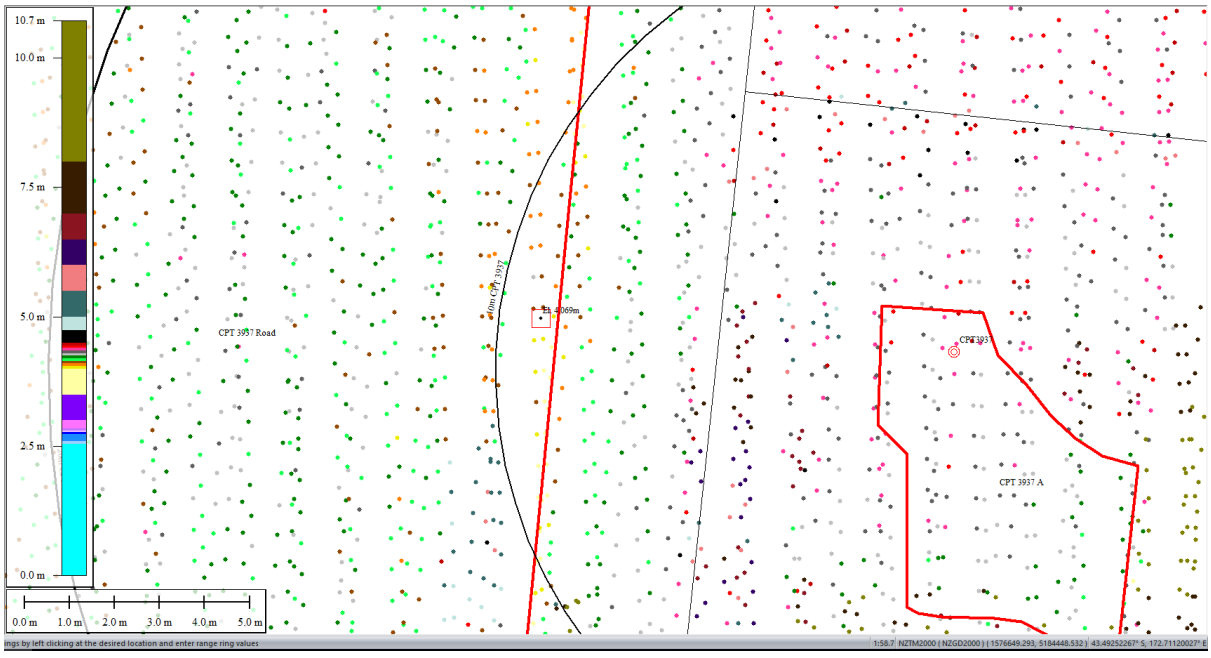

Figure 73: Ground surface elevation averaged over 10-m buffer for Road for Feb 2012 LiDAR survey.

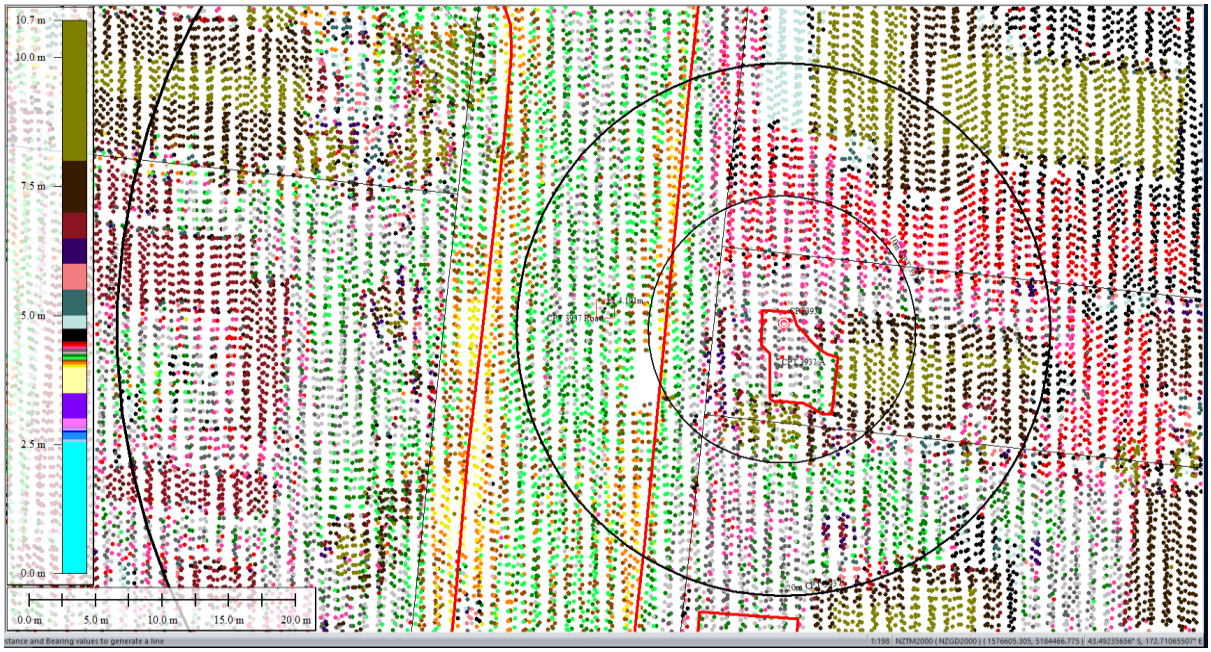

Figure 74: Ground surface elevation averaged over 20-m buffer for Road for Feb 2012 LiDAR survey.

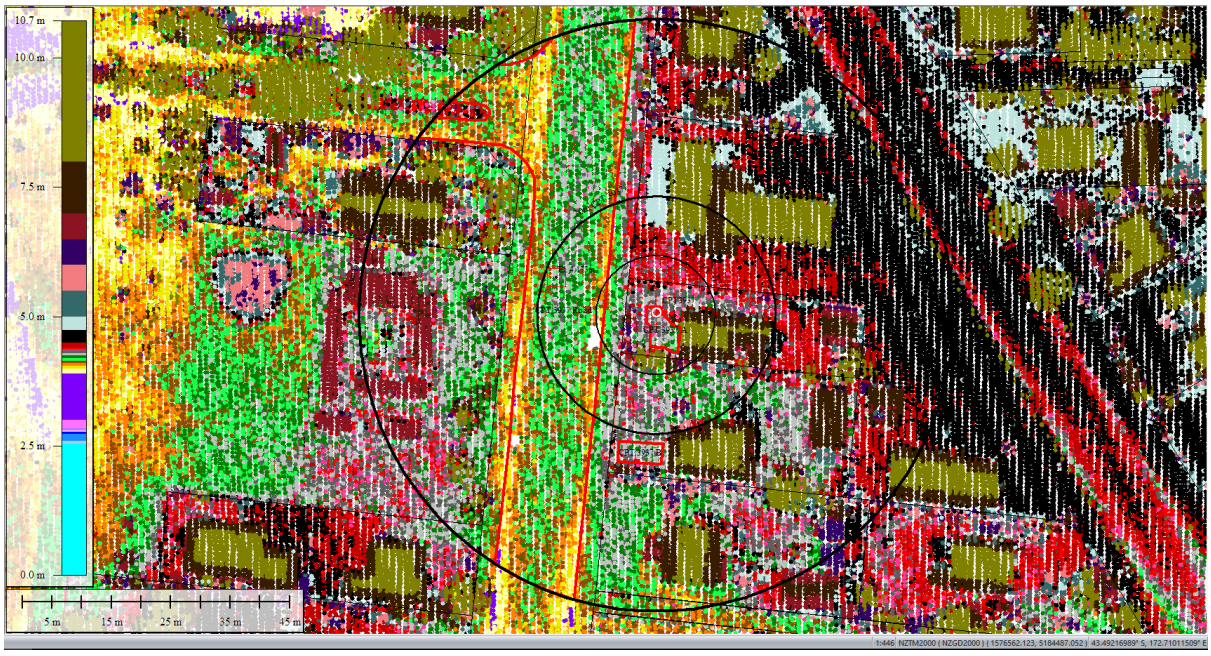

Figure 75: Ground surface elevation averaged over 50-m buffer for Road for Feb 2012 LiDAR survey.

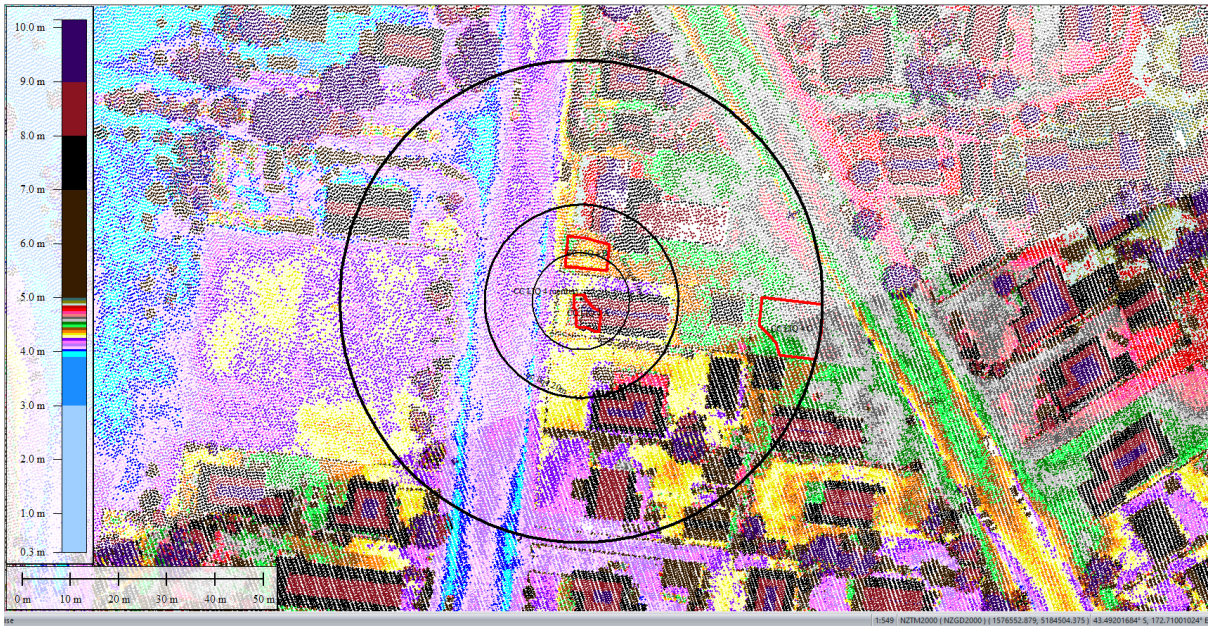

Figure 76: Oct 2015 LiDAR survey.

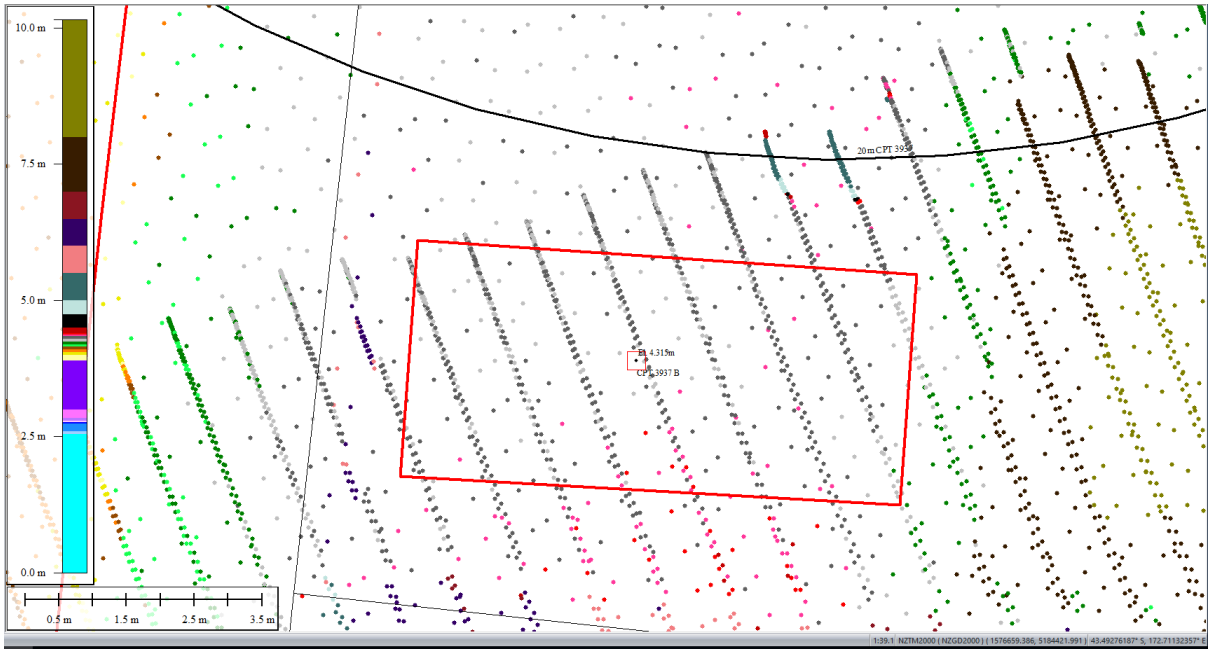

Figure 77: Ground surface elevation averaged over 50-m buffer for Patch B for Oct 2015 LiDAR survey.

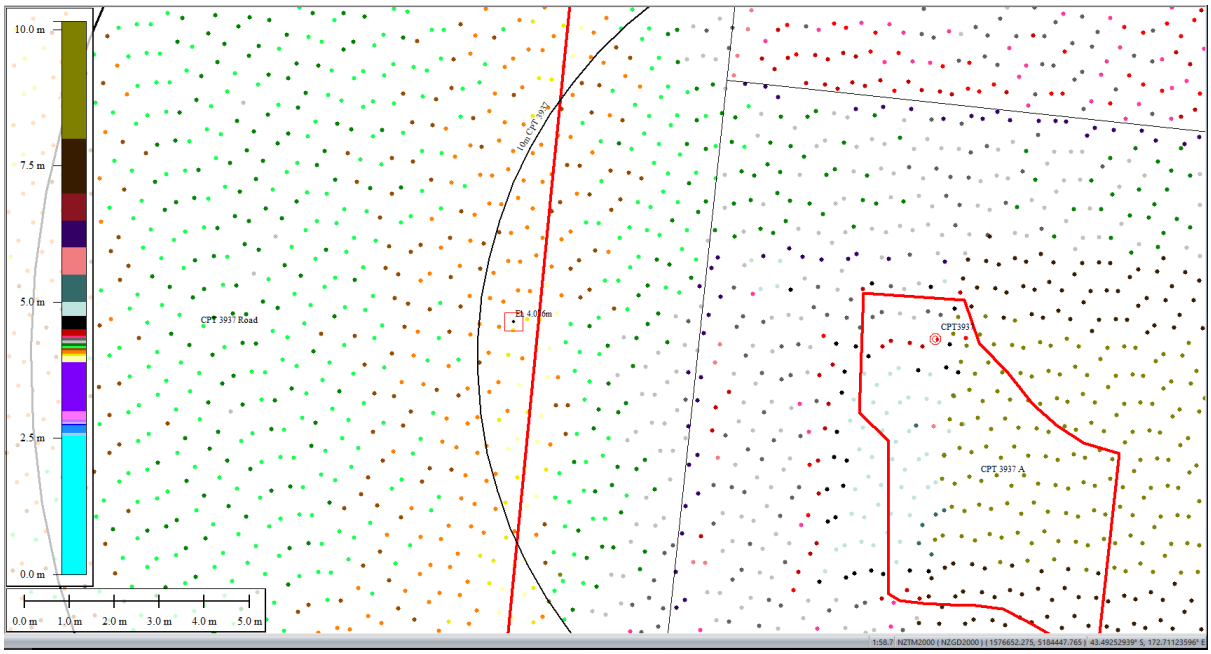

Figure 78: Ground surface elevation averaged over 10-m buffer for Road for Oct 2015 LiDAR survey.

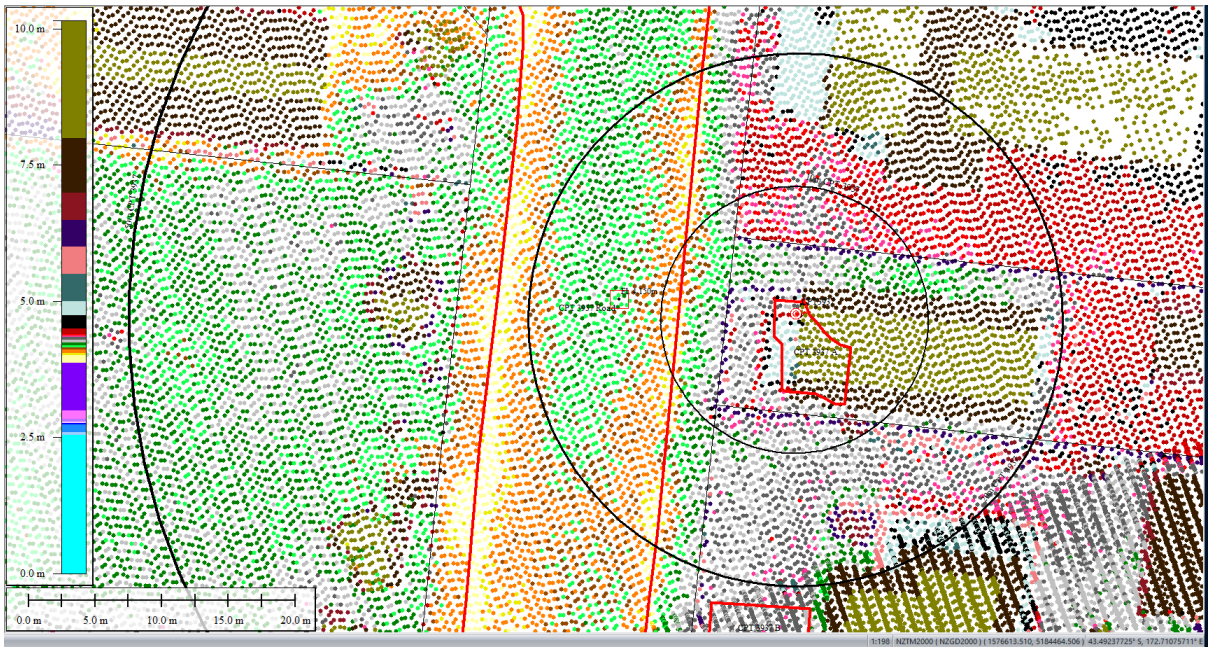

Figure 79: Ground surface elevation averaged over 20-m buffer for Road for Oct 2015 LiDAR survey.

Figure 80: Ground surface elevation averaged over 50-m buffer for Road for Oct 2015 LiDAR survey.

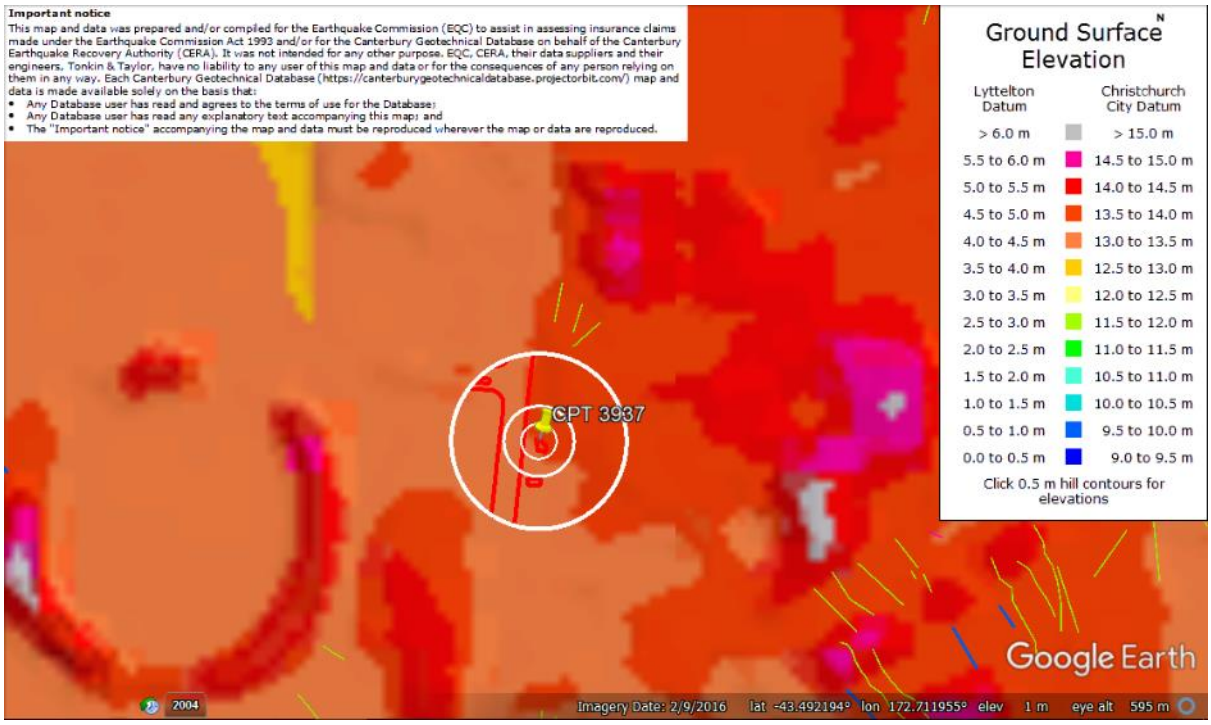

Figure 81: Ground surface elevation difference between the road and properties (LiDAR DEM for Sept 2010).

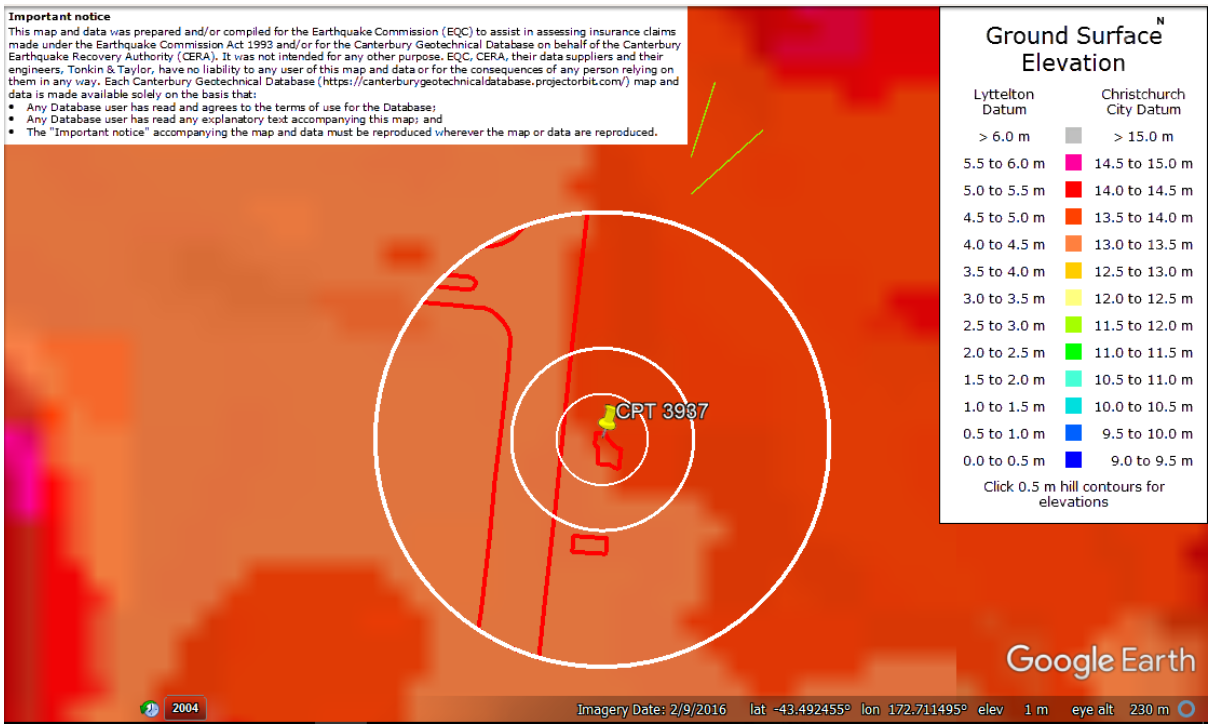

Figure 82: Enlarged view of ground surface elevation difference between the road and properties (LiDAR DEM for Sept 2010).

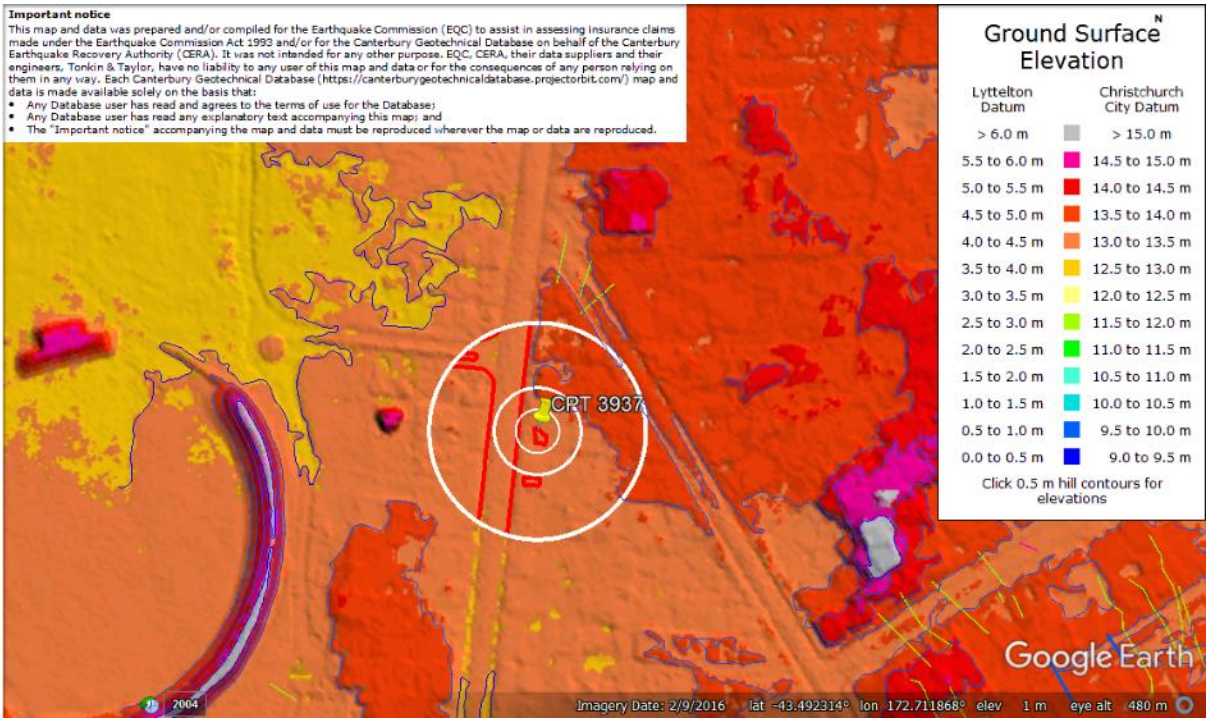

Figure 83: Ground surface elevation difference between the road and properties (LiDAR DEM for Sept 2011).

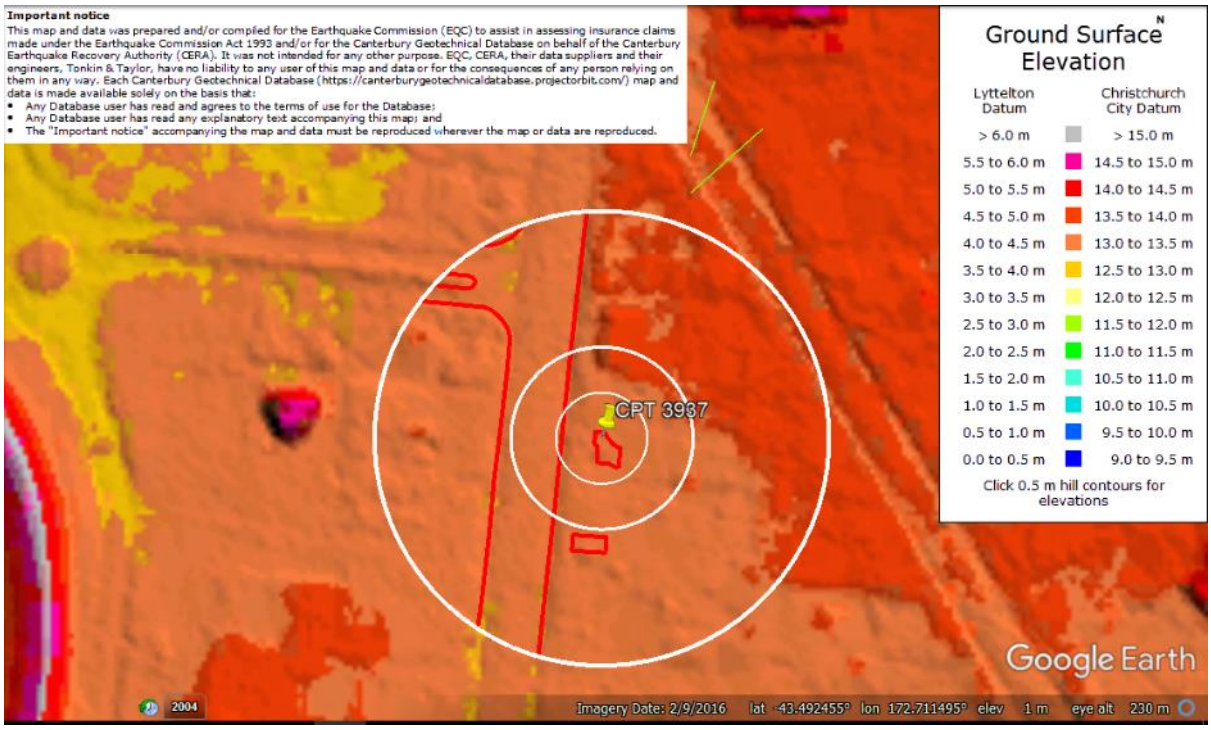

Figure 84: Enlarged view of ground surface elevation difference between the road and properties (LiDAR DEM for Sept 2011).

Figure 85: No ejecta for Sep-10 EQ.

Figure 86: Ejecta outline for Feb-11 EQ.

Figure 87: Presence of ejecta as seen in aerial photograph from 14-15 June 2011.

Figure 88: Ejecta outline for Jun-11 EQ.

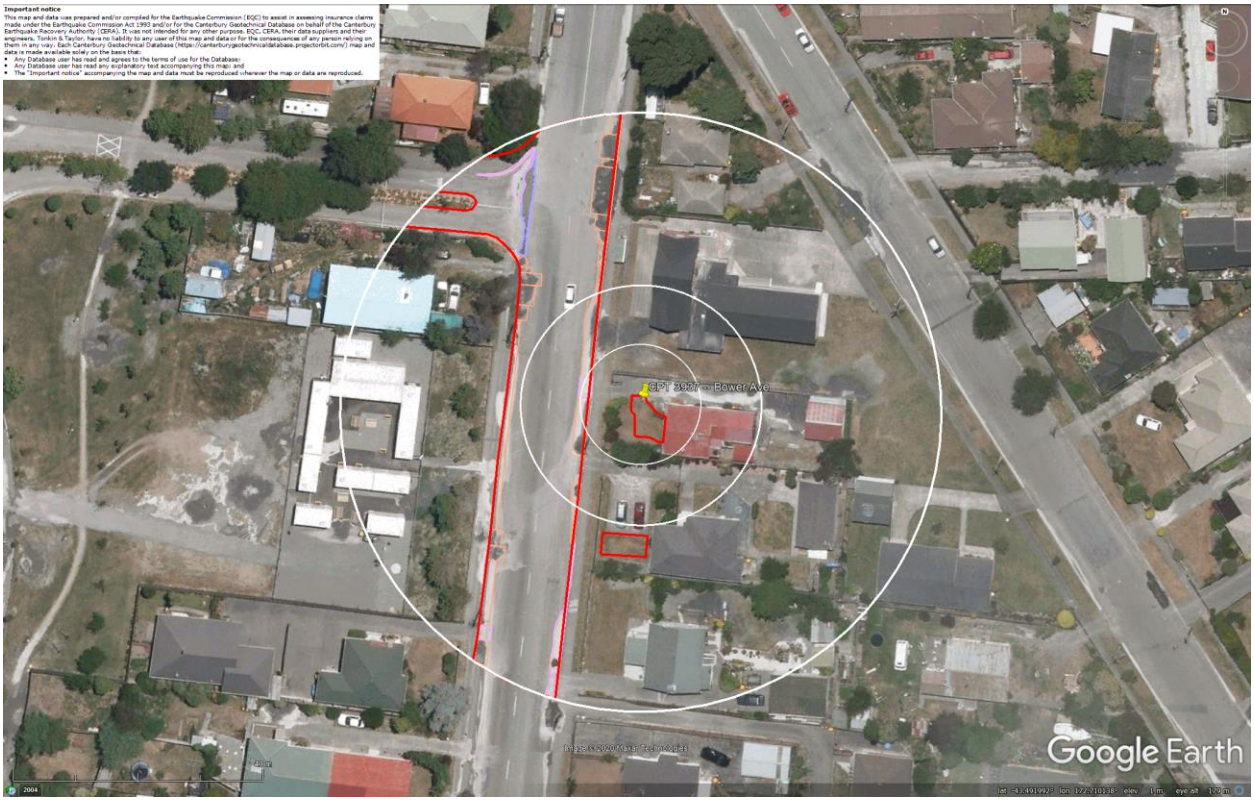

Figure 89: Ejecta outline for Dec-11 EQ.

Figure 90: Ground photo of Patch A.

Contents of this figure cannot be shared as doing so is restricted by a Non-Disclosure Agreement.

Figure 91: LDAT property inspection notes for Patch A.

Contents of this figure cannot be shared as doing so is restricted by a Non-Disclosure Agreement.

Figure 92: LDAT property inspection notes for Patch B.

Figure 93: PGA for Sep-10 EQ (st. dev. = 0.250-0.275 ln units).

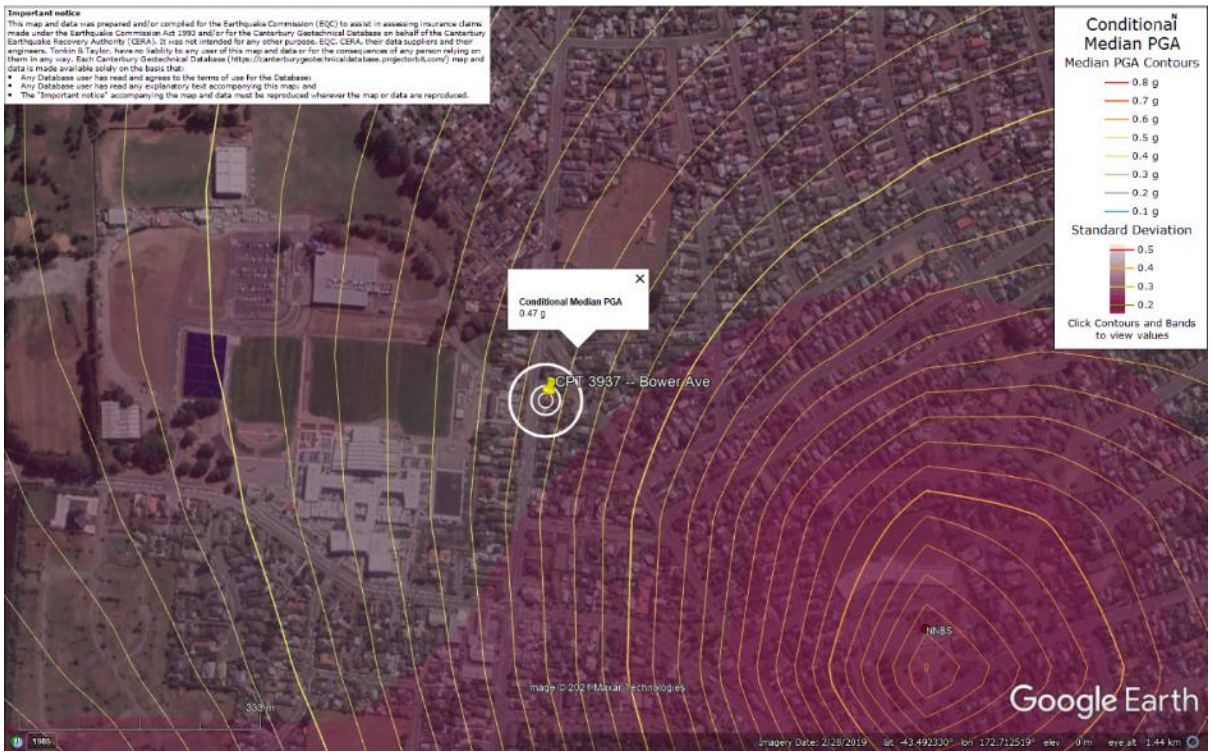

Figure 94: PGA for Feb-11 EQ (st. dev. = 0.275-0.300 ln units).

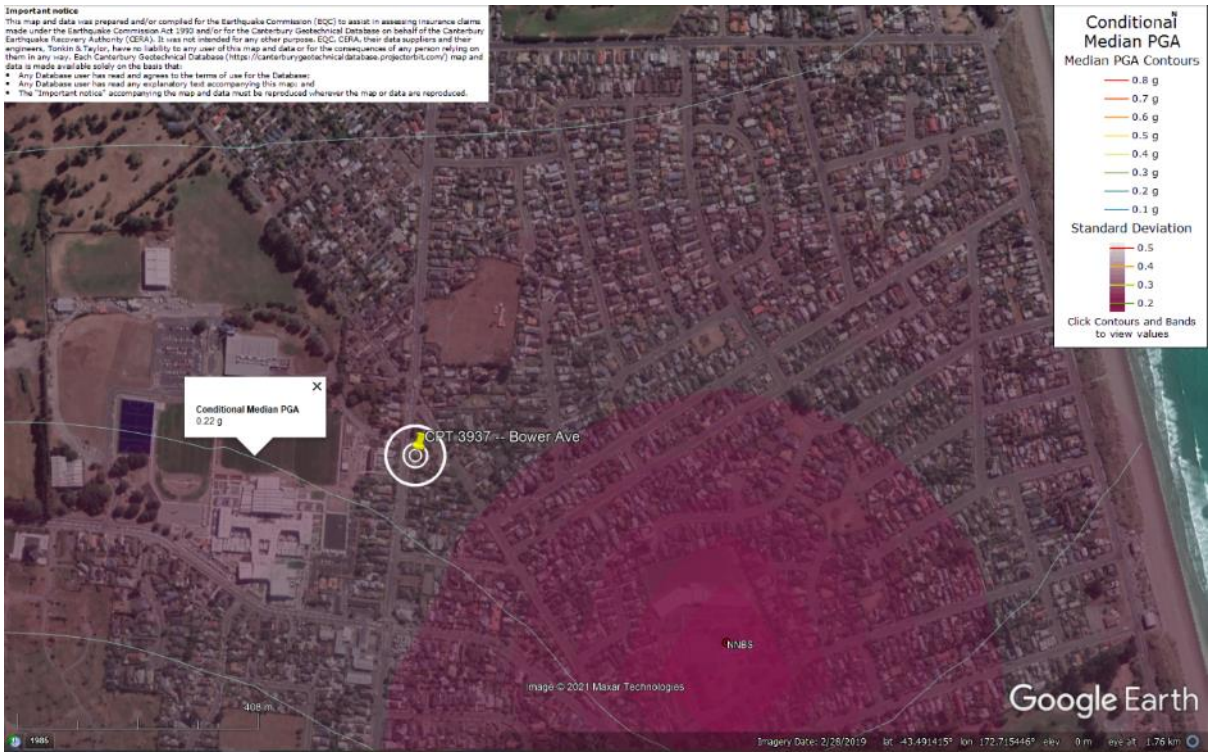

Figure 95: PGA for Jun-11 EQ (st. dev. = 0.275-0.325 ln units).

Figure 96: PGA for Dec-11 EQ (st. dev. = 0.375-0.400 ln units).

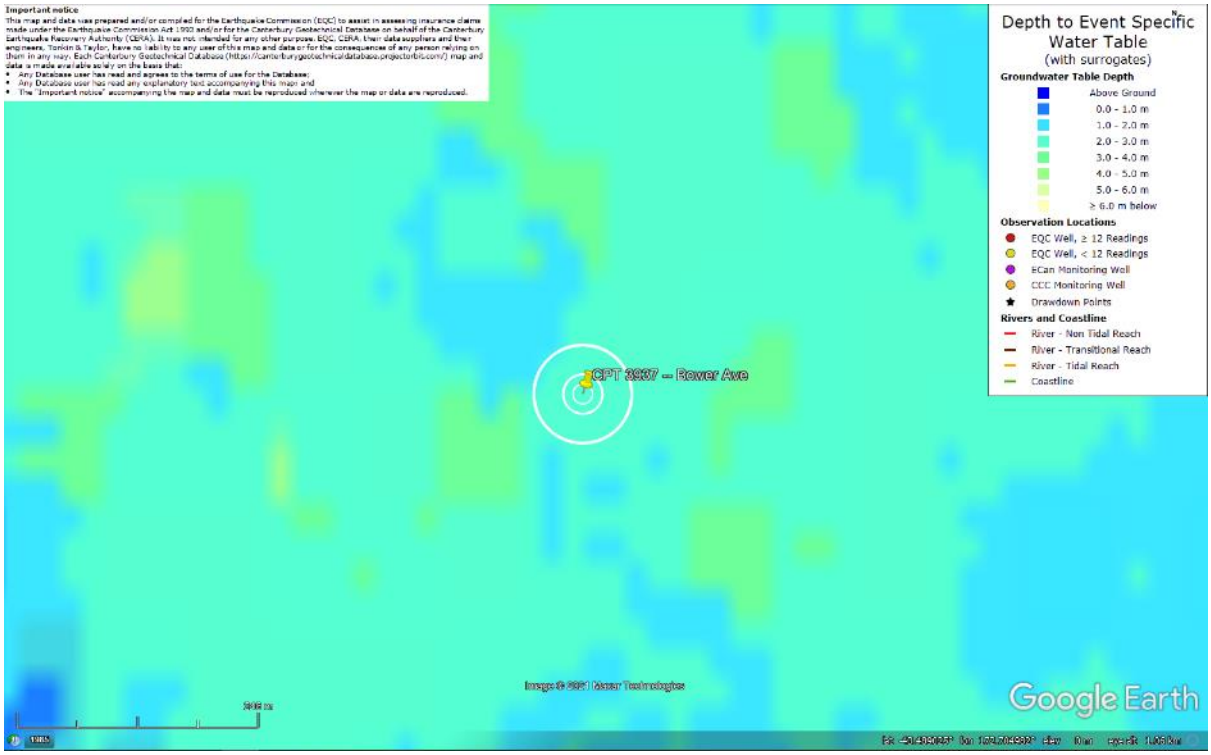

Figure 97: Depth to groundwater table for Sep-10 EQ.

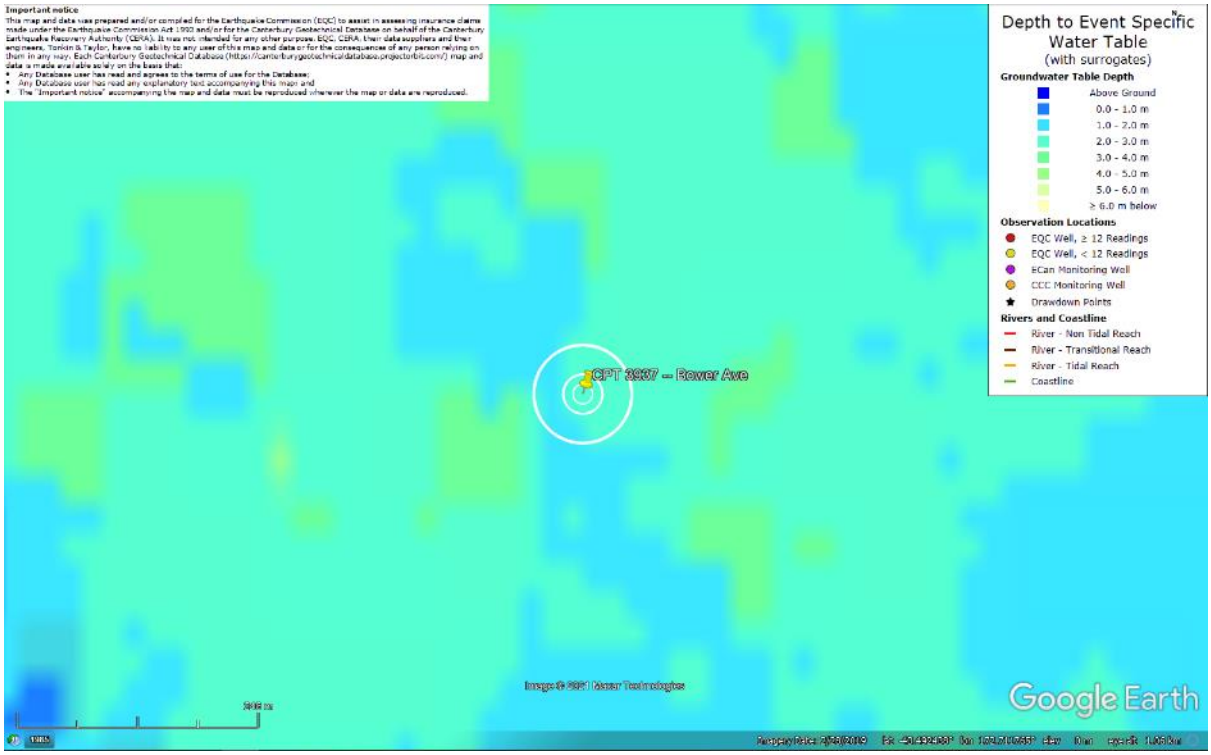

Figure 98: Depth to groundwater table for Feb-11 EQ.

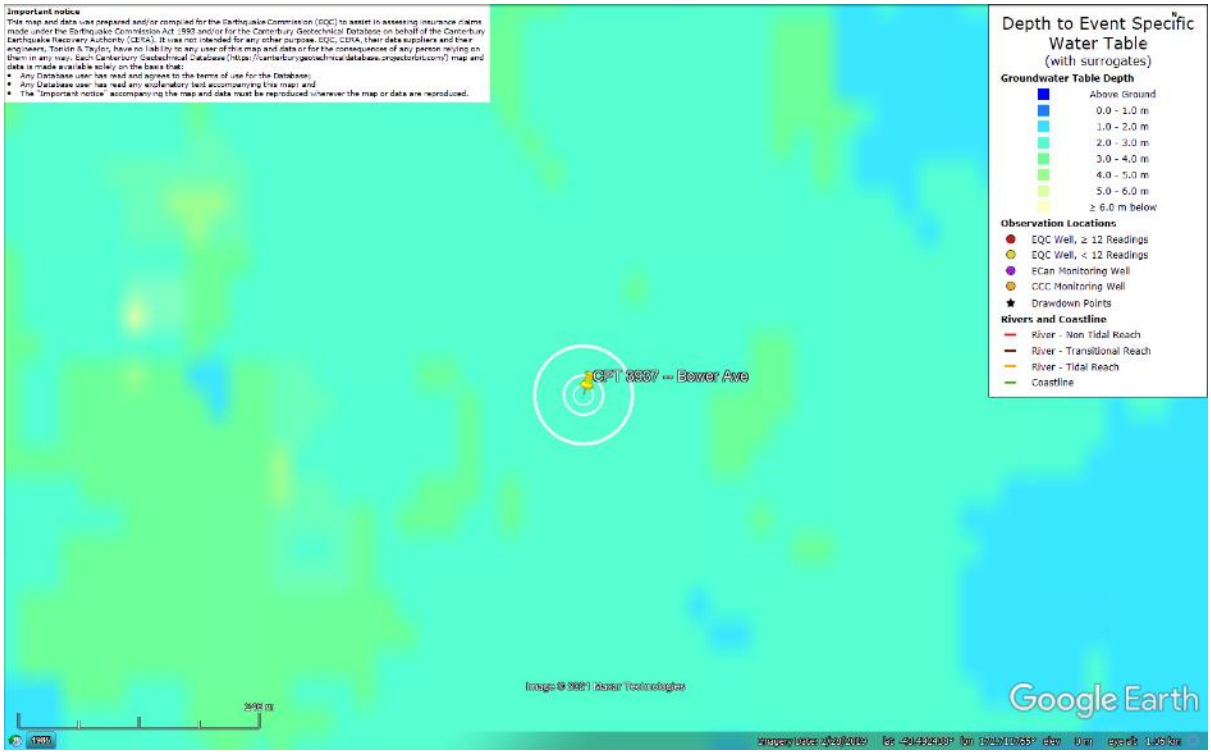

Figure 99: Depth to groundwater table for Jun-11 EQ.

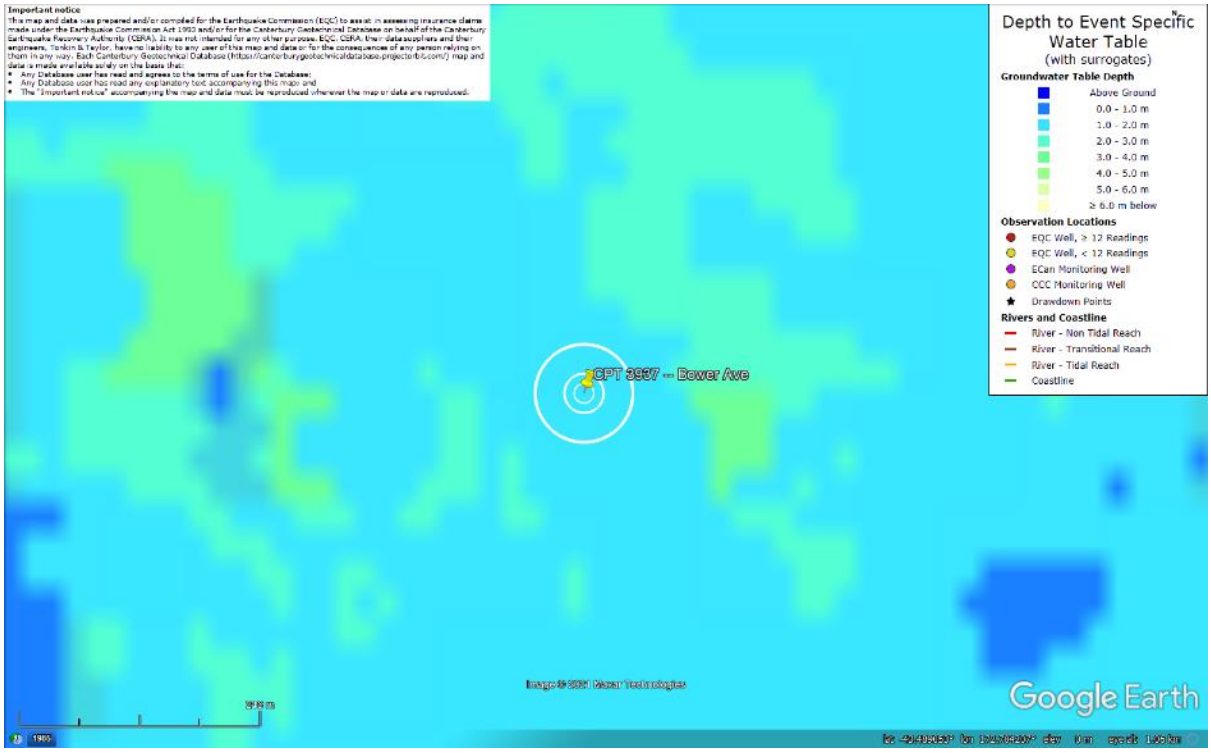

Figure 100: Depth to groundwater table for Dec-11 EQ.

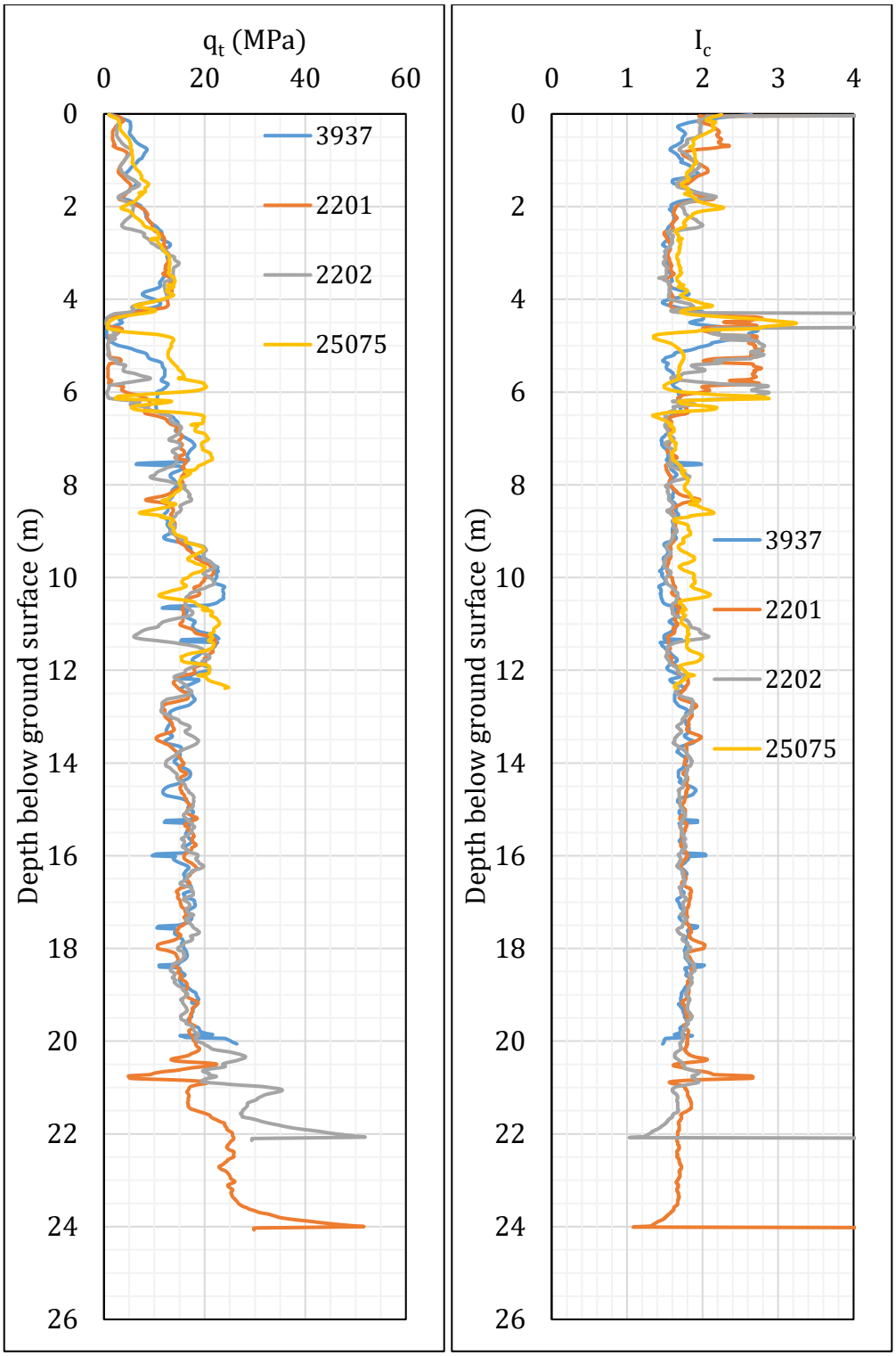

Figure 101: q_t and I_c profiles.

Note 7: The selection of CPTs for the area considered for settlement assessment (Figure 1) is based on the proximity of the CPTs to the considered areas. In accordance with that, the following table shows CPTs that were used for the volumetric settlement analysis in *Cliq v.3.0.3.2*, a CPT soil liquefaction software developed by GeoLogismiki. (The average volumetric settlements were reported in Table 8.)

Table 12: CPT profiles used in volumetric settlement analysis for areas selected for settlement assessment.

CPT ID No.	Patch A	Patch B	Road
3937	✓		✓
2201		✓	✓
2202			✓
25075			✓

Note: CPT 3937 was used to estimate the volumetric settlement for a depth range from 12.4 m to 20 m for CPT 25075.

Table 13: CPT-based results.

		CPT ID				
EQ Event	Parameter	3937	2201	2202	25075	$\Delta_{12.4m-20m}$*
Sep-10	S_{V1D} (mm)	16	8	10	1	4
	LSN	2	2	2	0	0
	LPI	0	0	0	0	0
	LPI_{ish}	0	0	0	0	--
	$D_{FS<1}$ (m)	undet.	undet.	undet.	undet.	--
Feb-11	S_{V1D} (mm)	98	45	63	13	34
	LSN	13	7	11	3	2
	LPI	7	5	7	2	1
	LPI_{ish}	5	1	4	1	--
	$D_{FS<1}$ (m)	3.78	4.58	2.21	undet.	--
Jun-11	S_{V1D} (mm)	20	11	15	2	4
	LSN	3	2	3	1	0
	LPI	1	0	0	0	0
	LPI_{ish}	0	0	0	0	--
	$D_{FS<1}$ (m)	undet.	undet.	undet.	undet.	--
Dec-11	S_{V1D} (mm)	65	36	53	10	10
	LSN	12	8	13	2	1
	LPI	4	4	5	1	0
	LPI_{ish}	3	0	3	1	--
	$D_{FS<1}$ (m)	4.26	4.58	1.75	undet.	--

Notes: $D_{FS<1}$ = Depth to the first liquefiable layer ($FS_L<1$) that is at least 200-mm thick, as determined by the Boulanger and Idriss (2016) liquefaction-triggering procedure (P_L=50%, C_{FC}=0.13, and $I_{c,cutoff}$ =2.6), and exported from *Cliq v.3.0.3.2*; undet. = the specified soil layer was not detected; * indicates the amount of S_{V1D}, LSN, and LPI to be added for CPT 25075 due to its penetration depth being shallower than 20 m.

Note 8: Based on the borehole log (BH 3813, Figure 1), the groundwater table is at a depth of 1.5 m below the ground surface. The soil profile consists of (1) topsoil (sandy silt) to a depth of 0.25 m, (2) fine to medium sand, SP, of the Christchurch formation to a depth of 5 m, (2) sandy silt, ML, of the Christchurch formation to a depth of 5.6 m, and (3) fine to medium sand, SP, of the Christchurch formation to a depth of 20 m.

Note 9: The ejecta-induced free-field settlement provided in Table 11 is an areal average settlement due to ejecta, which is based on the total settlement assessment area, A_T (provided in Table 9 and repeated in Table 14). However, the considered area was not always covered completely with ejecta; thus, it is important to provide the localized ejecta-induced settlement, too. The localized settlement due to ejecta is estimated using photographic evidence only as

$$S_{E,P\_localized} = \frac{V_E}{A_E}$$

where V_E is the total volume of ejecta within A_T and A_E is the total coverage area of ejecta within A_T. Please note that the areal ejecta-induced settlement provided in Table 14 as S_{E,P_areal} is the same as $S_{E,P}$ in Table 11, which was estimated as

$$S_{E,P\_areal} = S_{E,P} = \frac{V_E}{A_T}$$

where V_E is the total volume of ejecta within A_T and A_T is the total settlement assessment area.

Table 14a: Areal and localized ejecta-induced settlement estimates for Patch B (50-m buffer) based on photographic evidence.

Earthquake Event	A_T (m^2)	A_E (m^2)	V_E (m^3)	S_{E,P_areal} (mm)	$S_{E,P\_localized}$ (mm)
Sep-10	28.0	0	0	0	0
Feb-11	28.0	28.0	2.1-3.4	100±25	100±25
Jun-11	28.0	0	0	0	0
Dec-11	28.0	0	0	0	0

Notes: $S_{E,P\_areal} = S_{E,P}$ reported in Table 11 = areal ejecta-induced settlement; $S_{E,P\_localized}$ = localized ejecta-induced settlement; A_T = total settlement assessment area; V_E = total volume of ejecta within A_T; A_E = total area of ejecta within A_T; The estimates of both areal and localized ejecta-induced settlement are rounded to the nearest 5 mm; Final plus/minus values are also rounded to the nearest 5 mm.

Table 14c: Areal and localized ejecta-induced settlement estimates for Road (50-m buffer) based on photographic evidence.

Earthquake Event	A_T (m^2)	A_E (m^2)	V_E (m^3)	S_{E,P_areal} (mm)	$S_{E,P\_localized}$ (mm)
Sep-10	1491	0	0	0	0
Feb-11	1438	438	9.5-17.9	10±5	30±10
Jun-11	1377	1377	14.4-25.2	15±5	15±5
Dec-11	1491	356	7.0-12.6	5±5	30±5

Notes: S_{E,P_areal} = $S_{E,P}$ reported in Table 11 = areal ejecta-induced settlement; $S_{E,P\_localized}$ = localized ejecta-induced settlement; A_T = total settlement assessment area; V_E = total volume of ejecta within A_T; A_E = total area of ejecta within A_T; The estimates of both areal and localized ejecta-induced settlement are rounded to the nearest 5 mm; Final plus/minus values are also rounded to the nearest 5 mm.

Summary 2:

- **The best estimate of the localized ejecta-induced free-field ground settlement at the Bower Ave site for the SEP 2010, FEB 2011, JUN 2011, and DEC 2011 earthquake is 0 mm, 100±25 mm, 0 mm, and 0 mm, respectively.**
- **The best estimate of the localized ejecta-induced settlement of the road at the Bower Ave site for the SEP 2010, FEB 2011, JUN 2011, and DEC 2011 earthquake is 0 mm, 30±10 mm, 15±5 mm, and 30±5 mm, respectively.**